Stability and properties of heavy and superheavy nuclei in mean-field model with Skyrme energy density functional

A. Staszczak

Katedra Fizyki Teoretycznej UMCS Lublin

UMCS Uniwersytet Marii Curie-Skłodowskiej

Oak Ridge National Laboratory

The University of Tennessee

INT-13-3 University of Washington, 17 October 2013

The Segre chart of the SHN (A.D. 2013)

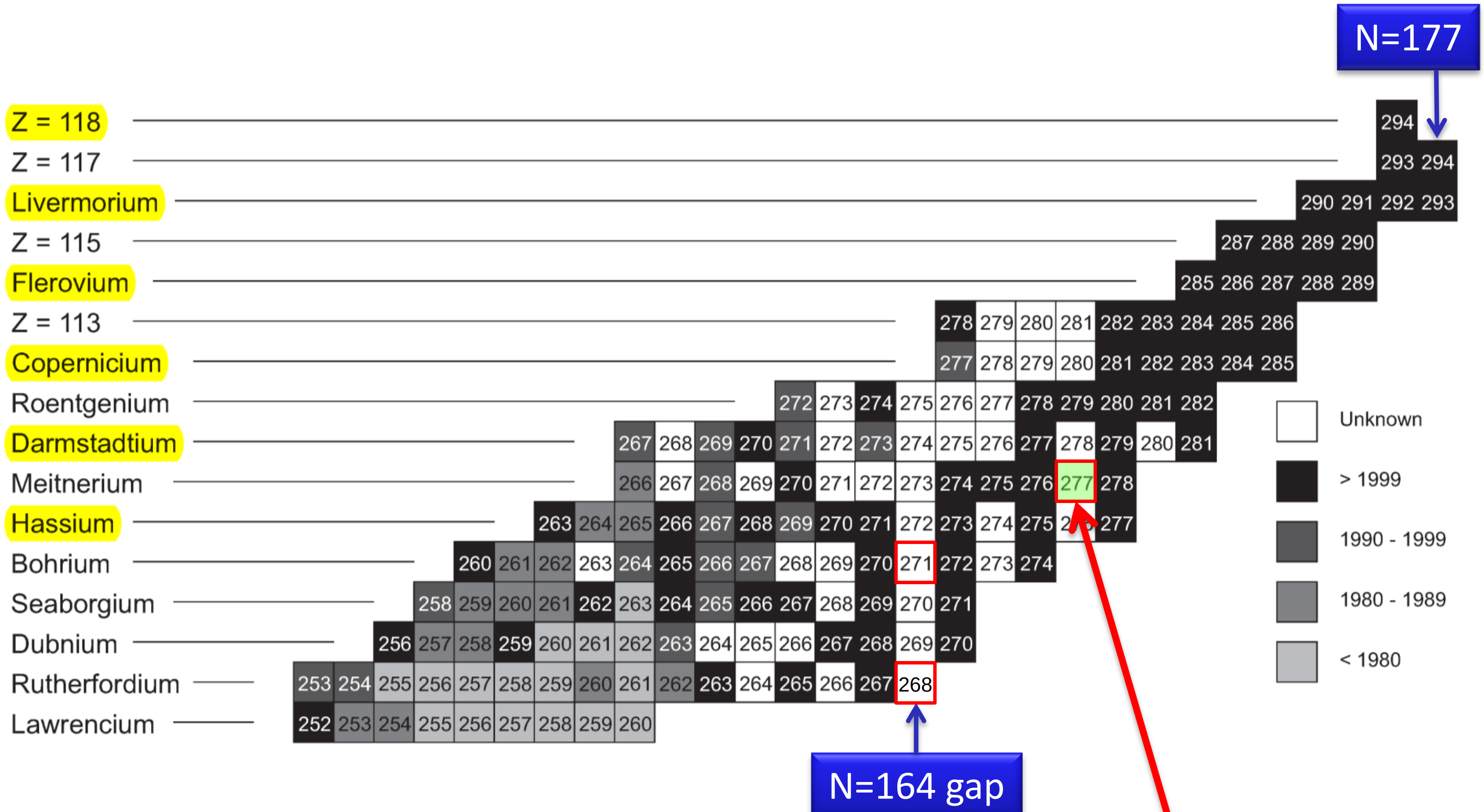

M. Thoennessen, Rep. Prog. Phys. **76**, 056301 (2013)

The new isotope ^{277}Mt.
Yu. Ts. Oganessian *et al.*, Phys. Rev. C **87**, 054621 (2013)

The Skyrme EDF

$$E_{Sk} = \sum_{t=0,1} \int \mathrm{d}^3\boldsymbol{r} \left(\mathcal{H}_t^{even}(\boldsymbol{r}) + \mathcal{H}_t^{odd}(\boldsymbol{r})\right),$$

time-even Skyrme EDF $\left(\rho_t,\ \tau_t,\ \mathbb{J}_t^{jk}\right)$ even-even nuclei

$$\begin{aligned}\mathcal{H}_t^{even}(\boldsymbol{r}) &= C_t^{\rho}[\rho_0]\rho_t^2 + C_t^{\Delta\rho}\rho_t\Delta\rho_t + C_t^{\tau}\rho_t\tau_t + C_t^{J0}\mathcal{J}_t^2 + C_t^{J1}\boldsymbol{J}_t^2 + C_t^{J2}\mathfrak{J}_t^2 \\ &+ C_t^{\nabla J}\rho_t\boldsymbol{\nabla}\cdot\boldsymbol{J}_t, \qquad \text{(spin-orbit term)}\end{aligned}$$

time-odd Skyrme EDF $\left(\boldsymbol{s}_t,\ \boldsymbol{T}_t,\ \boldsymbol{j}_t,\ \boldsymbol{F}_t\right)$

$$\begin{aligned}\mathcal{H}_t^{odd}(\boldsymbol{r}) &= C_t^{s}[\rho_0]\boldsymbol{s}_t^2 + C_t^{\Delta s}\boldsymbol{s}_t\cdot\Delta\boldsymbol{s}_t + C_t^{T}\boldsymbol{s}_t\cdot\boldsymbol{T}_t + C_t^{j}\boldsymbol{j}_t^2 \\ &+ C_t^{\nabla j}\boldsymbol{s}_t\cdot(\boldsymbol{\nabla}\times\boldsymbol{j}_t) \qquad \text{(spin-orbit term)} \\ &+ C_t^{\nabla s}(\boldsymbol{\nabla}\cdot\boldsymbol{s}_t)^2 + C_t^{F}\boldsymbol{s}_t\cdot\boldsymbol{F}_t, \qquad \text{(pure tensor terms)}\end{aligned}$$

The total energy in the Skyrme-HF/HFB model

$$\begin{aligned} E^{tot} &\equiv \langle \Phi_{HF} | \hat{H} | \Phi_{HF} \rangle \geqslant E_{g.s.} \\ &= \int \mathrm{d}^3\boldsymbol{r} \, \left[\mathcal{E}_{kin} + \mathcal{E}_{Sk} + \mathcal{E}_{Coul}^{dir} + \mathcal{E}_{Coul}^{ex} + \mathcal{E}_{pair} \right] + E_{corr}, \end{aligned}$$

$$\mathcal{E}_{kin} = \frac{\hbar^2}{2m} \tau_0(\boldsymbol{r}),$$

kinetic energy density

$$\mathcal{E}_{Coul}^{dir} = \tfrac{1}{2} e^2 \rho_p(\boldsymbol{r}) \int \mathrm{d}^3\boldsymbol{r}' \, \frac{\rho_p(\boldsymbol{r}')}{|\, \boldsymbol{r} - \boldsymbol{r}' \,|},$$

direct Coulomb en. density

$$\mathcal{E}_{Coul}^{ex} = -\tfrac{3}{4} e^2 \left(\tfrac{3}{\pi} \right)^{1/3} \rho_p^{4/3}(\boldsymbol{r})$$

exchange Coulomb en. density
(in the Slater approx.)

$$\mathcal{E}_{pair} = \sum_{q=p,n} \frac{V_q^0}{4} \left[1 - V^1 \left(\frac{\rho_0(\boldsymbol{r})}{\rho_{st}} \right)^{\beta} \right] \tilde{\rho}_q^2(\boldsymbol{r}),$$

Isovector pairing en. density

$V^1 = 0,\ 1,\ \text{or}\ 1/2$ for *volume-*, *surface-*, or *mix-*type pairing

$\rho_{st} = 0.16\,\mathrm{fm}^{-3}$, $\tilde{\rho}_q(\boldsymbol{r})$ - pairing density for protons and neutrons.

The equality-constrained prpblem (ECP)

$$\begin{cases} \min_{\bar{\rho}} E^{tot}[\bar{\boldsymbol{\rho}}] \\ \text{subject to:} \quad \sum_{q=p,n} \langle \Phi(\bar{\boldsymbol{\rho}}) | \hat{N}_q | \Phi(\bar{\boldsymbol{\rho}}) \rangle = N_q, \\ \qquad\qquad\qquad \sum_{\lambda\mu} \langle \Phi(\bar{\boldsymbol{\rho}}) | \hat{Q}_{\lambda\mu} | \Phi(\bar{\boldsymbol{\rho}}) \rangle = Q_{\lambda\mu}, \end{cases}$$

$$\begin{aligned} E^{tot}[\bar{\boldsymbol{\rho}}] &\equiv E^{tot}\left[\rho, \tau, \mathbb{J}; \boldsymbol{s}, \boldsymbol{T}, \boldsymbol{j}, \boldsymbol{F}; \tilde{\rho}\right] \\ &= \int \mathrm{d}^3\boldsymbol{r} \left(\mathcal{E}_{kin}(\boldsymbol{r}) + \mathcal{E}_{Sk}(\boldsymbol{r}) + \mathcal{E}^{dir}_{Coul}(\boldsymbol{r}) + \mathcal{E}^{ex}_{Coul}(\boldsymbol{r}) + \mathcal{E}_{pair}(\boldsymbol{r}) \right) + E_{corr} \end{aligned}$$

objective function

$$\langle \hat{Q}_{10} \rangle = \sqrt{\tfrac{4\pi}{3}} \sum_{i=1}^{A} \langle r_i Y_{10}(\theta_i, \phi_i) \rangle = \sum_{i=1}^{A} \langle z_i \rangle = 0$$

dipole moment condition
to avoid center of mass motion

$$\hat{Q}_{20} = \sqrt{\tfrac{16\pi}{5}} \sum_{i=1}^{A} r_i^2 Y_{20}(\theta_i, \phi_i) = \sum_{i=1}^{A} \left(2z_i^2 - x_i^2 - y_i^2\right)$$

quadrupole moment
stretching/squeezing

$$\hat{Q}_{30} = \sqrt{\tfrac{4\pi}{7}} \sum_{i=1}^{A} r_i^3 Y_{30}(\theta_i, \phi_i) = \sum_{i=1}^{A} \left[z_i^3 - \tfrac{3}{2} z_i \left(x_i^2 + y_i^2\right)\right]$$

octupole moment
mass-asymmetry

$$\hat{Q}_{40} = \sqrt{\tfrac{4\pi}{9}} \sum_{i=1}^{A} r_i^4 Y_{40}(\theta_i, \phi_i)$$

hexadecapole moment
necking

The augmented Lagrangian functional associated with ECP

$$E_c'[\bar{\boldsymbol{\rho}}, \boldsymbol{\lambda}, \boldsymbol{\Lambda}] = E^{tot}[\bar{\boldsymbol{\rho}}] - \sum_{q=p,n} \lambda_q \langle \Psi(\bar{\boldsymbol{\rho}}) | \hat{N}_q | \Psi(\bar{\boldsymbol{\rho}}) \rangle$$
$$+ \sum_{\lambda\mu} C_{\lambda\mu} \Big(\langle \Psi(\bar{\boldsymbol{\rho}}) | \hat{Q}_{\lambda\mu} | \Psi(\bar{\boldsymbol{\rho}}) \rangle - Q_{\lambda\mu} \Big)^2$$
$$\left[+ \sum_{\lambda\mu} \Lambda_{\lambda\mu} \Big(\langle \Psi(\bar{\boldsymbol{\rho}}) | \hat{Q}_{\lambda\mu} | \Psi(\bar{\boldsymbol{\rho}}) \rangle - Q_{\lambda\mu} \Big) \right]$$

quadratic penalty function (QPM)

linear penalty function (LCM)

$\lambda_p, \lambda_n, \Lambda_{\lambda\mu}$ *Lagrange multipliers*, $C_{\lambda\mu} > 0$ *penalty parameters*

<u>The augmented Lagrange method (ALM):</u>

$$\Lambda_{\lambda\mu}^{k+1} = \Lambda_{\lambda\mu}^{k} + 2C_{\lambda\mu}^{k} \Big(\langle \Psi(\bar{\boldsymbol{\rho}}^k) | \hat{Q}_{\lambda\mu} | \Psi(\bar{\boldsymbol{\rho}}^k) \rangle - Q_{\lambda\mu} \Big)$$

The first-order (necessary) variational condition

$$\frac{\delta}{\delta \bar{\boldsymbol{\rho}}} E_c'[\bar{\boldsymbol{\rho}}^*, \boldsymbol{\lambda}^*, \boldsymbol{\Lambda}^*] = 0 \quad \Rightarrow \quad E^{tot}[\bar{\boldsymbol{\rho}}^*] = E_{HF}^{tot}$$

and $\sum_{q=p,n} \langle \Psi(\bar{\boldsymbol{\rho}}^*) | \hat{N}_q | \Psi(\bar{\boldsymbol{\rho}}^*) \rangle = N_q\,, \;\; \sum_{\lambda\mu} \langle \Psi(\bar{\boldsymbol{\rho}}^*) | \hat{Q}_{\lambda\mu} | \Psi(\bar{\boldsymbol{\rho}}^*) \rangle = Q_{\lambda\mu}$

Eur. Phys. J. A **46**, 85 (2010)

The augmented Lagrangian method (ALM)

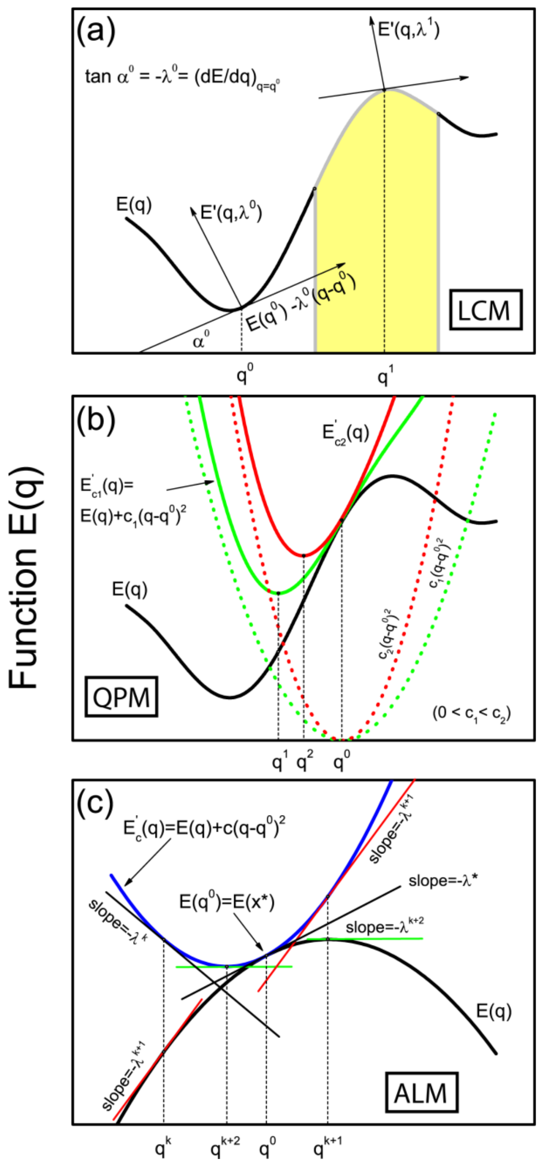

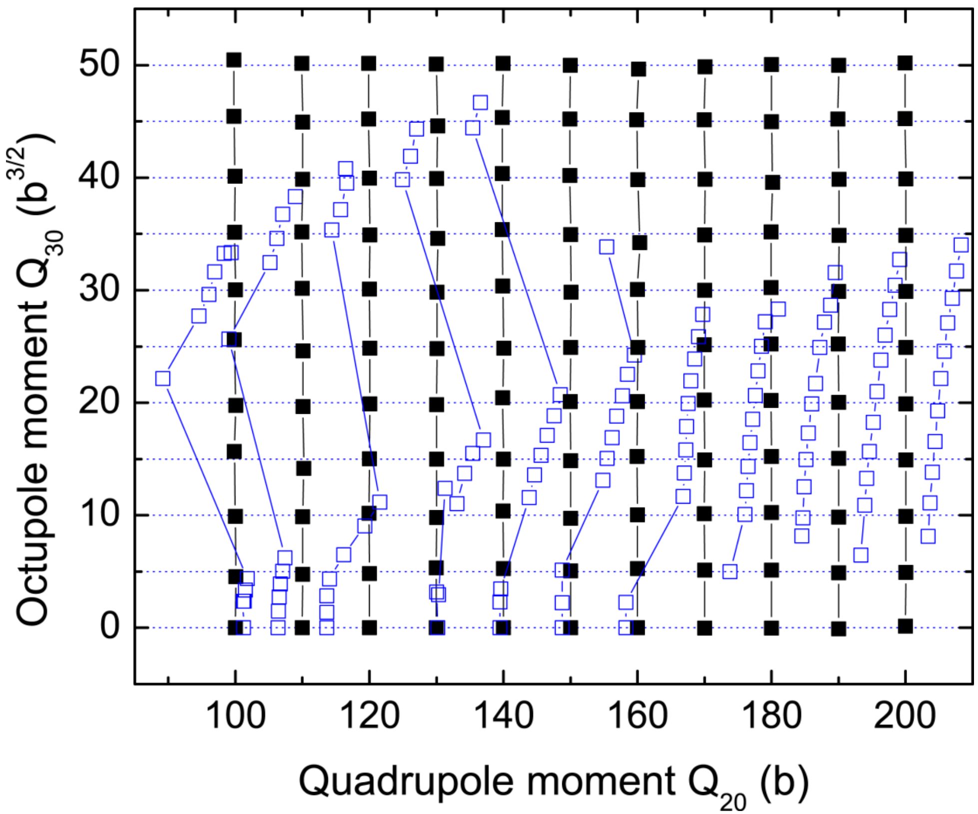

QPM vs. ALM

Eur. Phys. J. A **46**, 85 (2010)

HFODD: the self-consistent symmetries

- time-reversal $\hat{T}$
- parity $\hat{P}$
- x-, y-, z-signature $\hat{R}_{x,y,z} = \exp(-i\pi \hat{J}_{x,y,z})$
- x-, y-, z-simplex $\hat{S}_{x,y,z} = \hat{P}\hat{R}_{x,y,z}$
- x-, y-, z-simplex*T $\hat{S}^T_{x,y,z} = \hat{T}\hat{S}_{x,y,z}$

$\hat{T}$	$\hat{S}_y$	$\hat{S}^T_y$
$\hat{P}$	$\hat{S}_y$	$\hat{R}_y$
$\hat{R}_y$	$\hat{S}^T_x$	$\hat{S}^T_z$
1	1	1
1	0	0
0	1	0
0	0	1
0	0	0

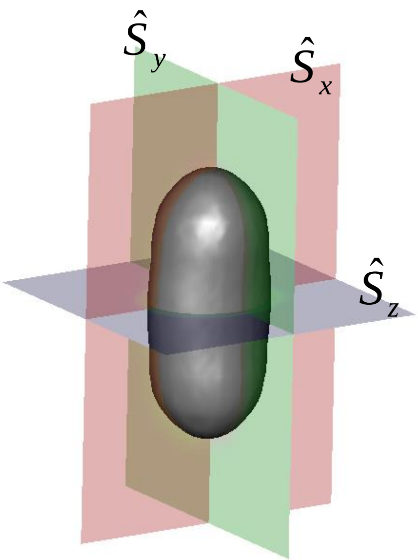

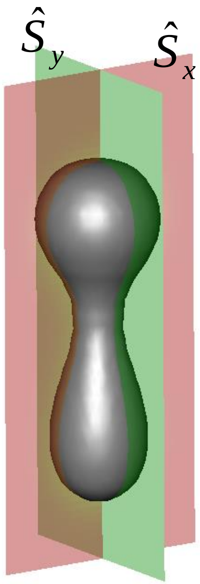

$$\hat{S}_y = 1 \Rightarrow Q_{\lambda\mu} = \langle \hat{Q}_{\lambda\mu} \rangle \in \mathbb{R}$$

$$Q_{\lambda-odd,\mu} \neq 0 \;\; only \;\; for \;\; \hat{P} = 0$$

HFODD: all allowed symmetries (for T=1)

$\hat{T}$(ITIREV)						**1**							
$\hat{P}$(ISIQTY)			1						0				
$\hat{S}_y$(ISIMPY)	1			0			1				0		
$\hat{S}_y^T$(JSIMTY)	1			0			1				0		
$\hat{R}_y$(ISIGNY)	1			0			0		1			0	
$\hat{S}_x^T$(ISIMTX)	1	0	1	0	0	1	0	0	1	0	1	0	0
$\hat{S}_z^T$(ISIMTZ)	1	0	0	1	0	0	1	0	1	0	0	1	0
No.	1	2	3	4	5	6	7	8	9	10	11	12	13

symmetric fission

asymmetric fission

HFODD: all allowed symmetries (for *T*=0)

$\hat{T}$(ITIREV)									**0**												
$\hat{P}$(ISIQTY)				1										0							
$\hat{S}_y$(ISIMPY)	1			0			0			1				0					0		
$\hat{S}^T_y$(JSIMTY)	0			1			0			0				1					0		
$\hat{R}_y$(ISIGNY)	1			0			0			0		1			0		1			0	
$\hat{S}^T_x$(ISIMTX)	1	0	1	0	0	1	0	0	1	0	0	1	0	1	0	0	1	0	1	0	0
$\hat{S}^T_z$(ISIMTZ)	1	0	0	1	0	0	1	0	0	1	0	1	0	0	1	0	1	0	0	1	0
No.	1	2	3	4	5	6	7	8	9	10	11	12	13	14	15	16	17	18	19	20	21

Model

The symmetry unrestricted code HFODD [1] and an augmented Lagrangian method [2] were used to solve constrained HFB equations with SkM* Skyrme force [3] in the p-h channel and a density dependent mixed pairing [4, 5] interaction in the p-p channel.

The stretched harmonic oscillator basis of HFODD was composed of states having not more than N_0 = 26 quanta in either of the Cartesian directions, and not more than 1140 states in total.
The collective mass tensor of the fissioning superfluid nucleus was computed by means of the perturbative cranking approximation to the adiabatic time-dependent Hartree-Fock-Bogoliubov approach [6].

	SkM*	SLy4	Units/Comments
t_0	-2645.0	-2488.913	MeV fm^3
t_1	410.0	486.818	MeV fm^5
t_2	-135.0	-546.395	MeV fm^5
t_3	15595.0	13777.0	MeV fm$^{3+\alpha}$
x_0	0.09	0.834	-
x_1	0.0	-0.344	-
x_2	0.0	-1.000	-
x_3	0.0	1.354	-
$1/\alpha$	6.0	6.0	-
W_0	120.0	123.0	MeV fm^5
C_t^J	0.0	0.0	(spin-orbit tensor term, $\mathbb{J}^2$)
ρ_{st}	0.16	0.16	fm^{-3}
β	1.0	1.0	-
E_{cut}	60	-	MeV (HFB)
E_{cut}	-	N or Z	(no. of s.p. states, BCS)
V^1	0.5	1	(0.5-mixed, 1-surface pairing)
V_n^0	-268.9	-842.0	MeV fm^3
V_p^0	-332.5	-1020.0	MeV fm^3

[1] N. Schunck *et al.*, **183**, 166 (2012).
[2] A. Staszczak, M. Stoitsov, A. Baran, and W. Nazarewicz, Eur. J. Phys. A **46**, 85 (2010).
[3] J. Bartel *et al.*, Nucl. Phys. A **386**, 79 (1982).
[4] J. Dobaczewski, W. Nazarewicz, and M. V. Stoitsov, Eur. J. Phys. A **15**, 21 (2002).
[5] A. Staszczak, A. Baran, J. Dobaczewski, and W. Nazarewicz, Phys. Rev. C **80**, 014309 (2009).
[6] A. Baran, J. A. Sheikh, J. Dobaczewski, W. Nazarewicz, and A. Staszczak, Phys. Rev. C **84**, 054321 (2011).

Model

The Skyrme EDF in the case of even-even nuclei (time-reversal symmetry)

$$\mathcal{E}_{Sk}^{even}(\boldsymbol{r}) = \sum_{t=0,1}\left(C_t^{\rho}[\rho_0]\rho_t^2 + C_t^{\Delta\rho}\rho_t\Delta\rho_t + C_t^{\tau}\rho_t\tau_t + \cancel{C_t^{J}\mathbb{J}_t^2}\right) \quad \text{(central terms)}$$

$$+ \sum_{t=0,1}\left(C_t^{\nabla J}\rho_t\boldsymbol{\nabla}\cdot\boldsymbol{J}_t\right), \quad \text{(spin-orbit term)}$$

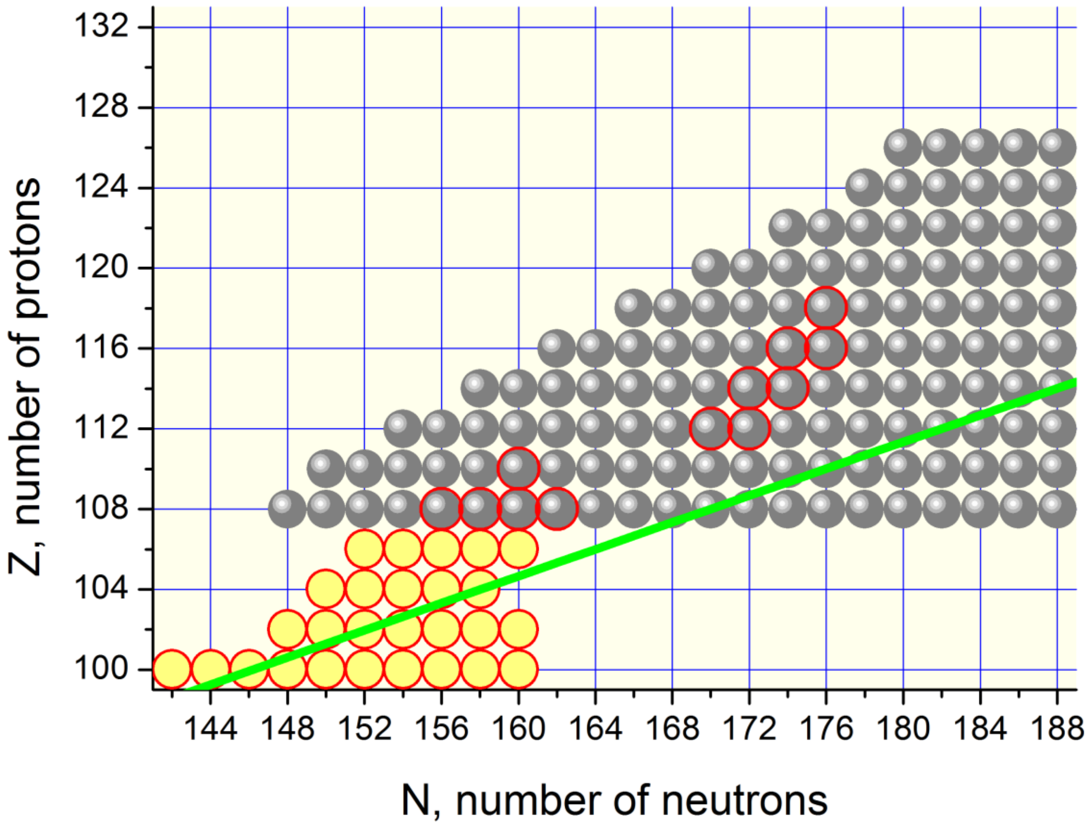

130 e-e nuclei
$108 \leq Z \leq 126$
$148 \leq N \leq 188$

Ground state pairing properties of e-e SHN

$\Delta_n \approx 0$ MeV for N = 184

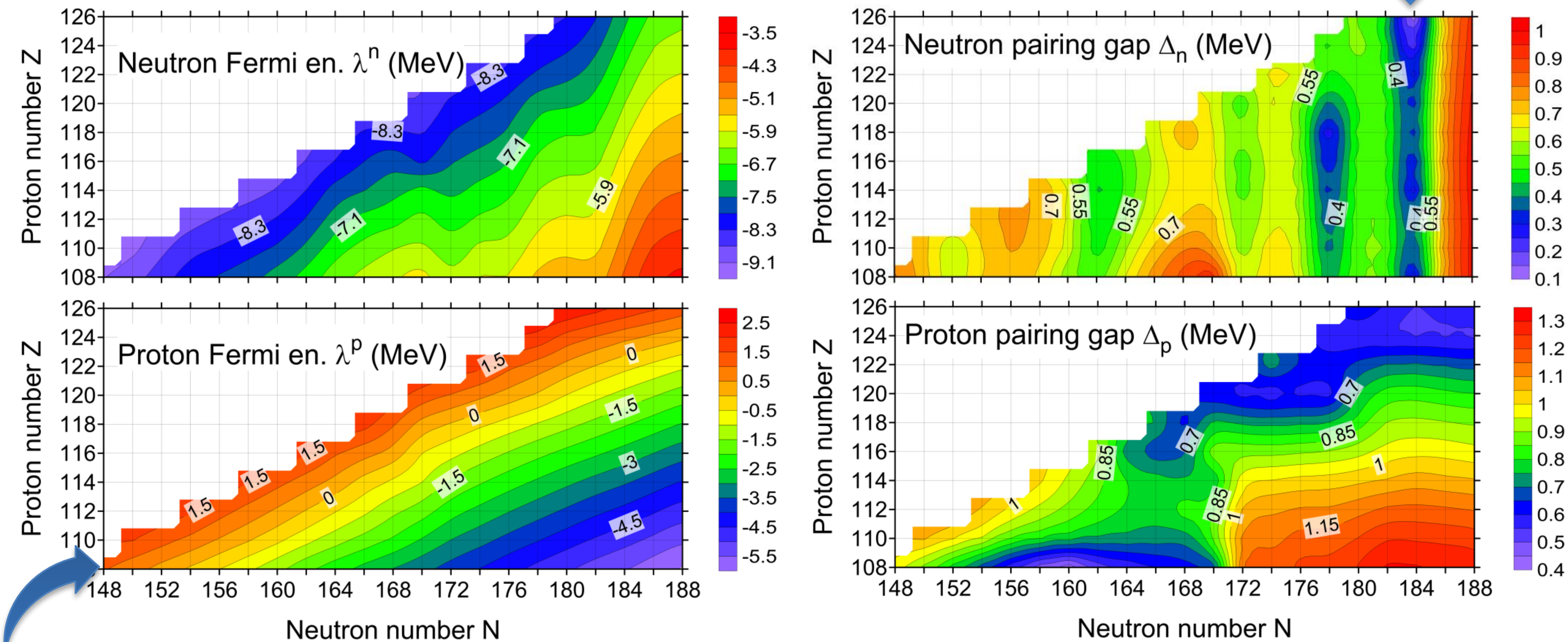

<u>Proton *drip line*</u>:
Fermi energy $\lambda^p \leq 2$ MeV.

Geometric sizes

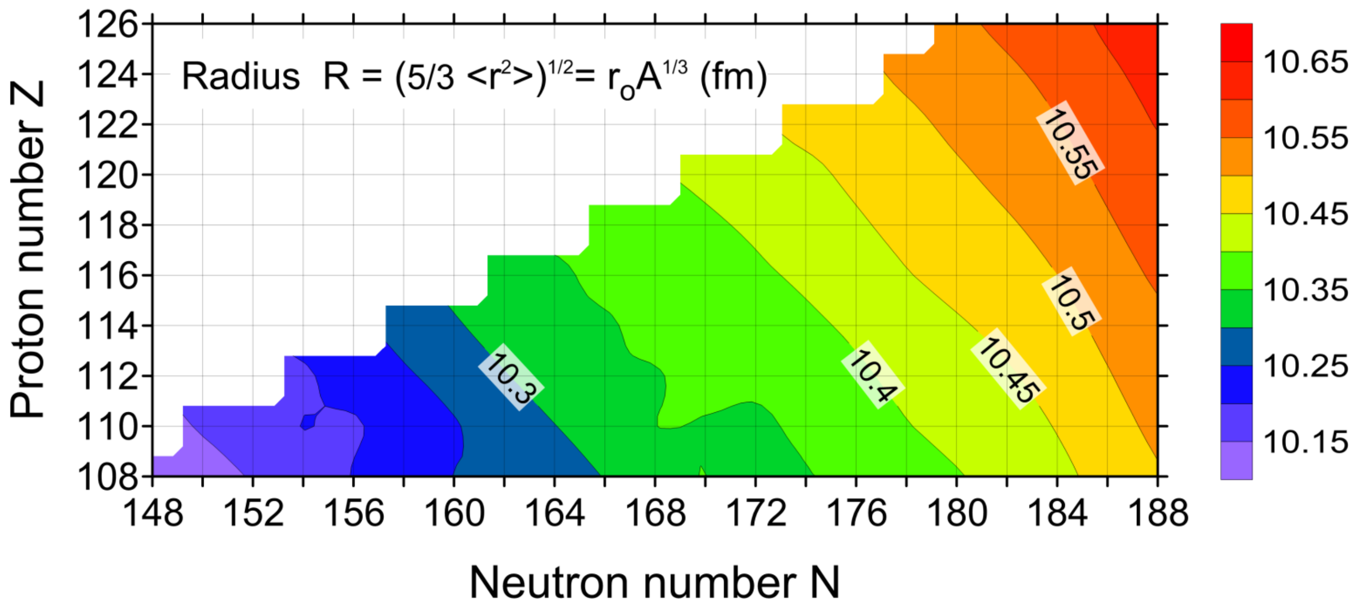

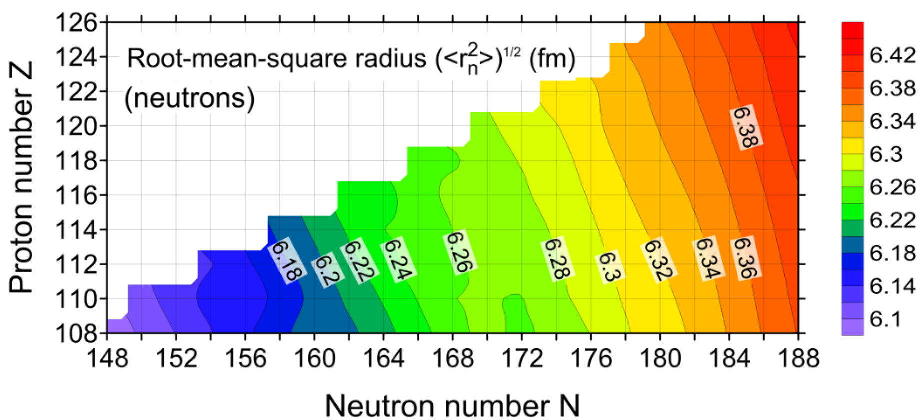

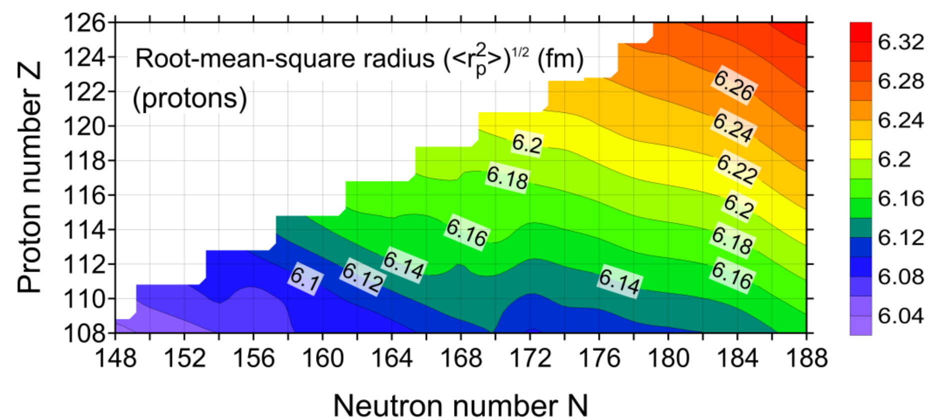

Groud state deformations

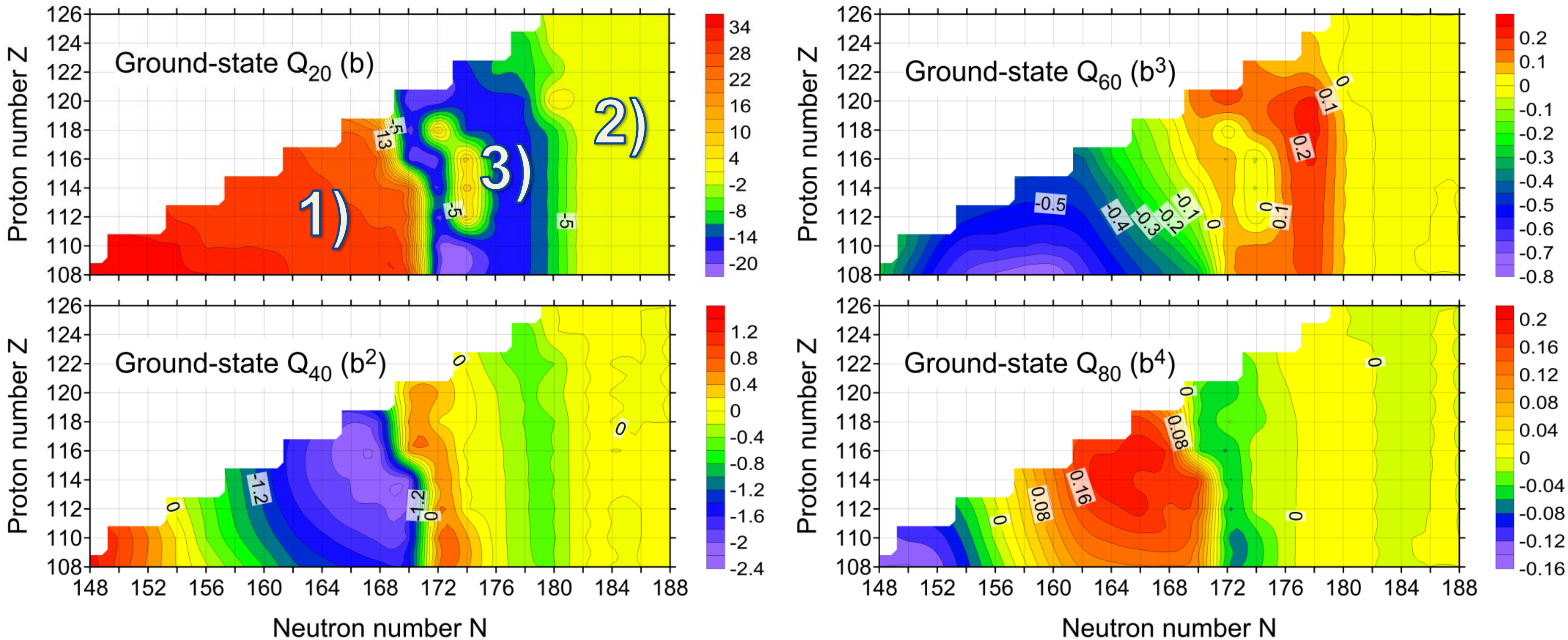

<u>The e-e SHN form three regions:</u>

1) a prolate-deformed (for N < 172),
2) spherical (N>180),
3) the transitional region (between the former two).

Shape phase transitions and critical-point phenomena in atomic nuclei
R.F. Casten, Nature Physics **2**, 811 - 820 (2006)

Geometric collective model (GCM) - A. Bohr (1952)

$$V(\beta,\gamma) = A\beta^2 + B\beta^3 \cos 3\gamma + C\beta^4, \quad (C>0)$$

$A = A_1 = 0$: *spinodal* point

$A = A_c = B^2/(4C)$: *critical* point

$A = A_2 = 9B^2/(32C)$: *antispinodal* point

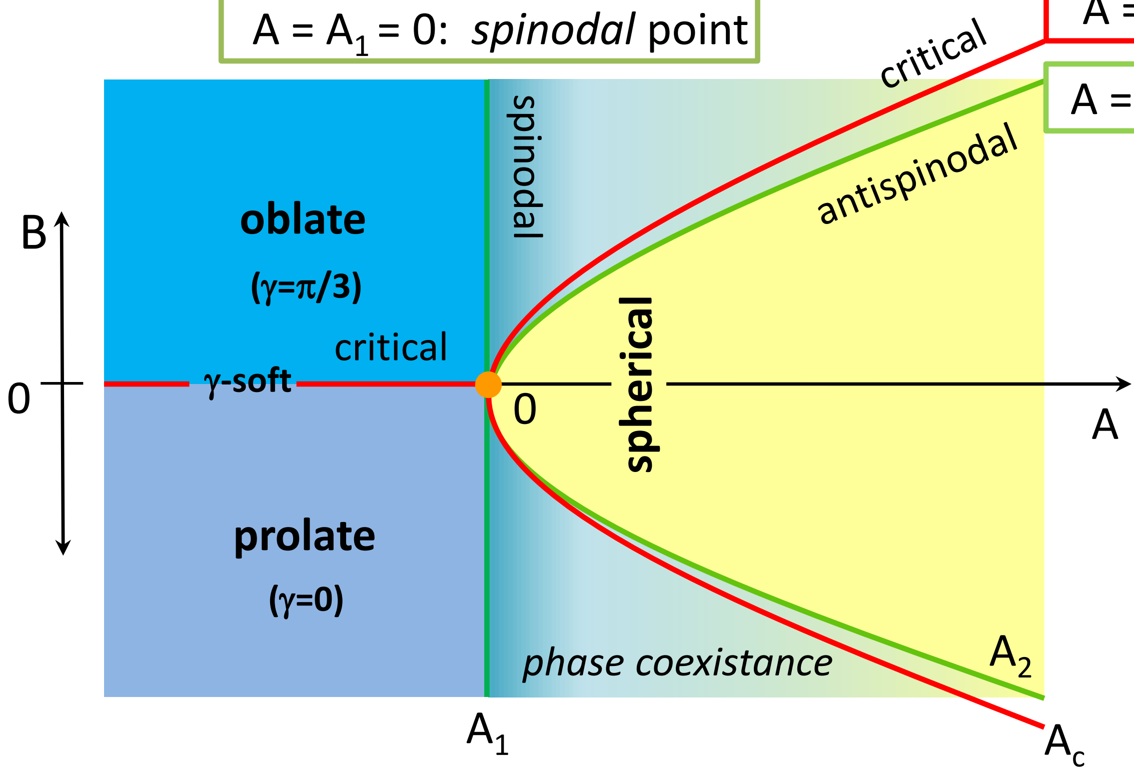

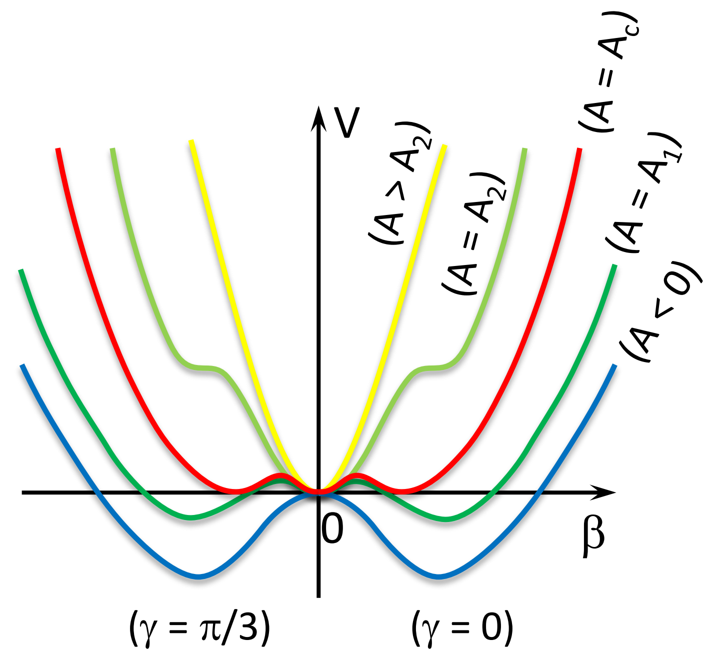

$A = A_c$ ($B \neq 0$) and $A < 0$ ($B = 0$): *first-order* phase transition lines

$A = B = 0$: *second-order* phase transition point (*triple-point*)

Interacting boson approximation (IBA-1) – Arima, Iachello

$$U(6) \supset U(5) \supset O(5) \supset O(3)$$
$$U(6) \supset SU(3) \supset O(3)$$
$$U(6) \supset O(6) \supset O(5) \supset O(3)$$

$$U(6) \supset \overline{SU(3)} \supset O(3)$$
$$U(6) \supset \overline{O(6)} \supset O(5) \supset O(3)$$

Dynamical symmetries:

$U(5)$ (vibrational)

$SU(3), \overline{SU(3)}$ (rotational)

$O(6), \overline{O(6)}$ (γ-soft)

Critical-point solutions:

$$V(\beta,\gamma) = A\beta^2 + B\beta^3\cos 3\gamma + C\beta^4$$
$$V(\beta,\gamma) \approx V_1(\beta) + V_2(\gamma)$$

$X(5)$: $V_1 = V_{well}(\beta)$, $V_2 = c(\gamma-\gamma_o)^2, (c>0)$

$E(5)$: $V_1 = V_{well}(\beta)$, $V_2 \equiv 0$

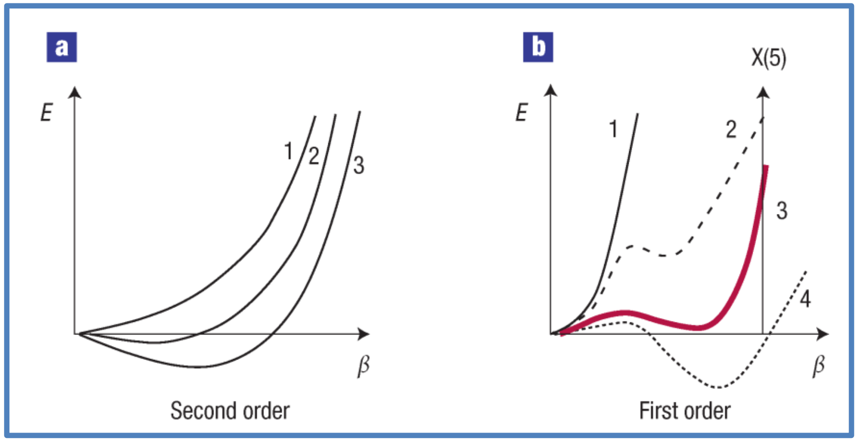

F. Iachello, PRL **85**, 3580 (2000); **87**, 052502 (2001).

(Fig. Casten)

Extended triangle of IBA-1 – R. Casten

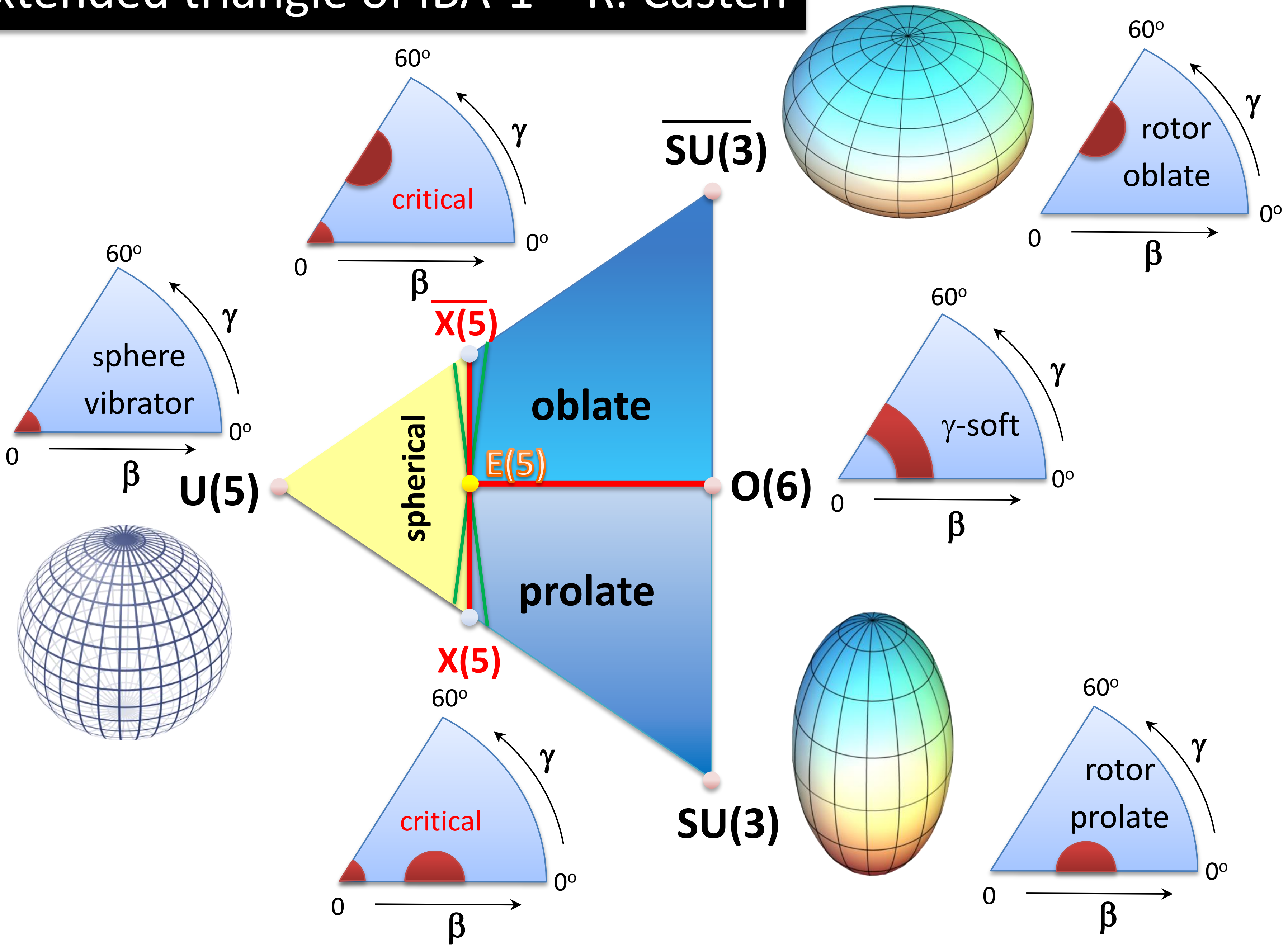

Nuclear shape phase transitions

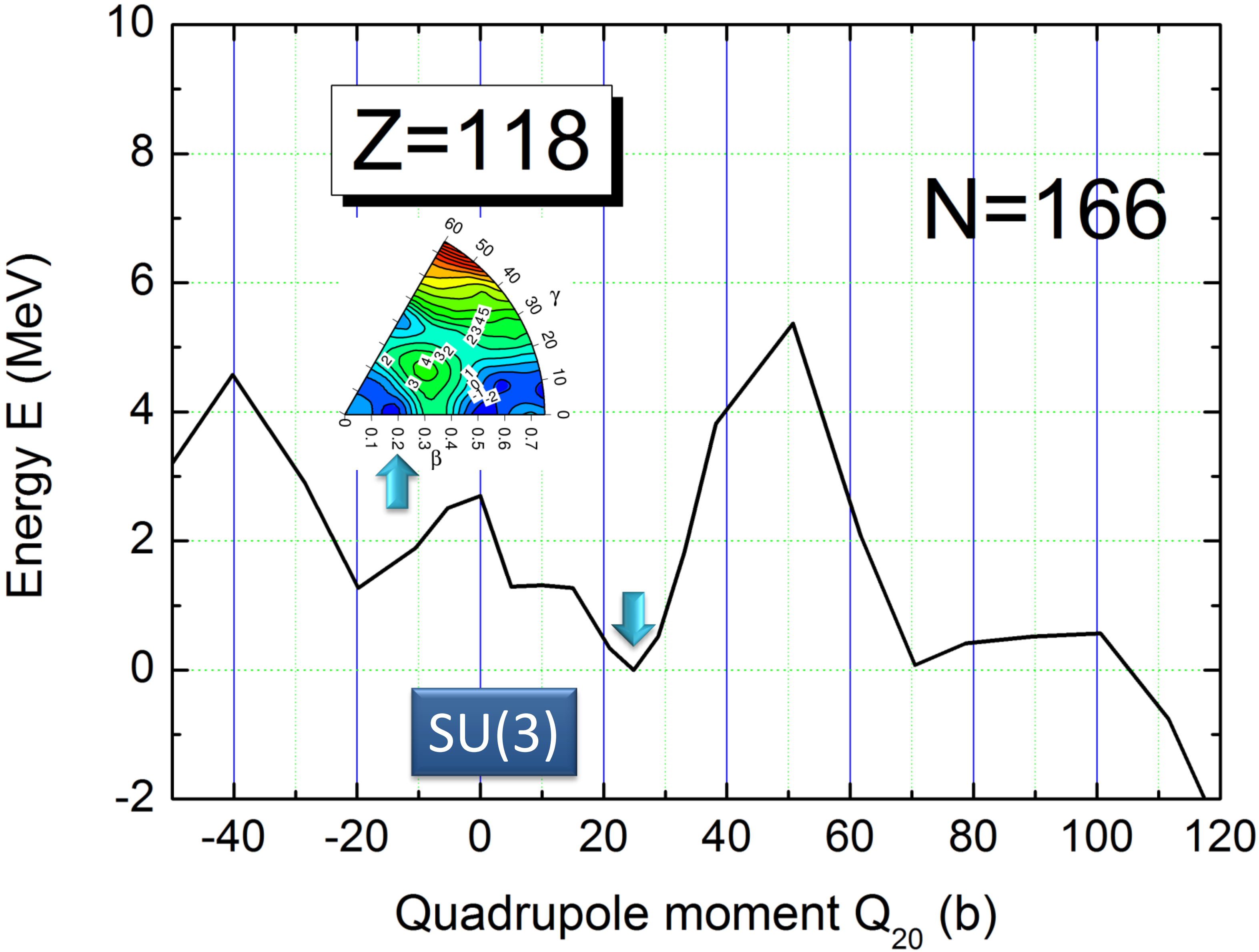

Second order phase transition O(6) – U(5)

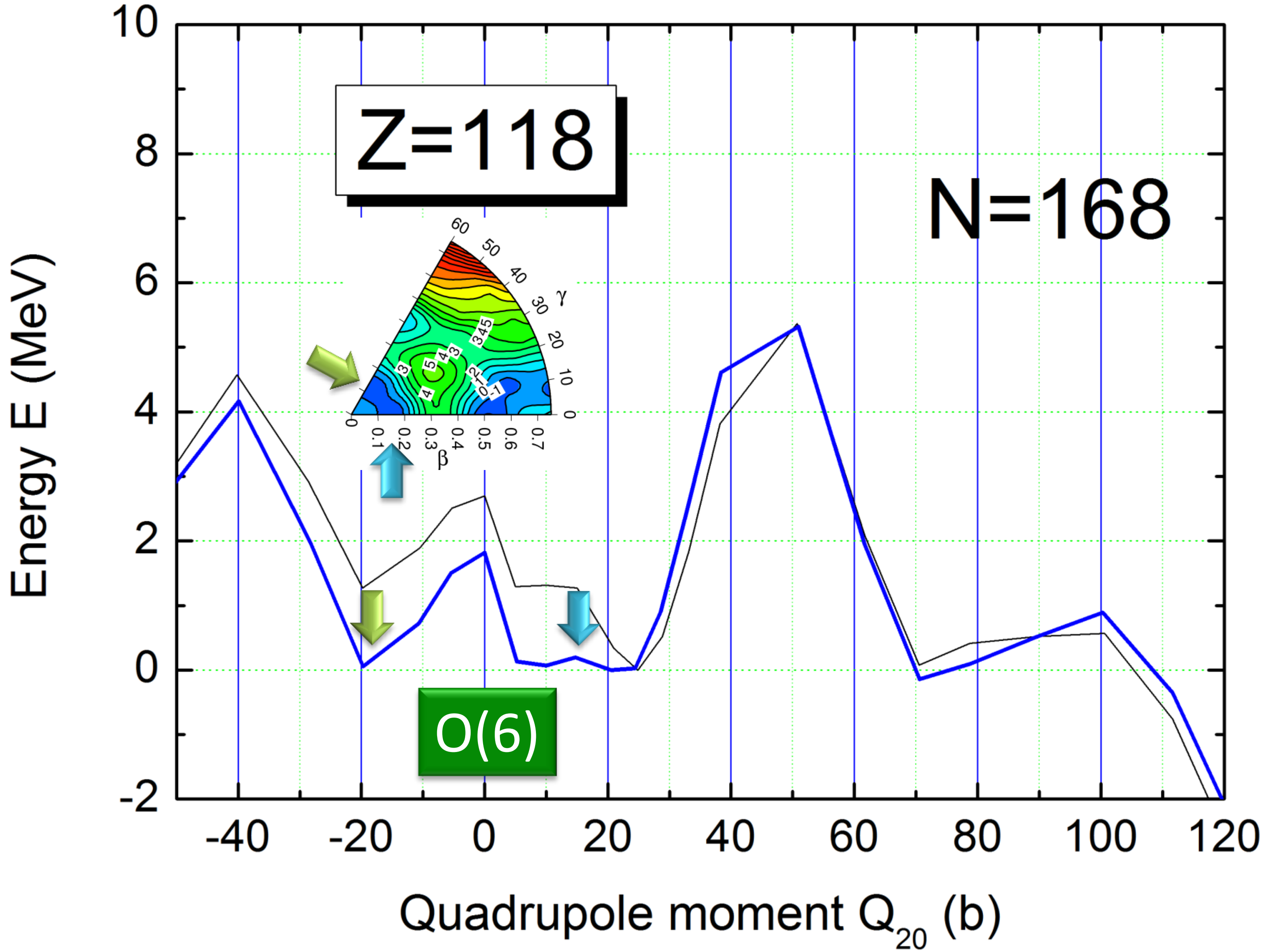

Second order phase transition O(6) – U(5)

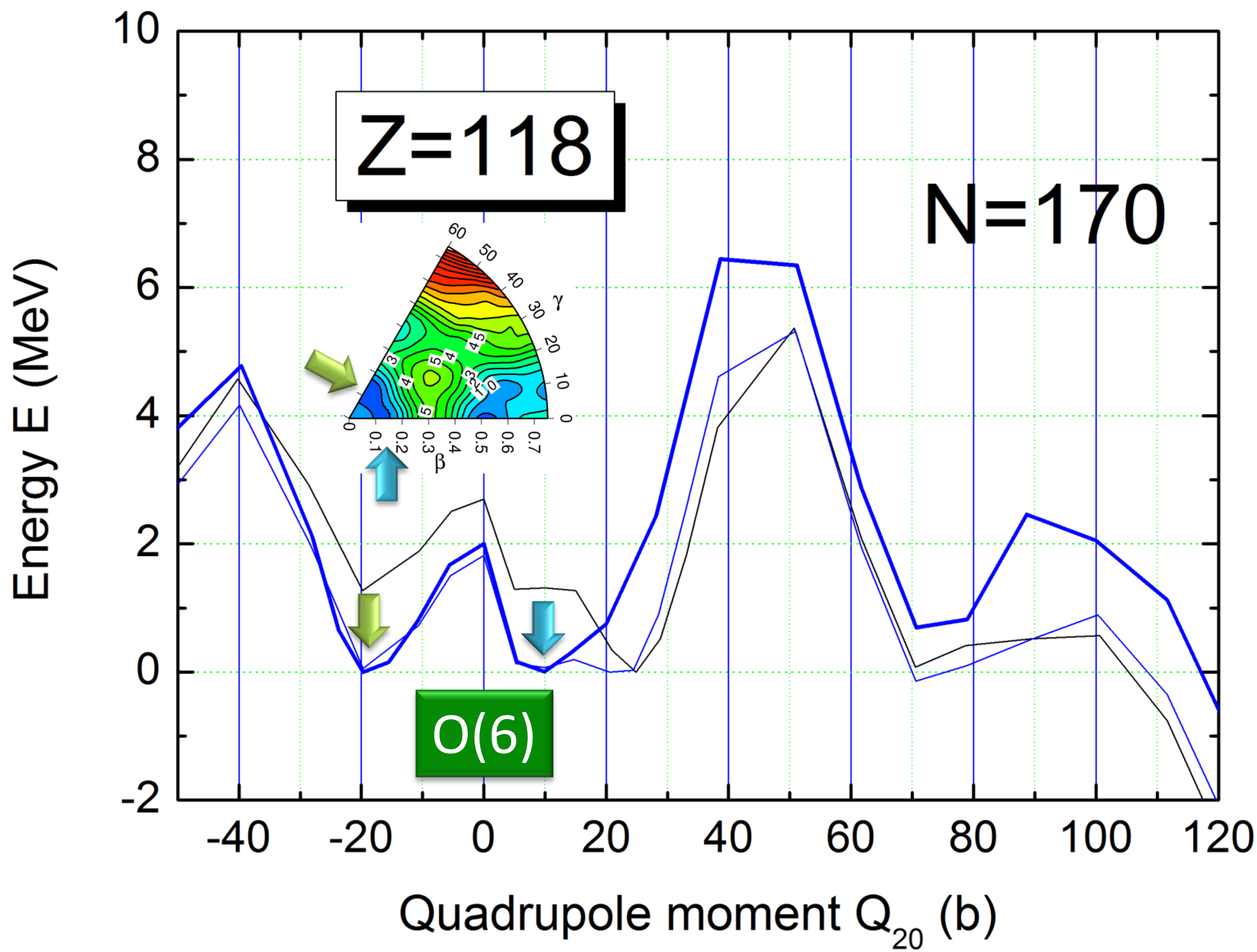

Second order phase transition O(6) – U(5)

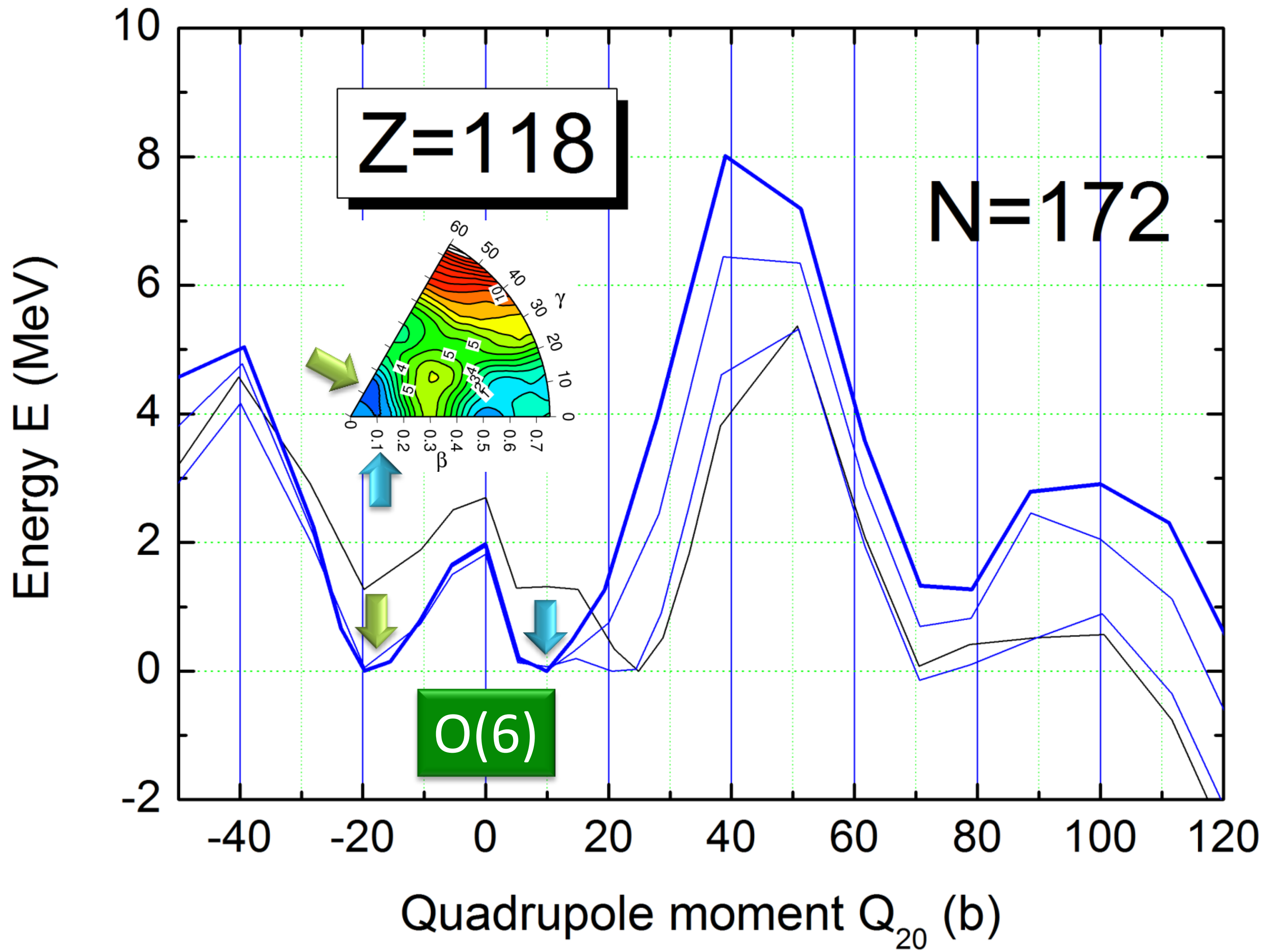

Second order phase transition O(6) – U(5)

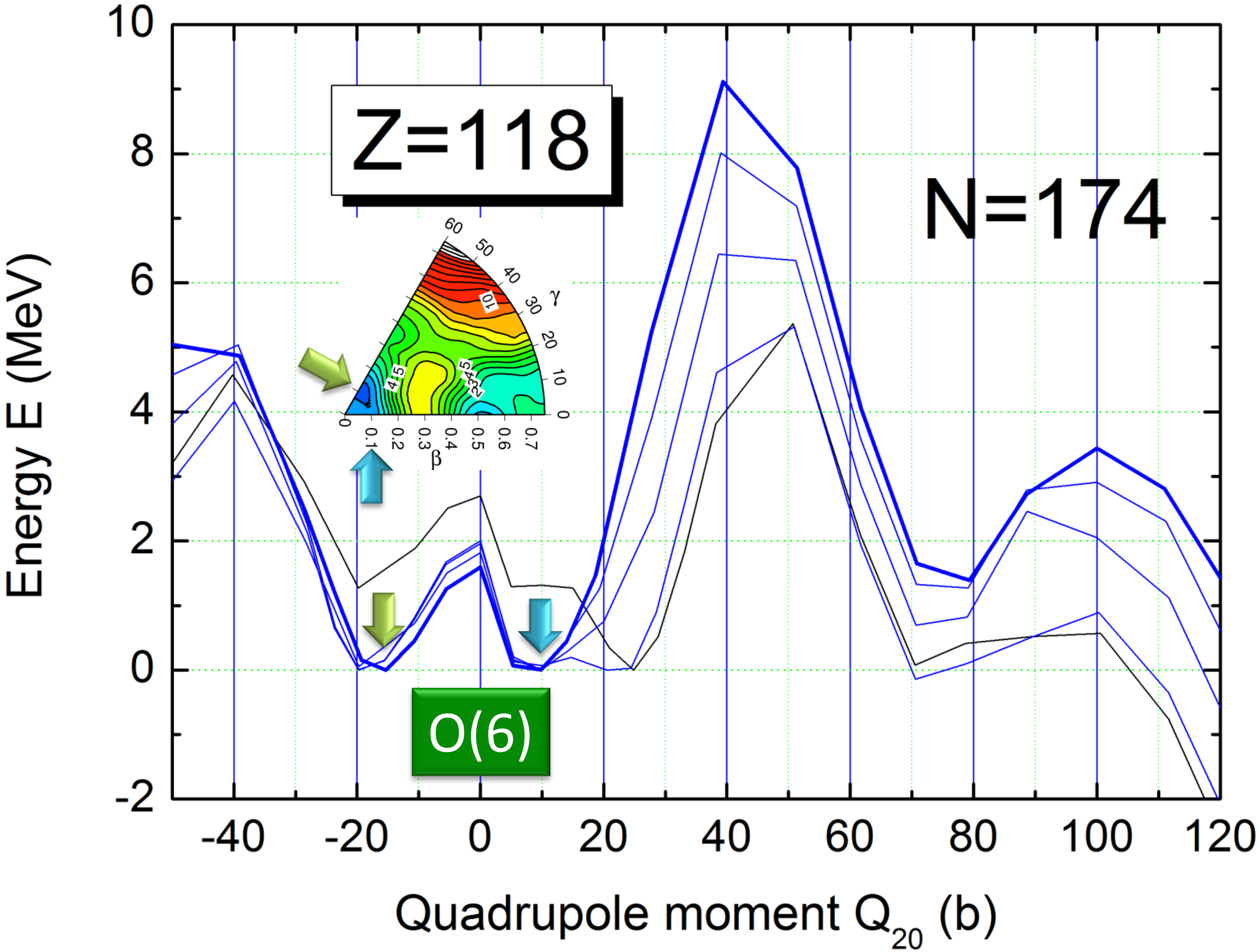

Second order phase transition O(6) – U(5)

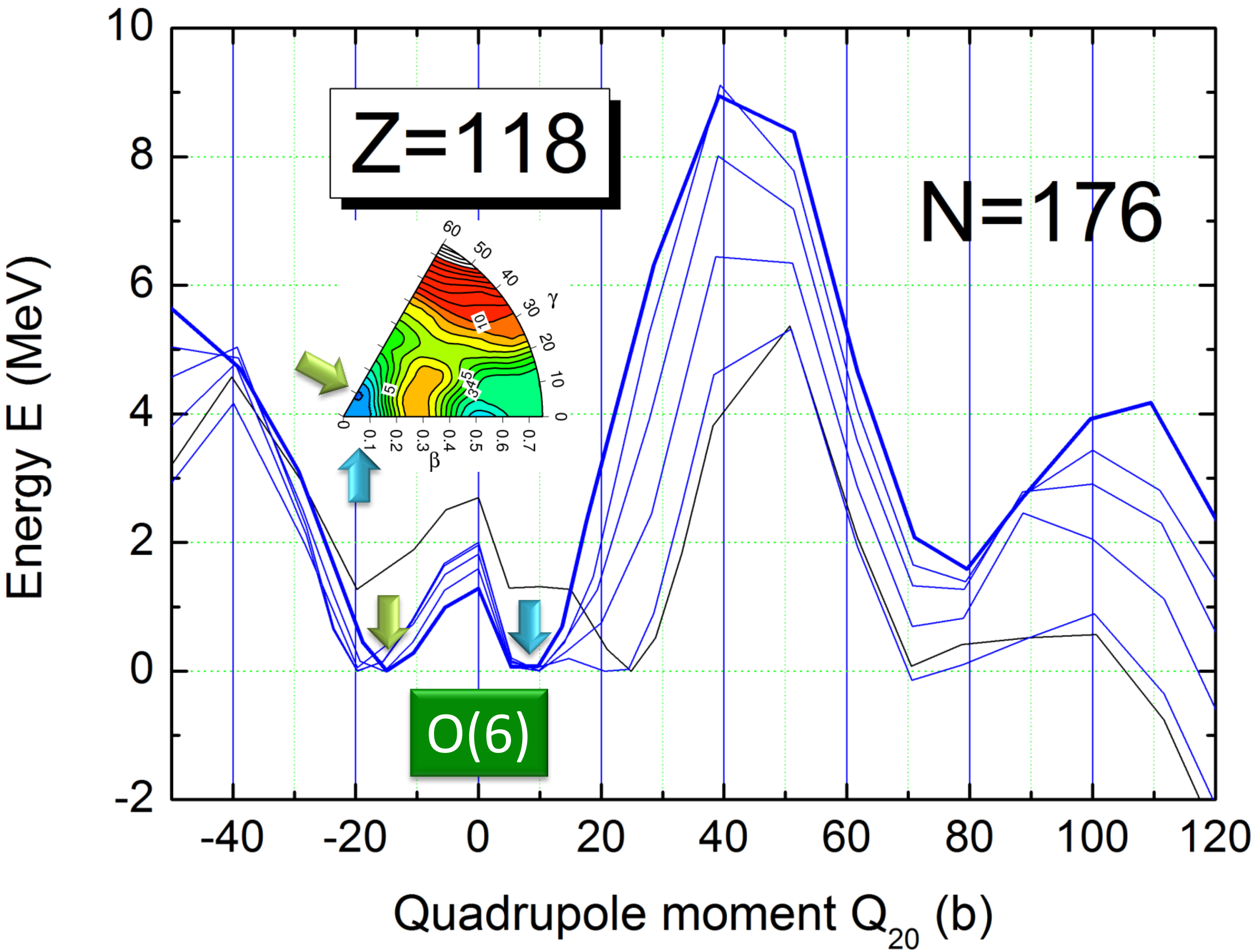

Second order phase transition O(6) – U(5)

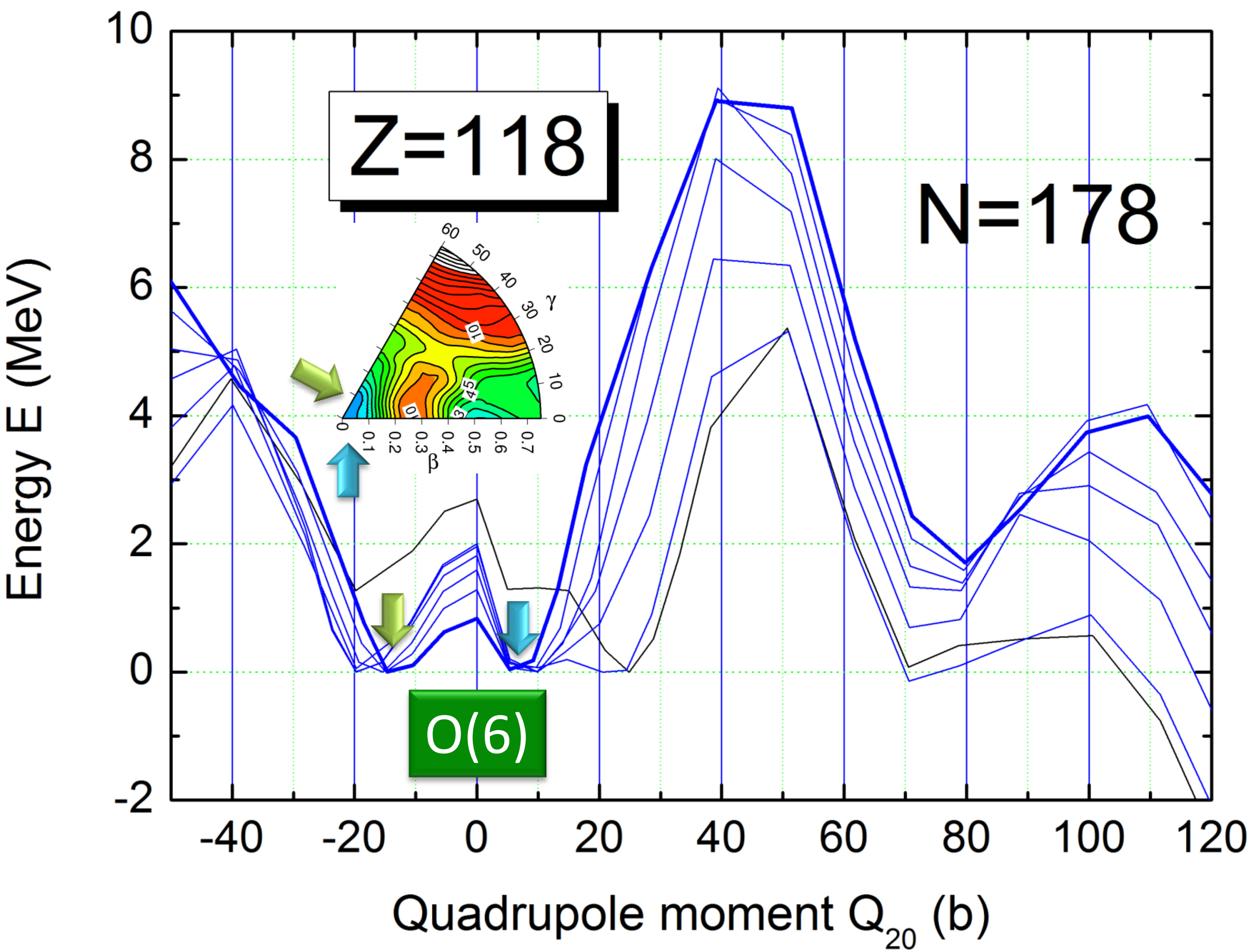

Critical (triple) point E(5)

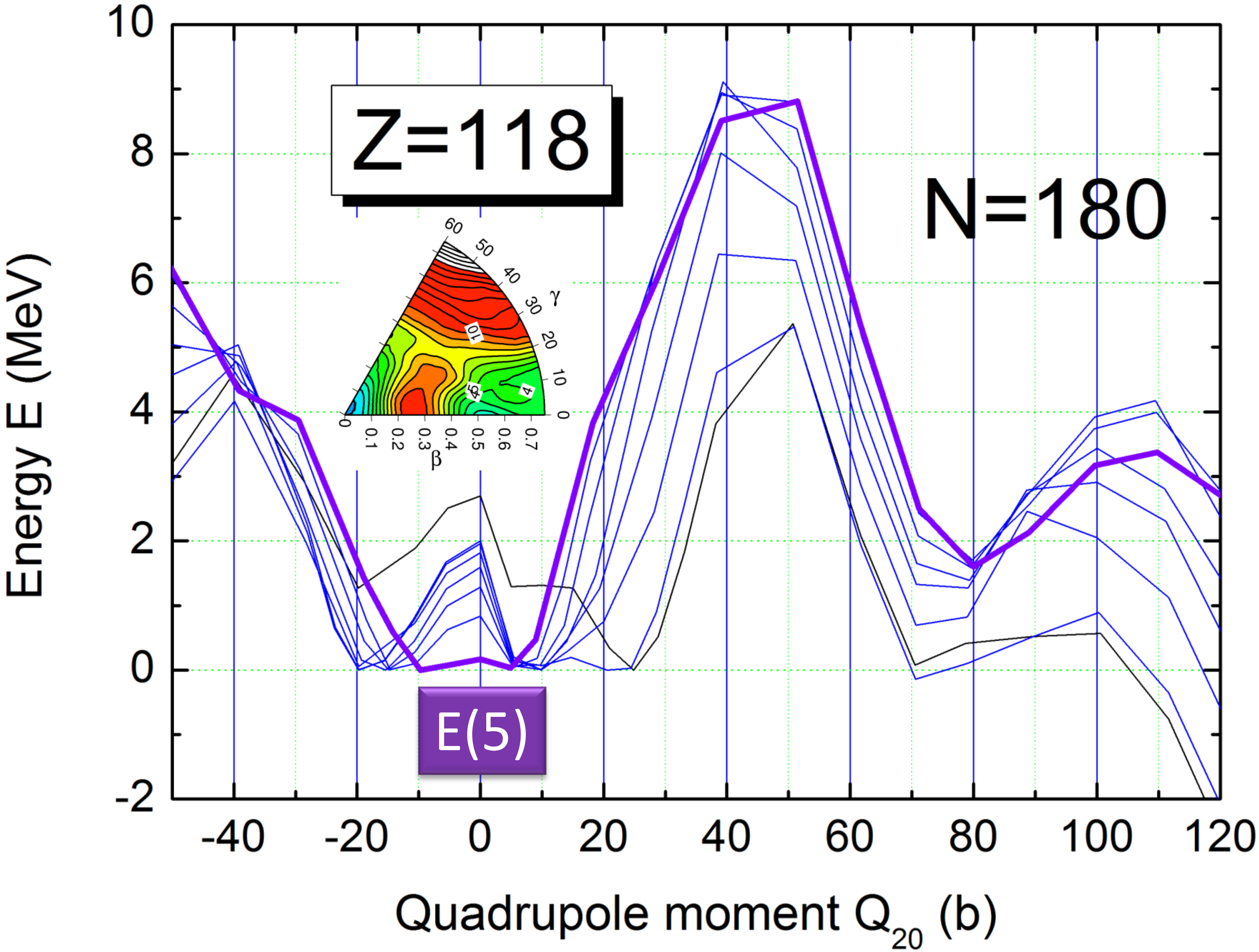

Second order phase transition O(6) – U(5)

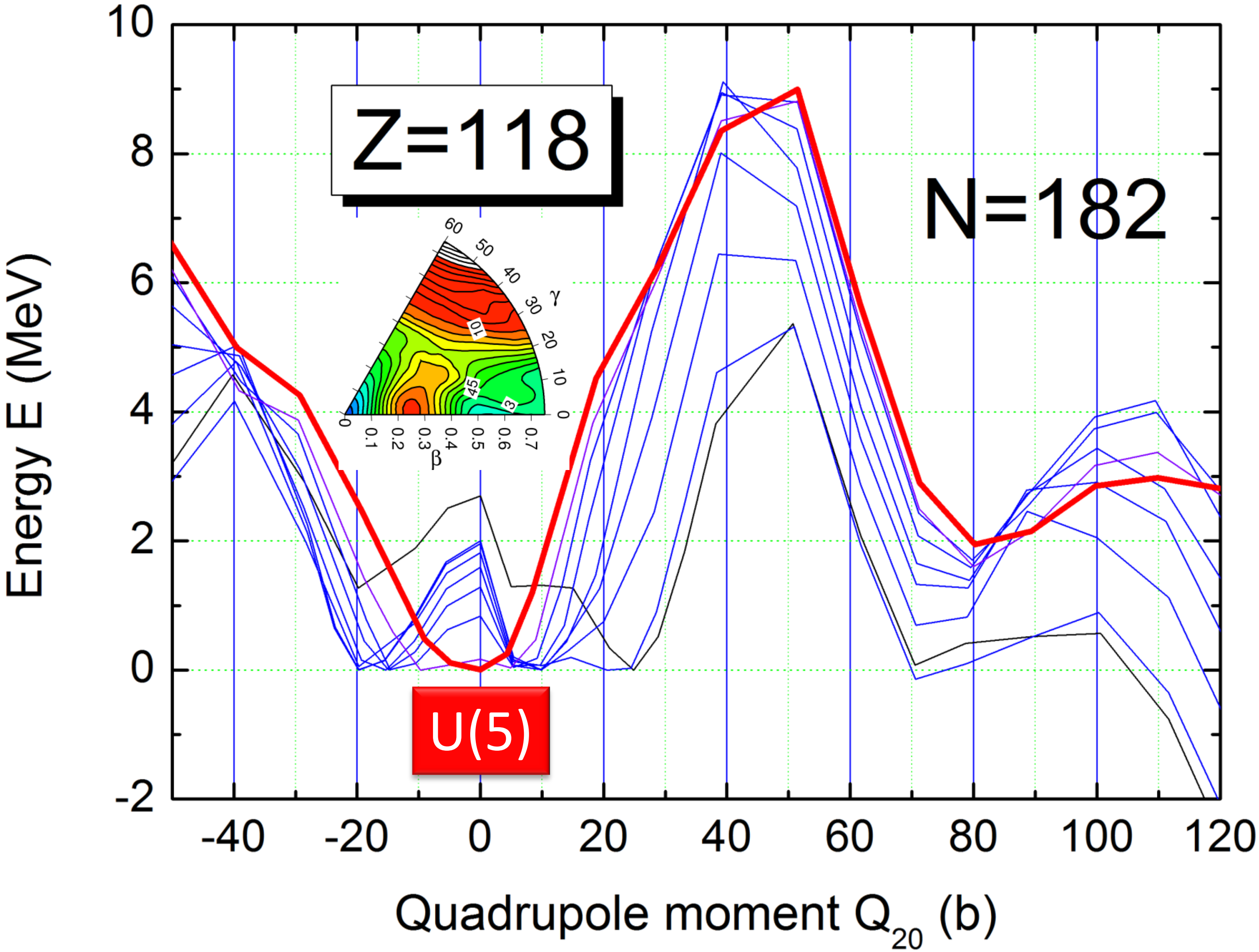

Second order phase transition O(6) – U(5)

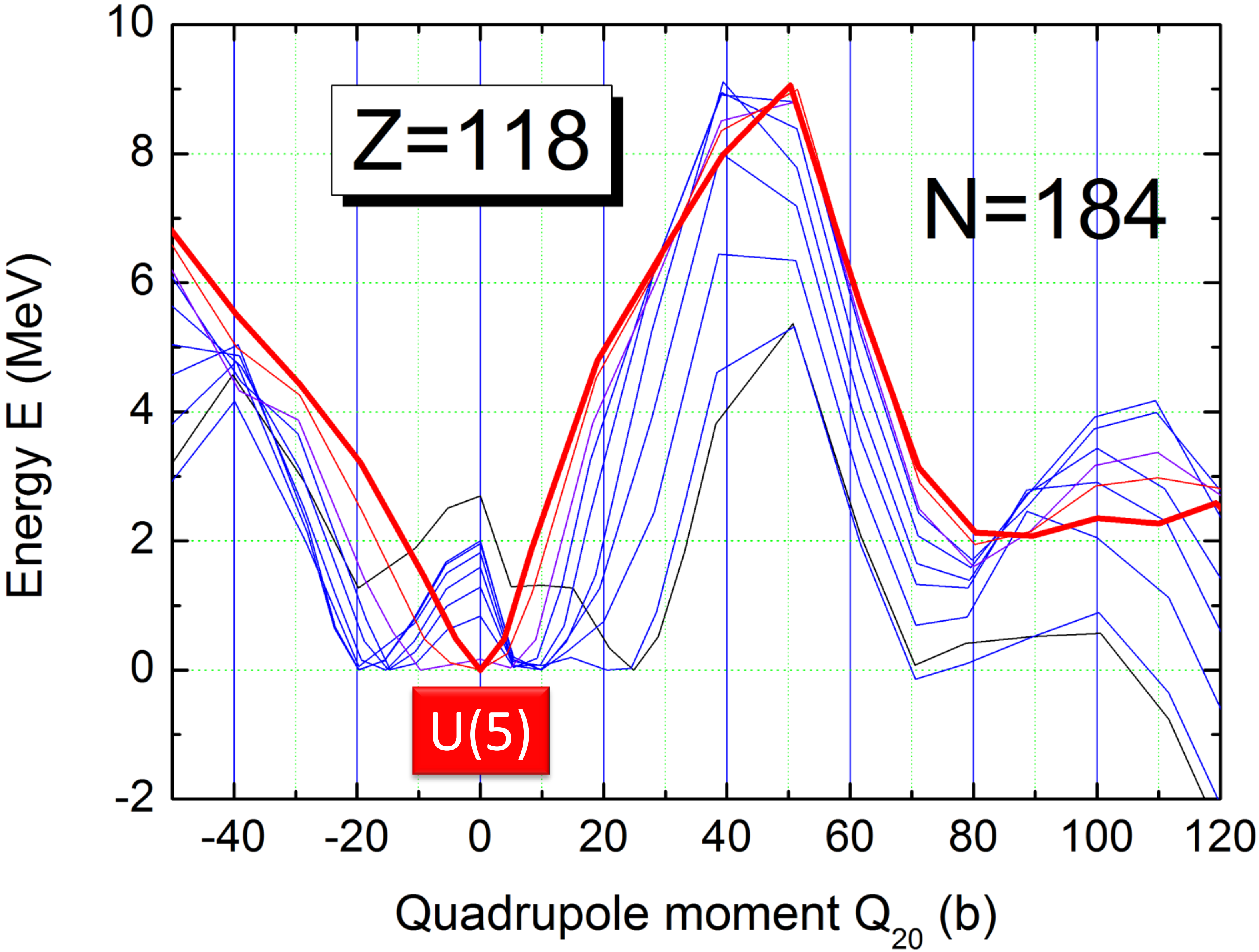

Second order phase transition O(6) – U(5)

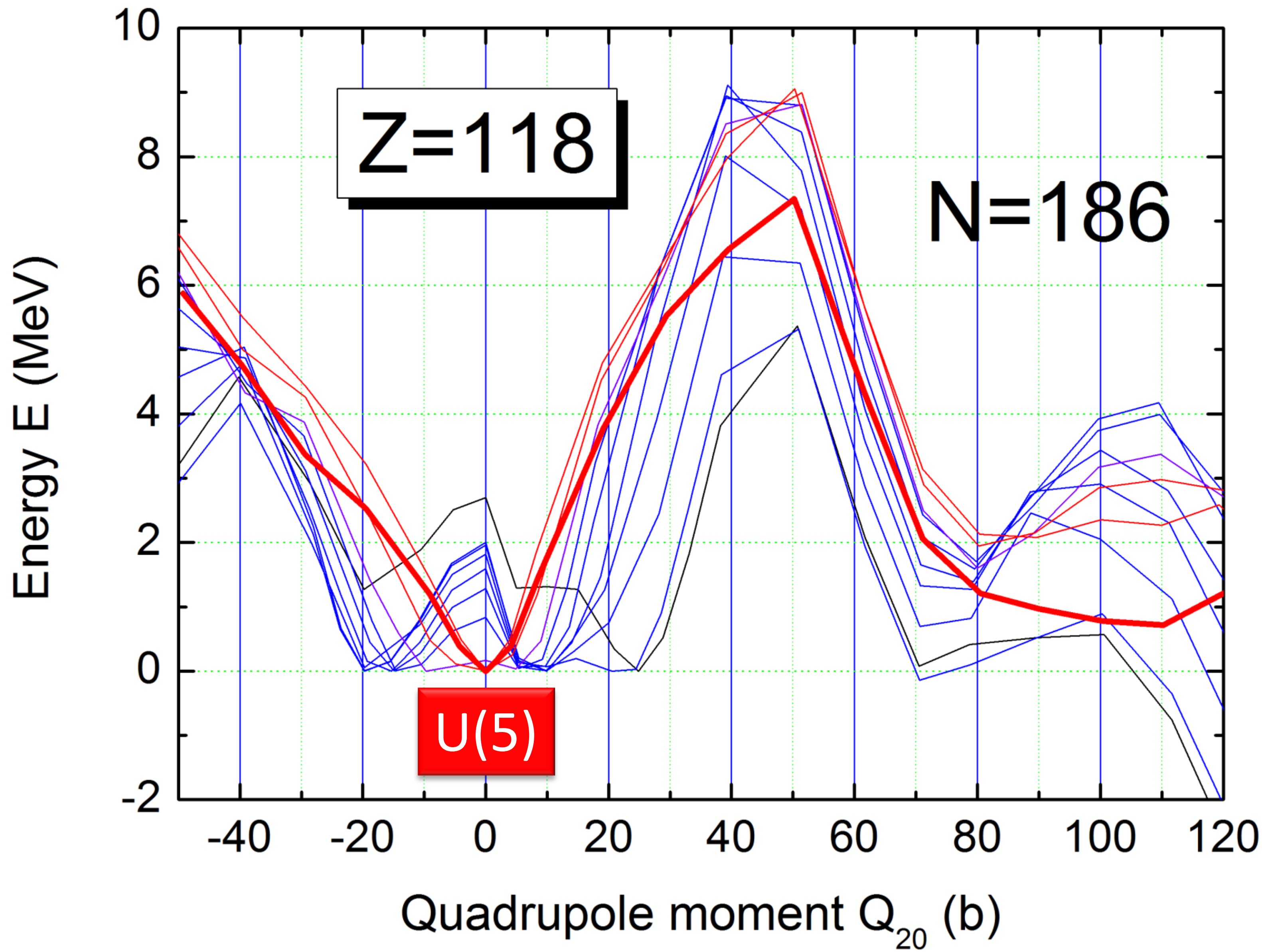

Second order phase transition O(6) – U(5)

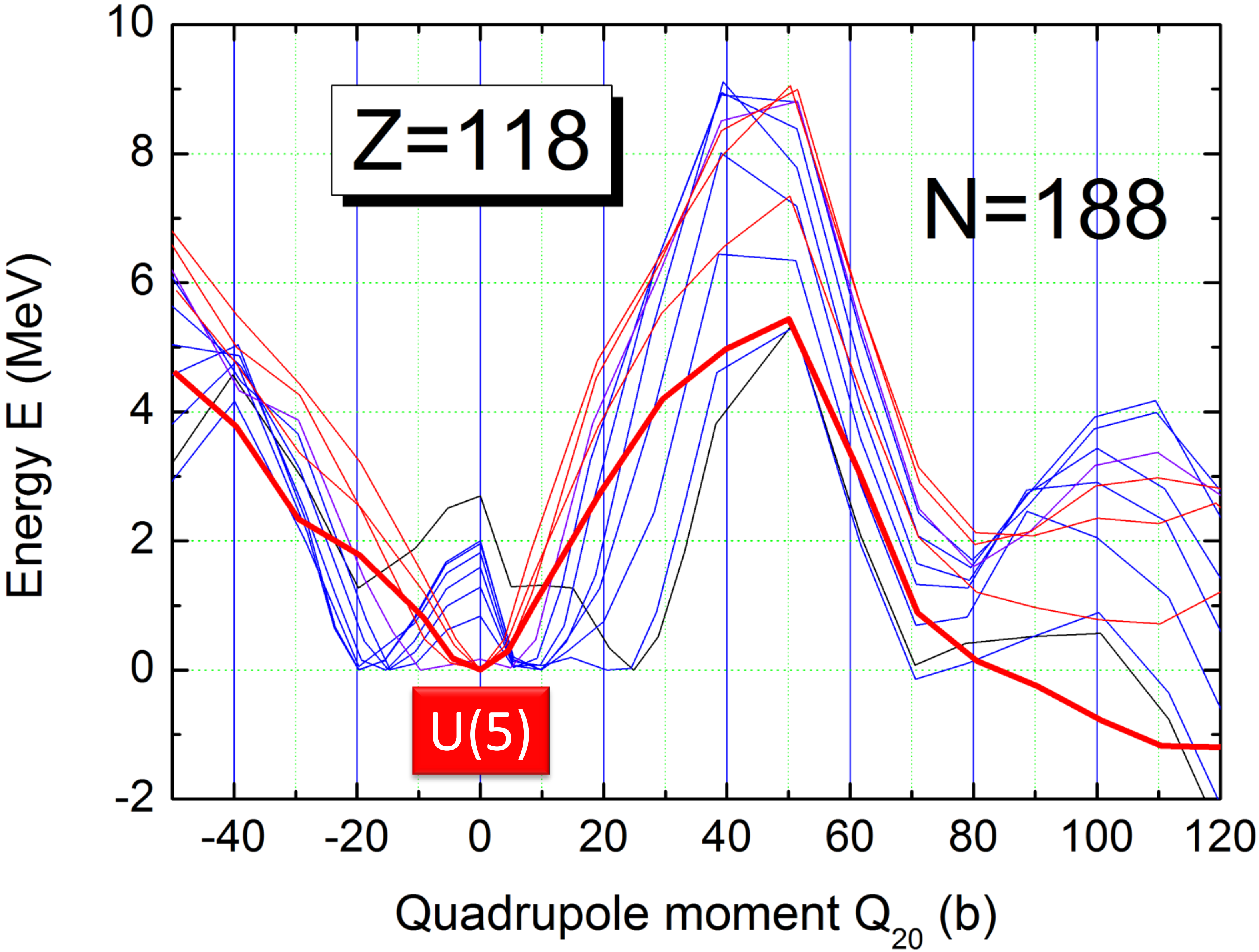

Superdeformed oblate (SDO) SHN?

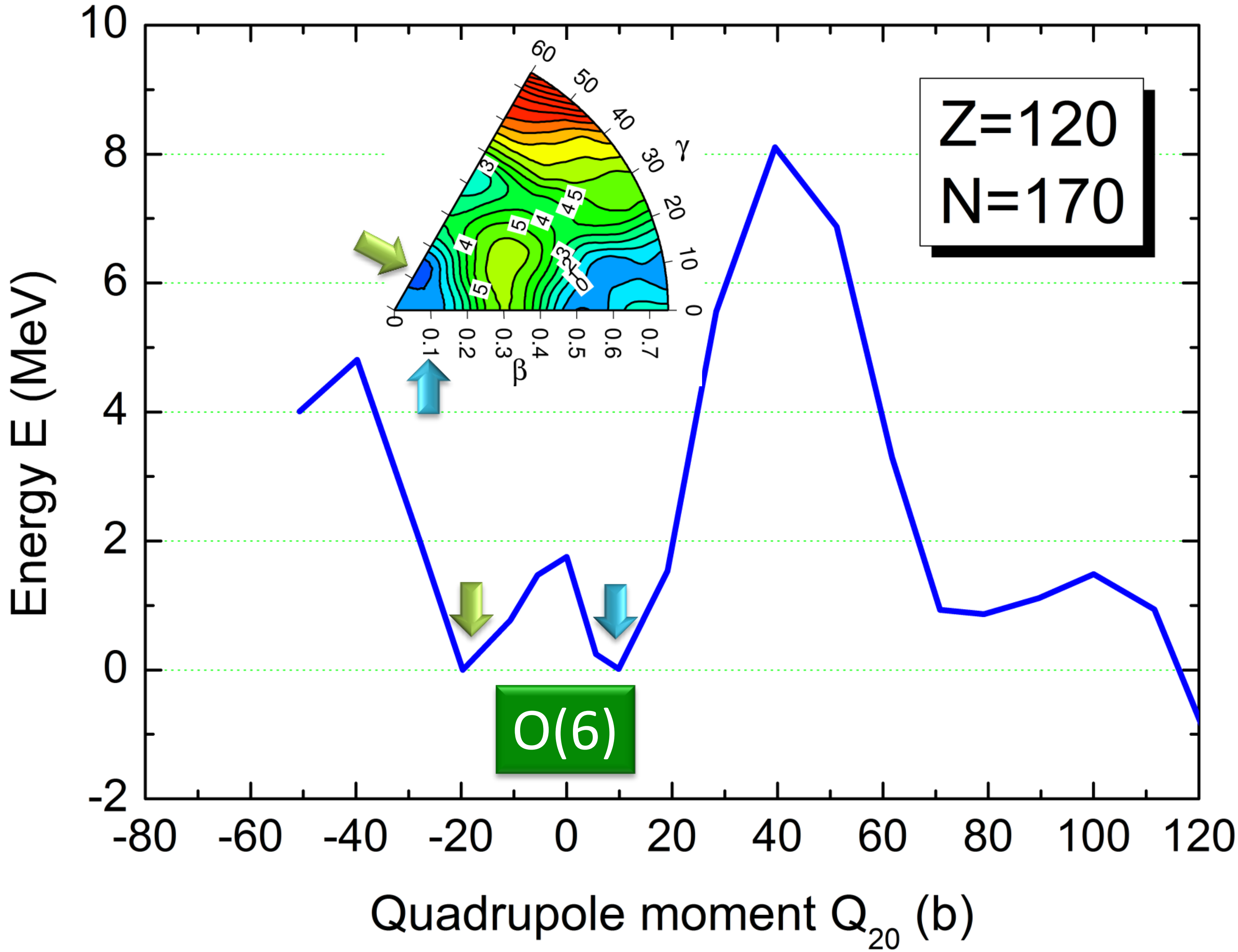

Superdeformed oblate (SDO) SHN?

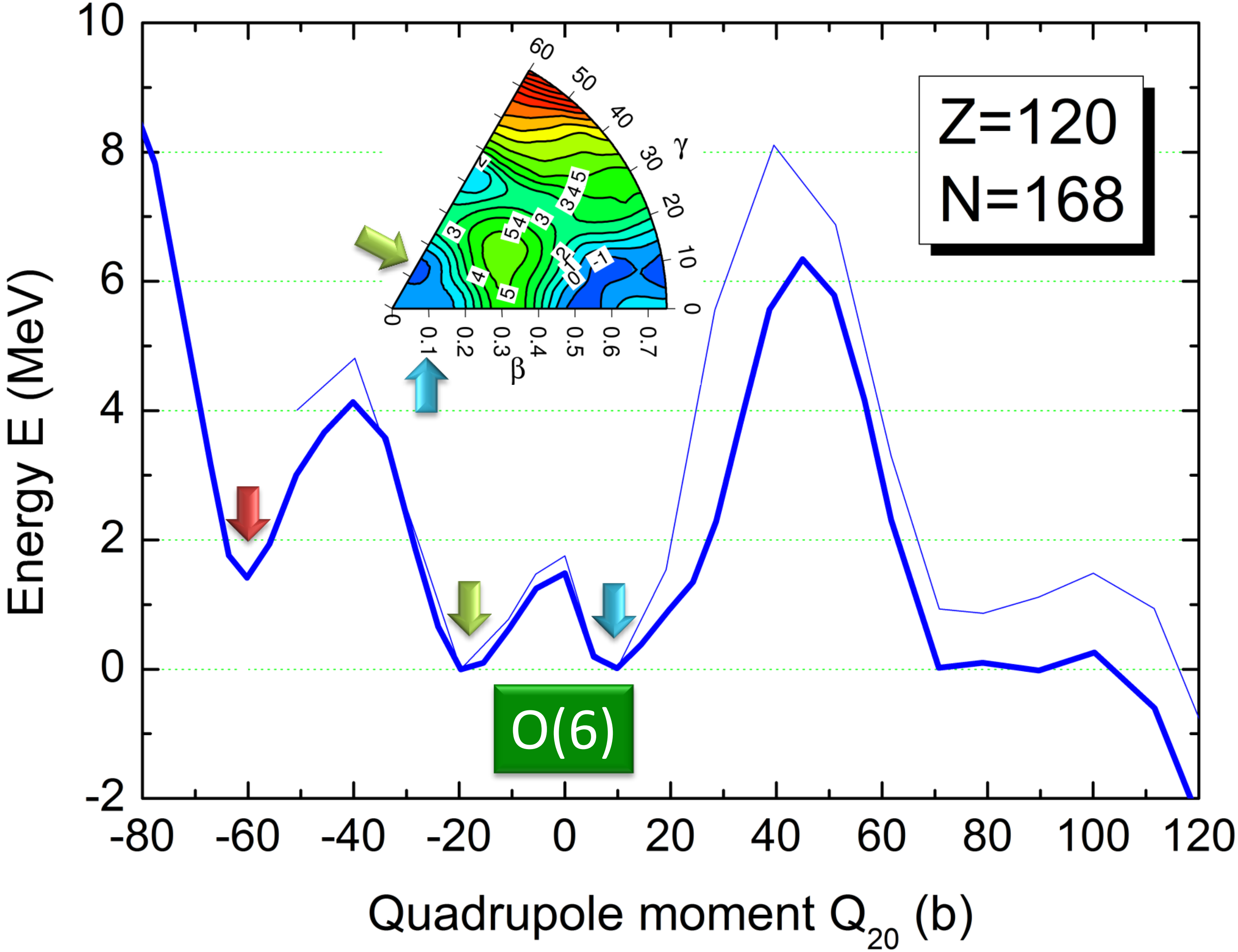

Superdeformed oblate (SDO*) SHN

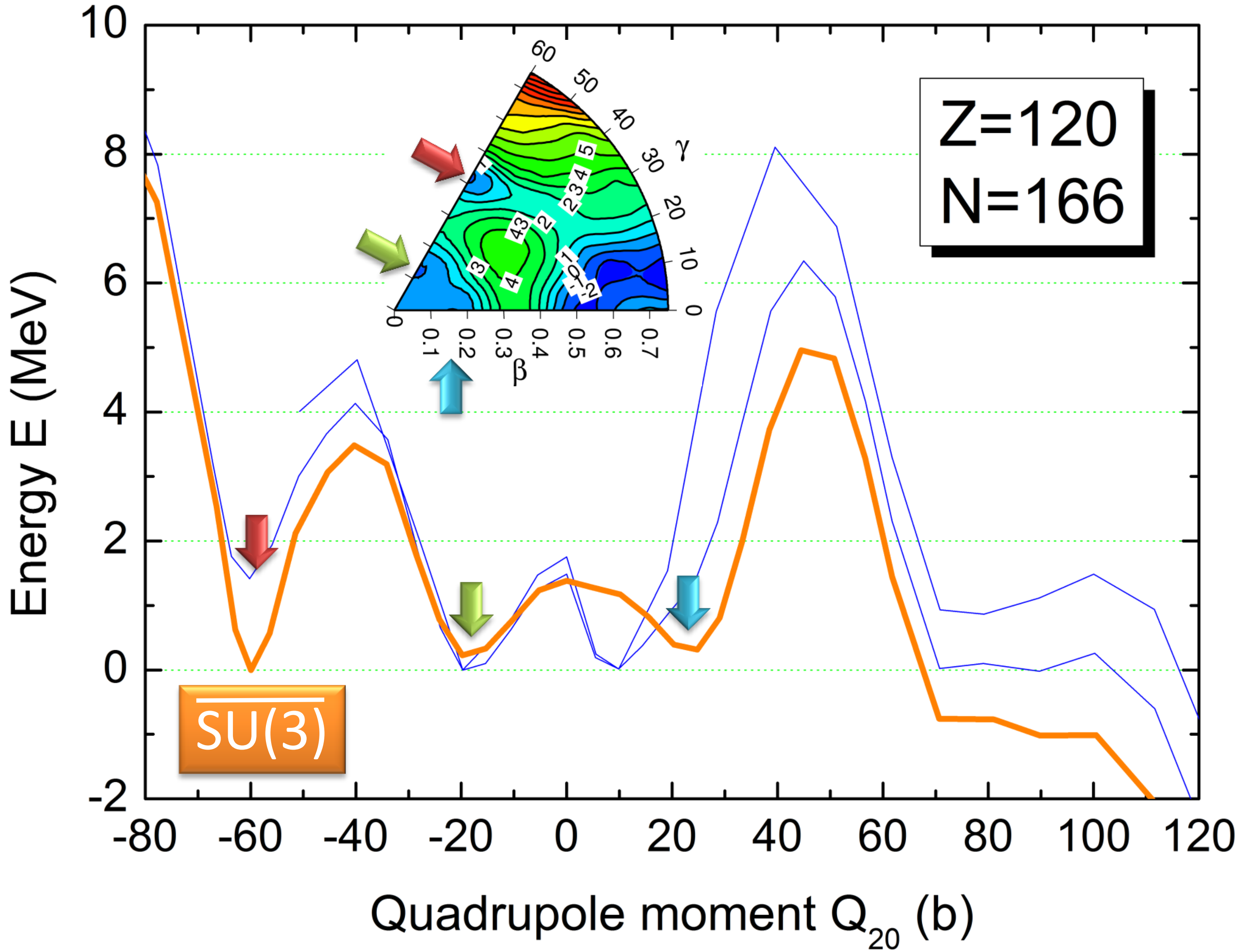

*P. Jachimowicz, M. Kowal, J. Skalski, Phys. Rev. C **83**, 054302 (2011)
L. Próchniak, A. S., Acta Phys. Polonica B **44**, 287 (2013)

Superdeformed oblate (SDO) SHN

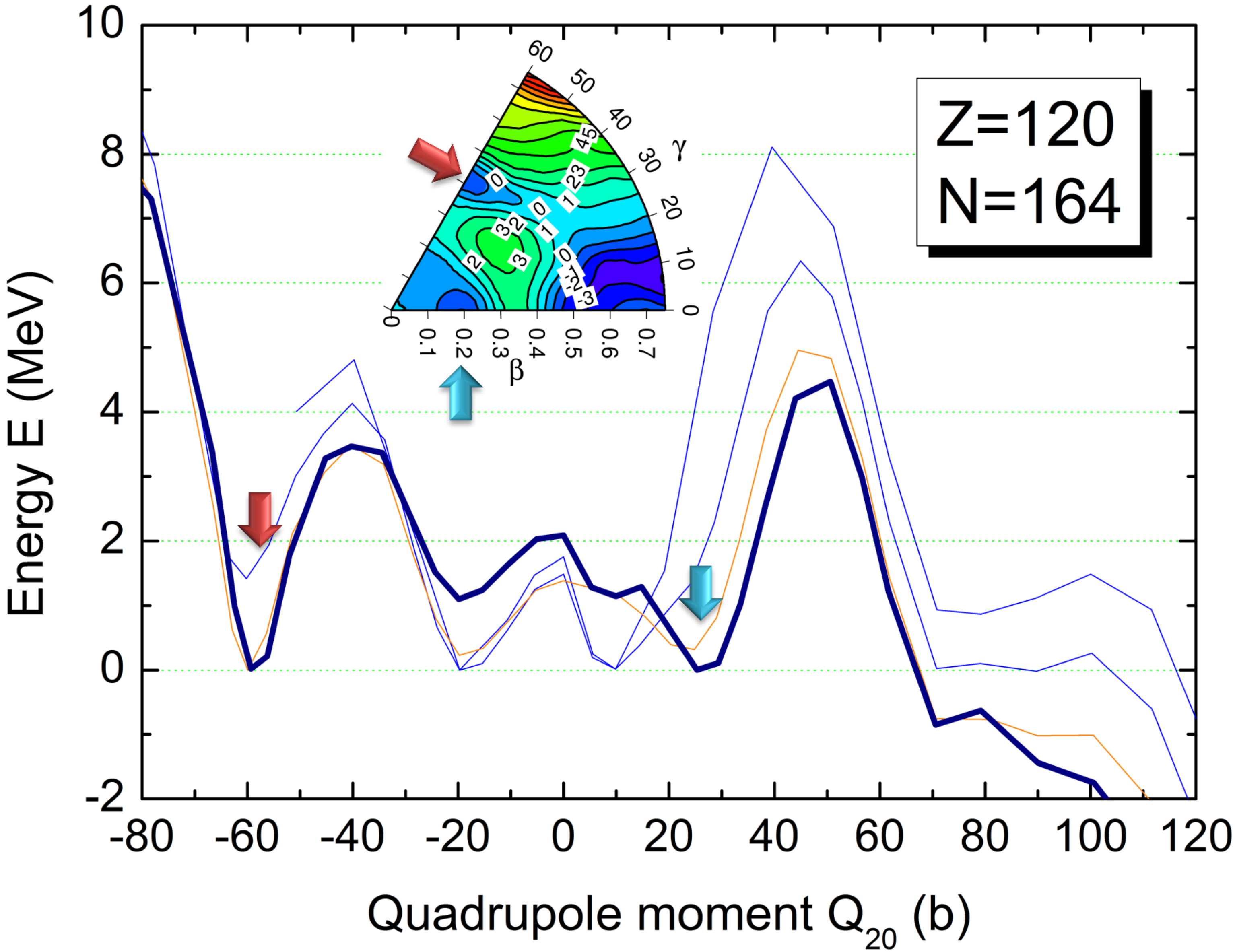

Superdeformed oblate (SDO) SHN

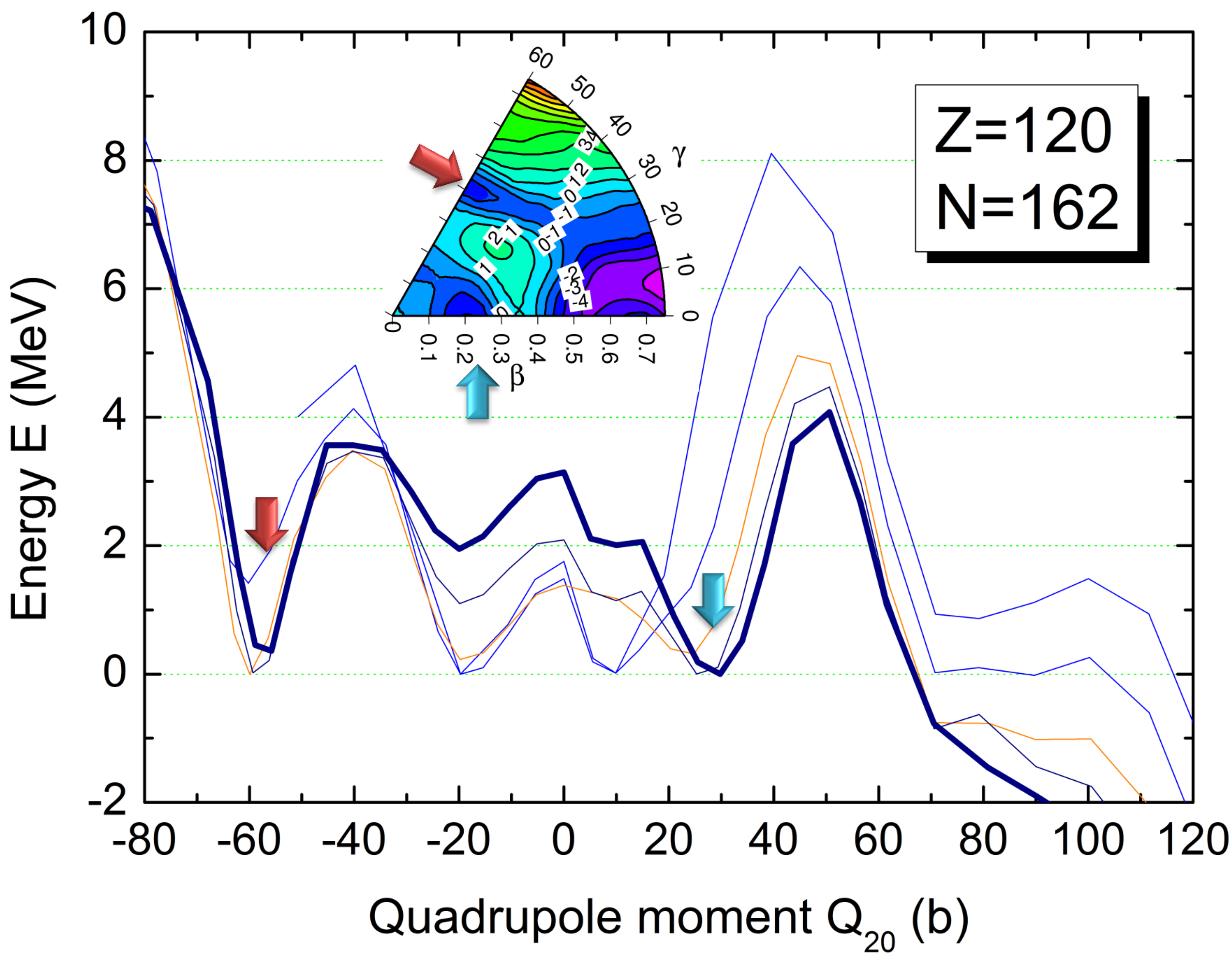

Superdeformed oblate (SDO) SHN

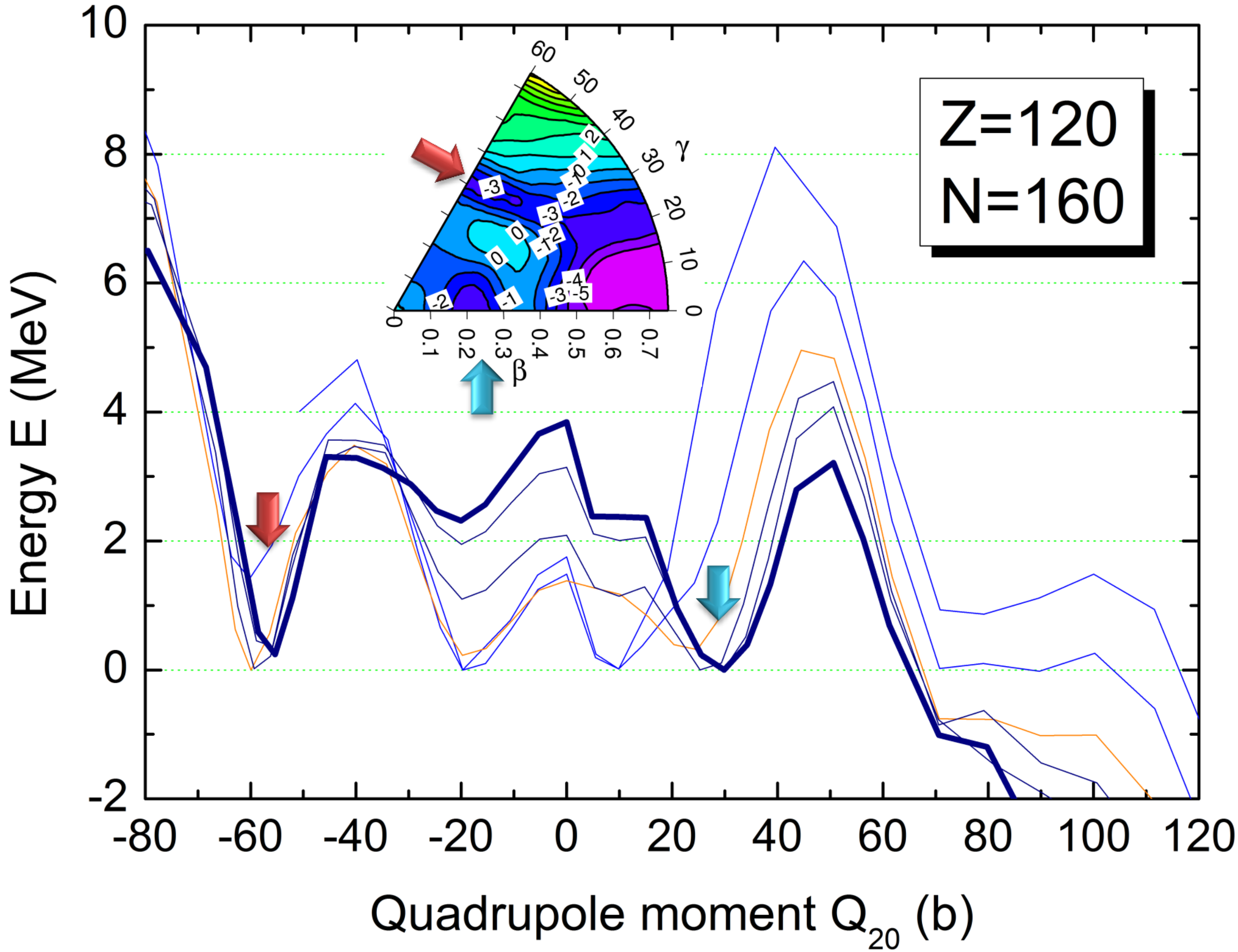

SHN phase diagram *(Natura non facit saltus)*

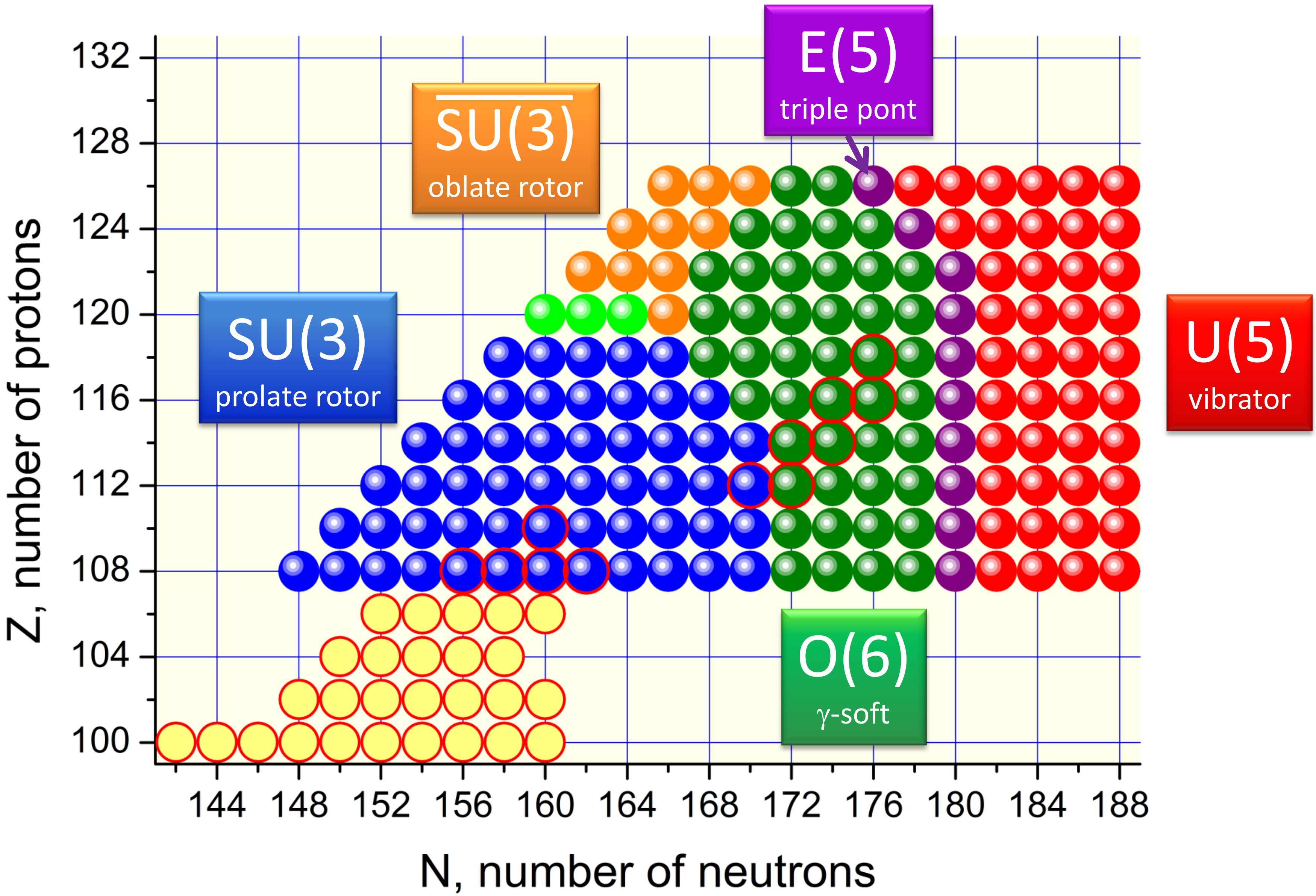

G.s. properties of SHN - Conclusions

- ✓ The e-e SHN form three regions: the prolate-deformed SU(3) (for $N < 172$), spherical U(5) (for $N>180$), and transitional region (γ-soft) O(6) between the former two.
- ✓ On the border between the O(6) and U(5) regions (for $N = 180$) nuclei exhibit a rather flat potential bottom and acquire the triple-point solutions - E(5).
- ✓ The existence of superdeformed oblate (SDO) nuclei - $\overline{SU(3)}$ for $N \leq 166$ and $Z \geq 120$ was validated.
- ✓ The heaviest even-even nuclei produced by ^{48}Ca induced reactions on actinide targets fall into the class of O(6) γ-soft nuclei.

SHN: alpha emission

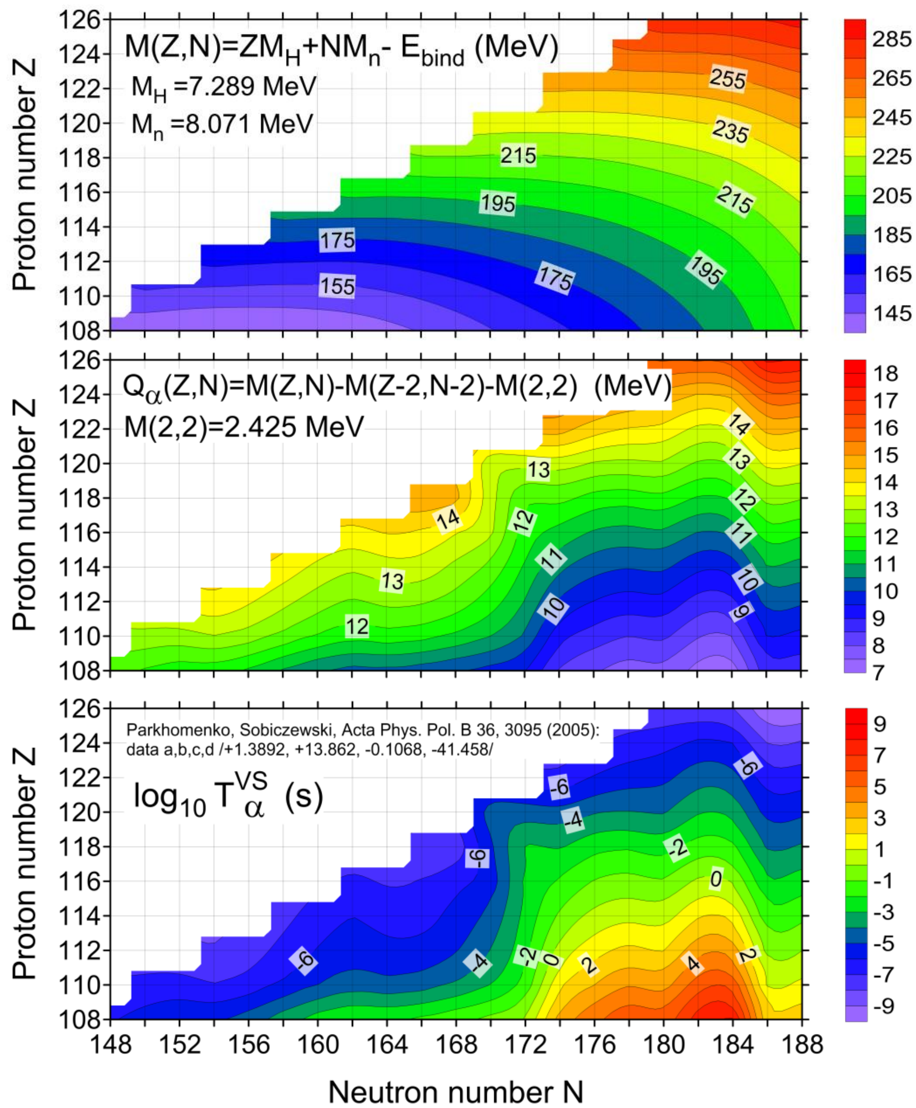

SHN: Q_α- values

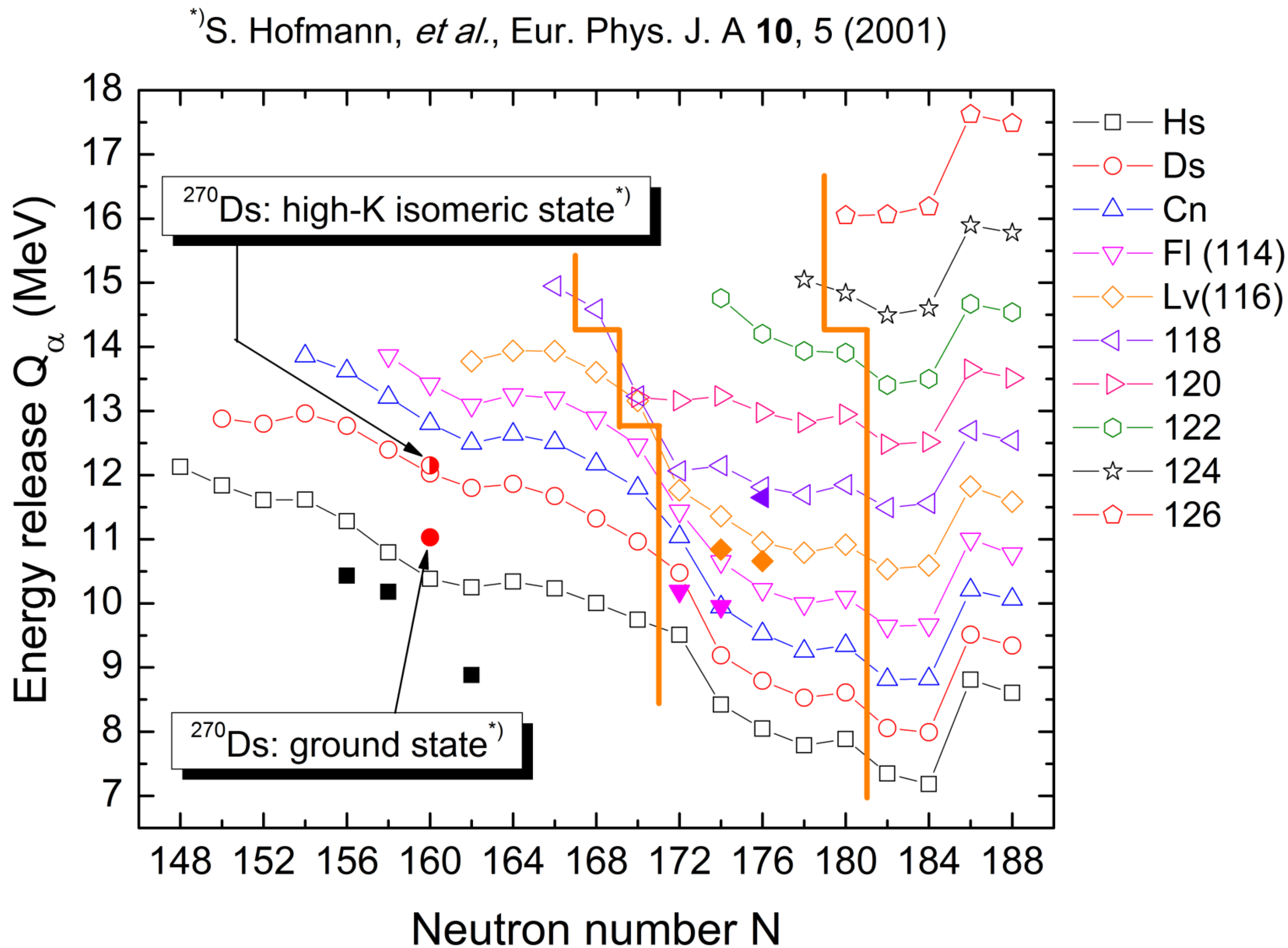

PRC 87, 024320 (2013)

The spontaneous-fission half-life is inversely proportional to the probability of penetration through the barrier

$$T^{sf}_{\frac{1}{2}} = \frac{\ln 2}{n}\frac{1}{P}, \qquad n \approx 10^{20.38} s^{-1}, \qquad \frac{\ln 2}{n} = 10^{-20.54} s.$$

In the WKB semi-classical approximation for the probability P

$$T^{sf}_{\frac{1}{2}}\left[s\right] = \frac{10^{-20.54}}{\hbar\omega_0}\left[1+\exp\left(2S\left(L\right)\right)\right],$$

where the action-integral calculated along a fission path $L(s)$ in the multi-dimensional deformation space $\left\{q^{\lambda}\right\}$ is

$$S\left(L\right) = \int_{s_1}^{s_2}\left\{2/\hbar^2 B_{eff}\left(s\right)\left[V\left(s\right)-E\right]\right\}^{\frac{1}{2}} ds$$

The effective inertia associated with the fission motion along the path $L(s)$ is

$$B_{eff}\left(s\right) = \sum_{k,l} B_{q^k q^l}\frac{dq^k}{ds}\frac{dq^l}{ds},$$

Barriers of even-even Fm isotopes

PRC **80**, 014309 (2009)

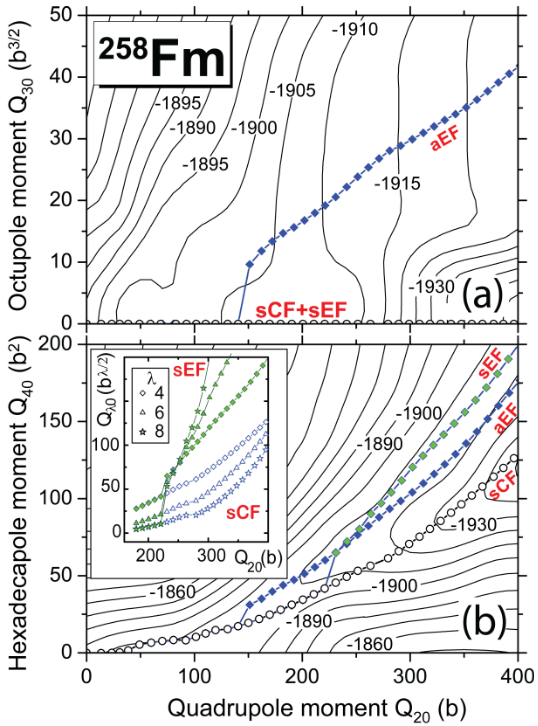

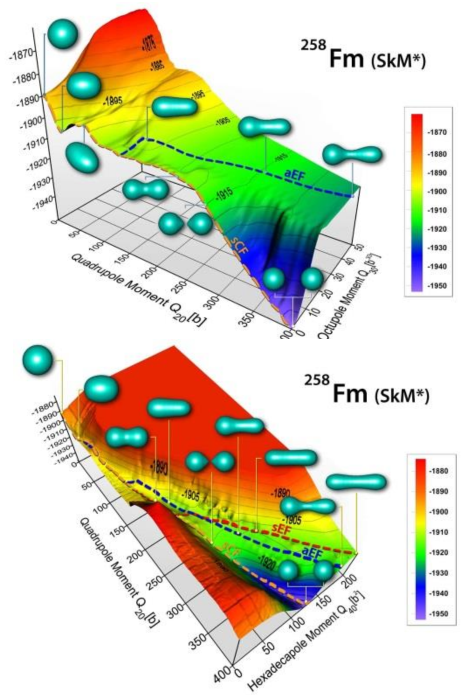

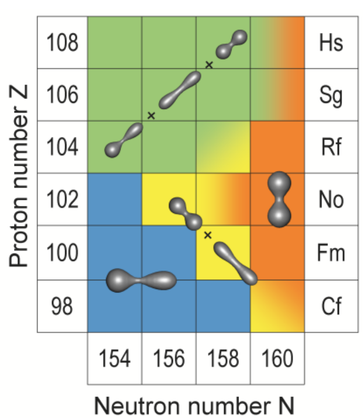

Multimodal fission

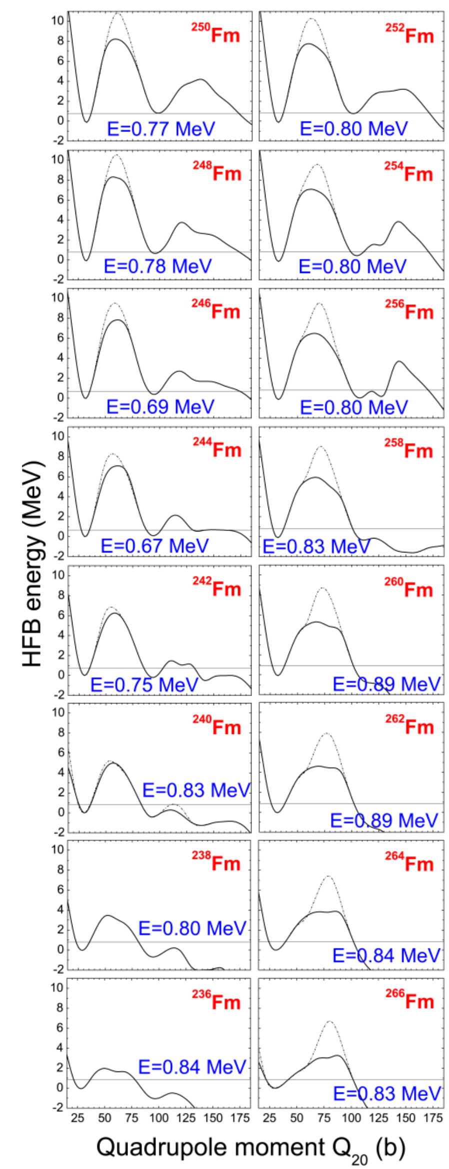

SF half-lives of even-even Fm isotopes

PRC **87**, 024320 (2013)

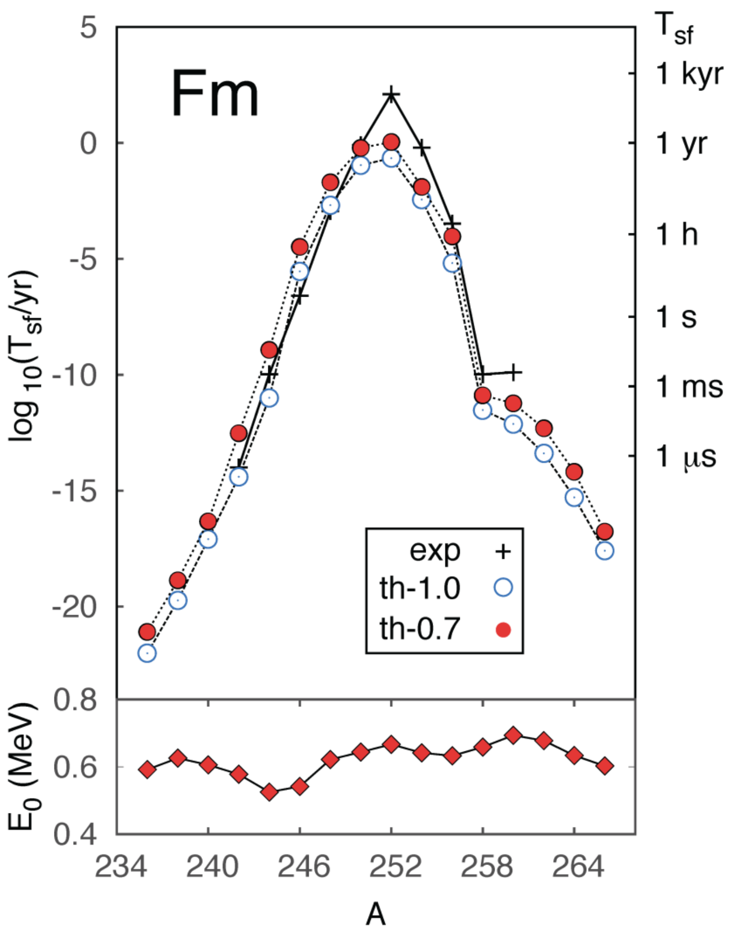

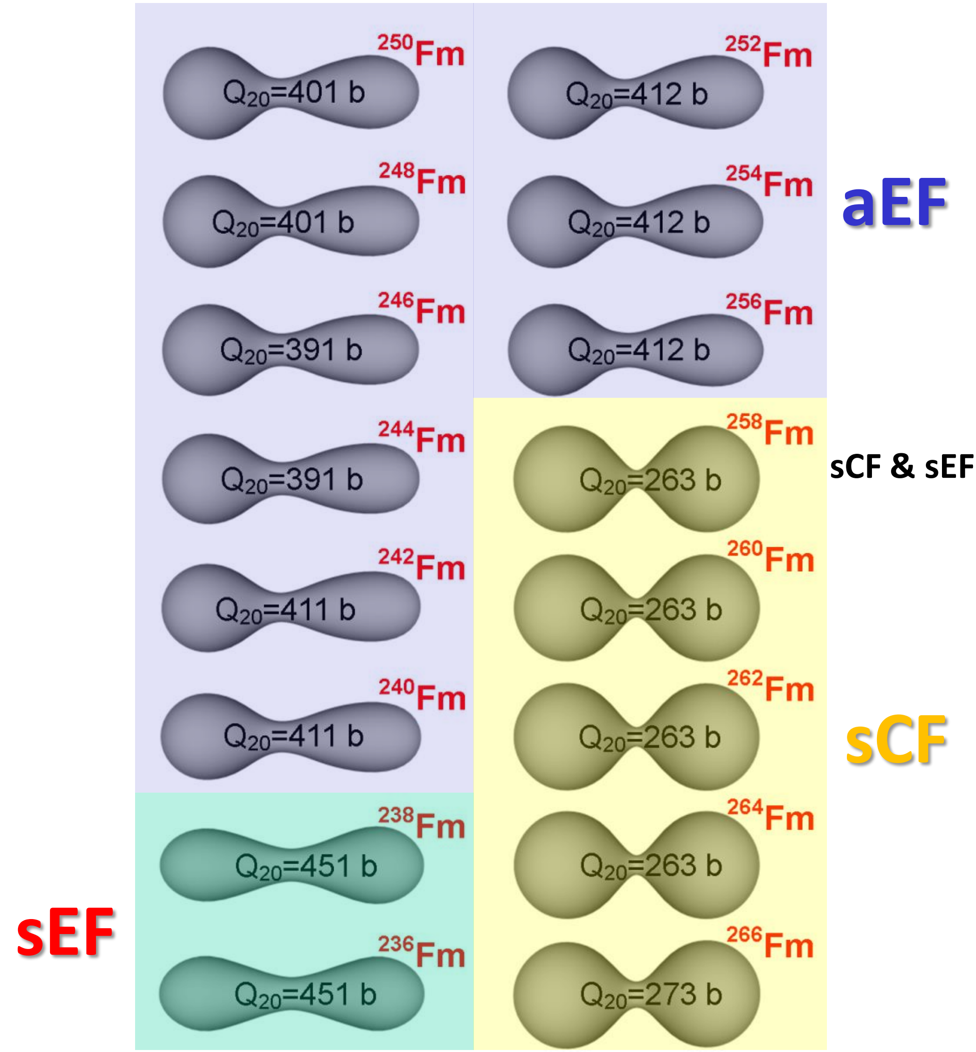

Experimental fission half-lives from:

- E. Holden and D.C. Hoffman, Pure Appl. Chem. 72, 1525 (2000).
- J. Khuyagbaatar *et al.,* Eur. Phys. J. A 37, 177 (2008).

E^{tot} and $B_{20\,20}$ along sEF and aEF fission paths in $^{306}122$

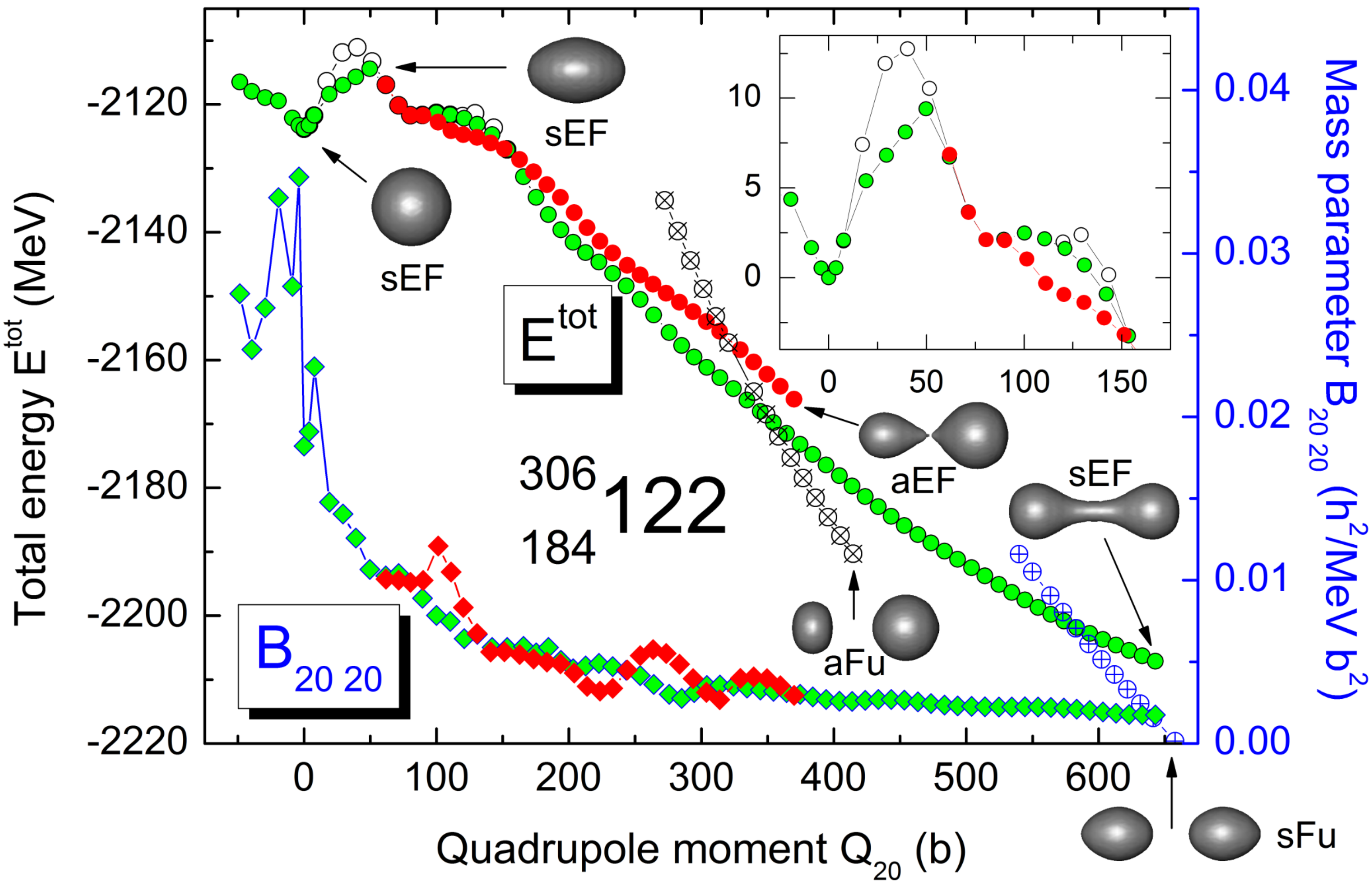

PRC **87**, 024320 (2013)

PES with the sEF and aEF fission paths in $^{304}120$

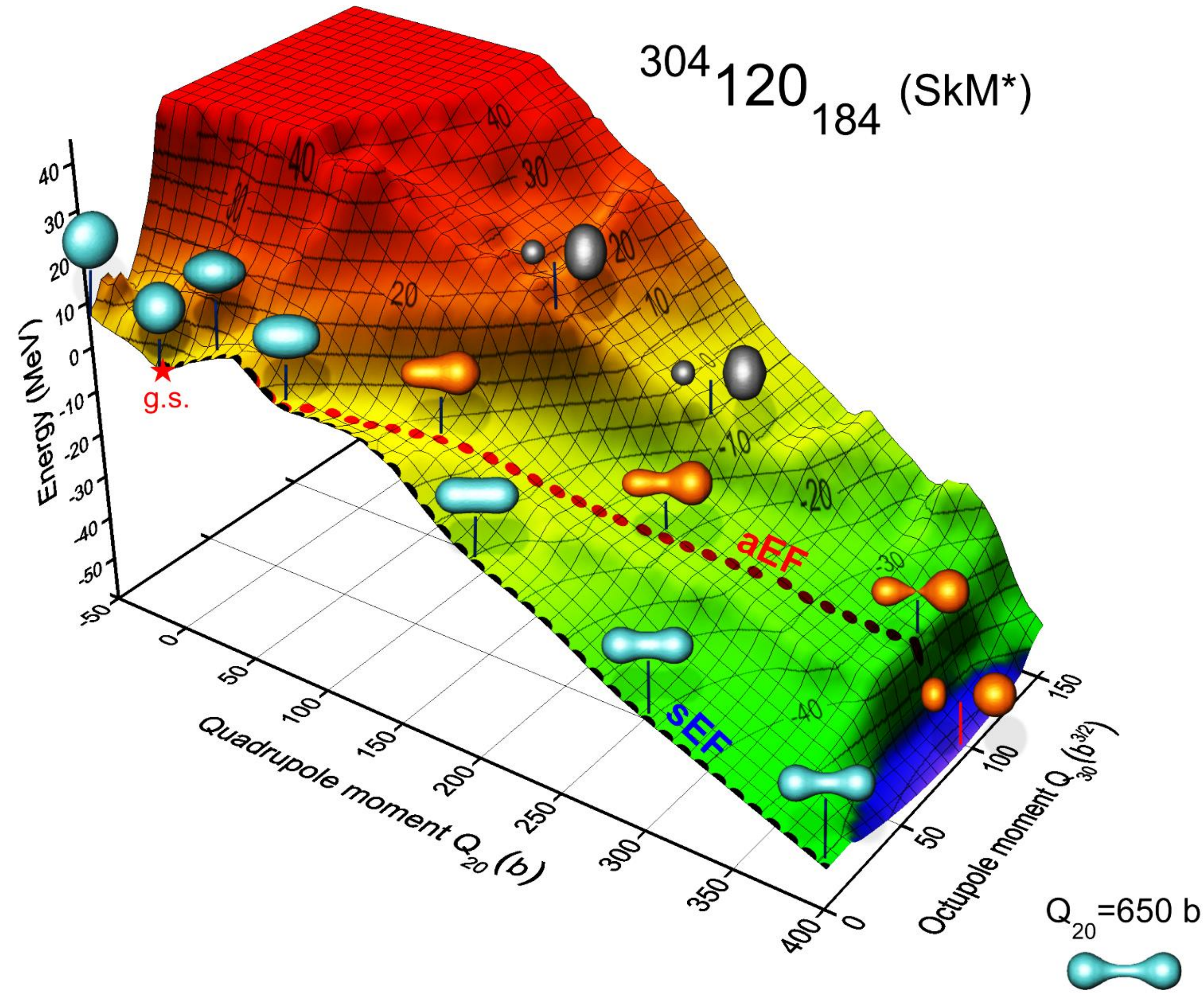

PES with the sEF and aEF fission paths in $^{304}120$

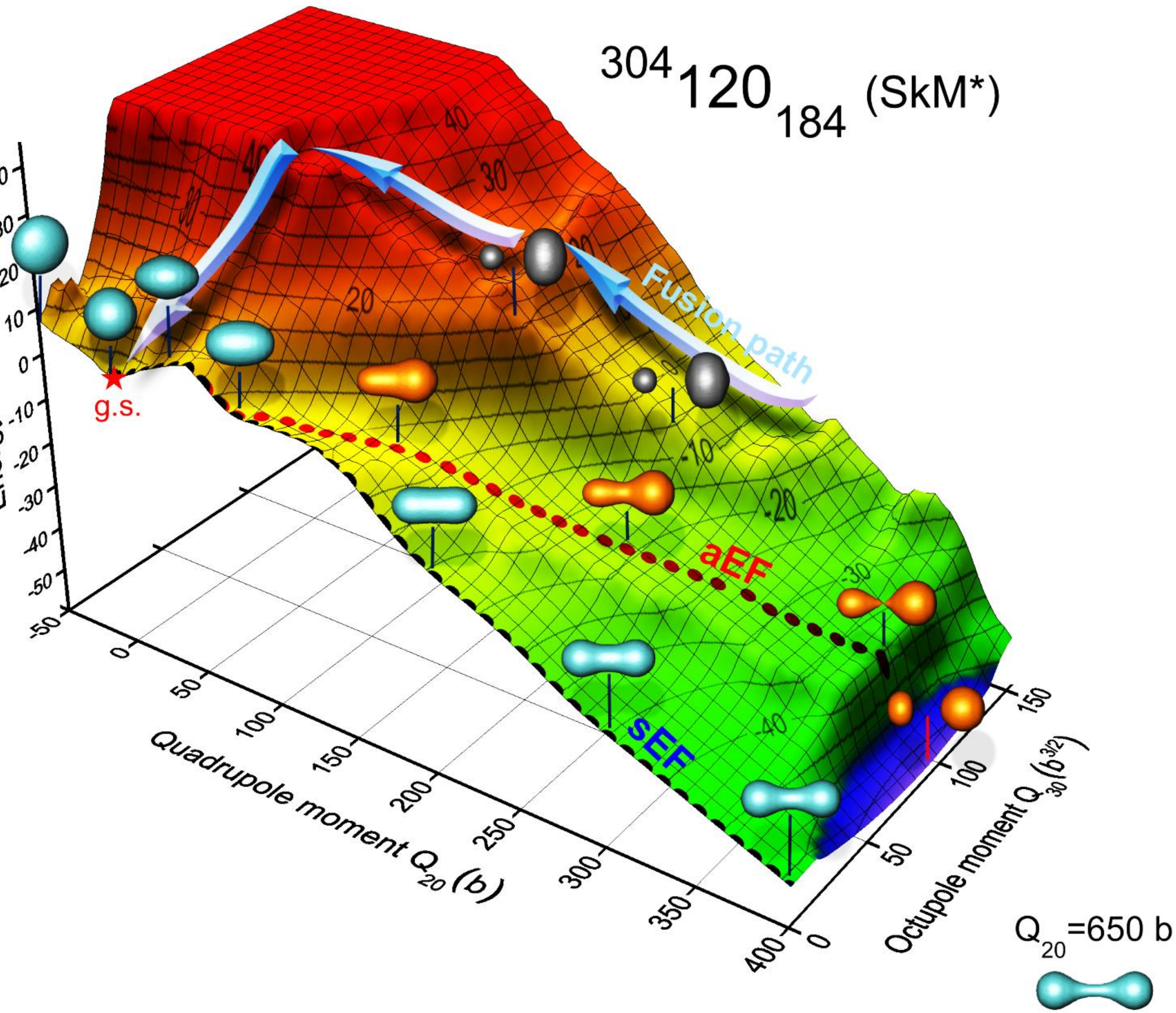

$^{306}122_{184}$ – sEF path

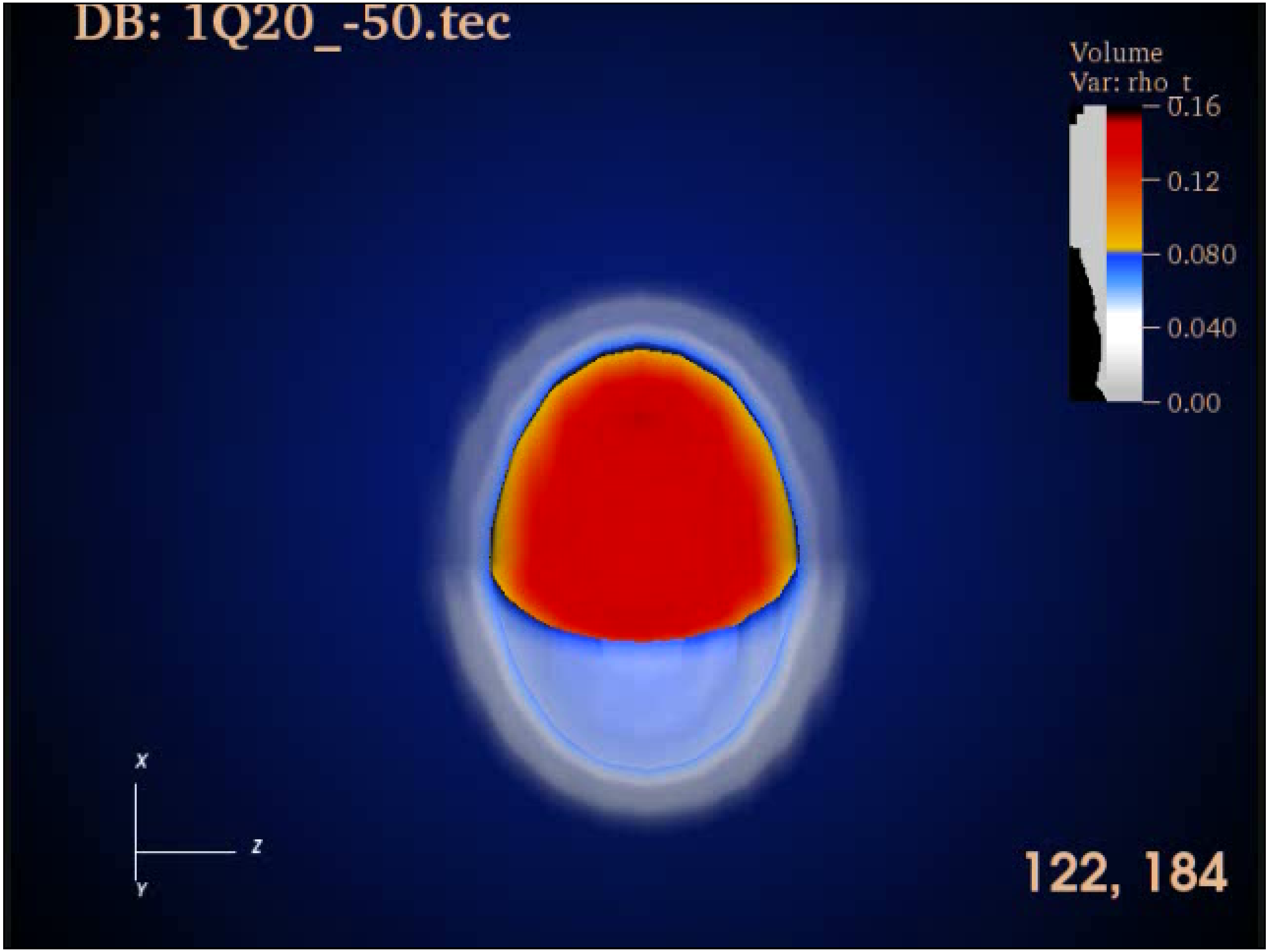

$^{306}122_{184}$ – aEF path

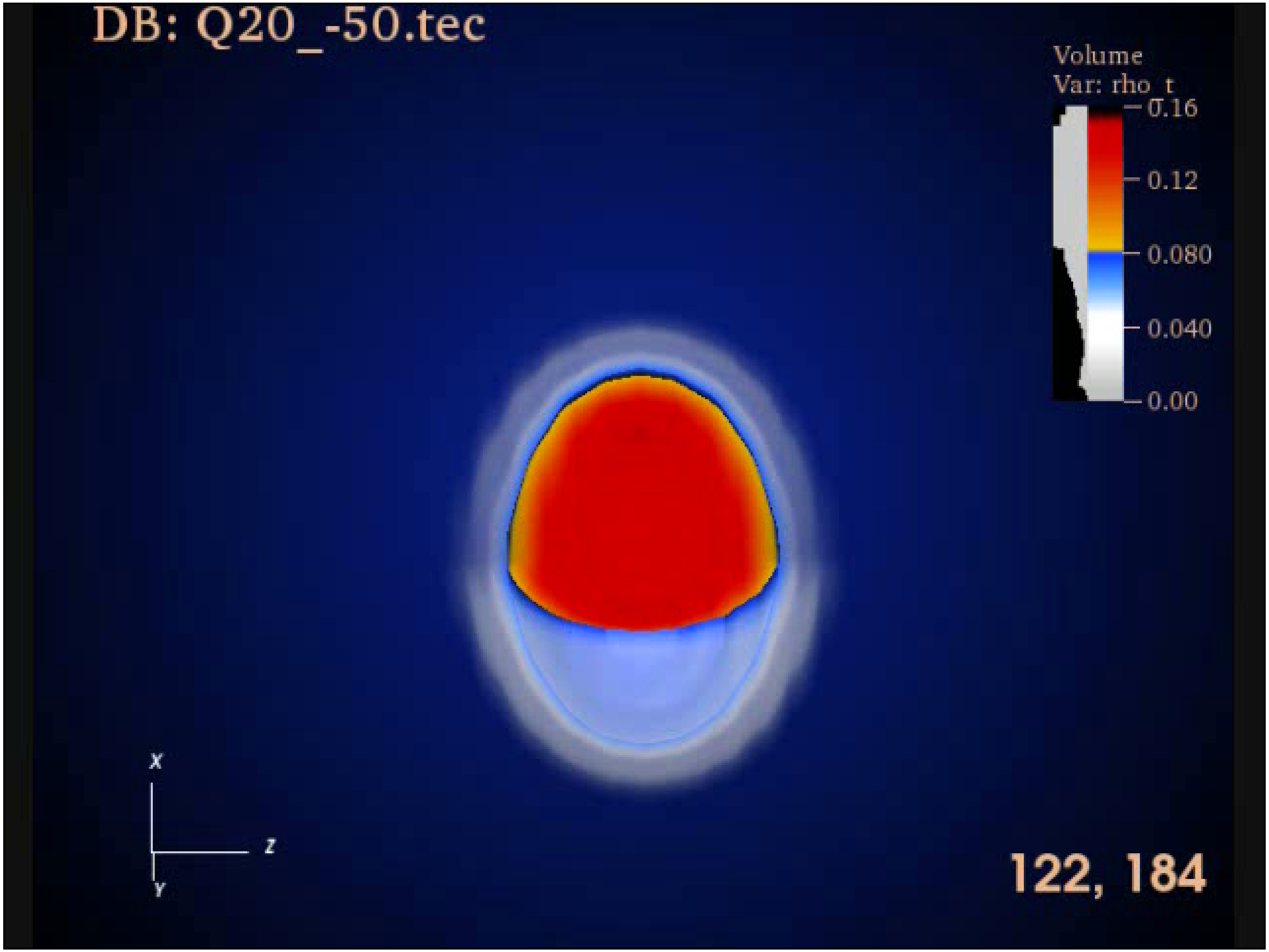

sEF and aEF SF modes in even-even SHN

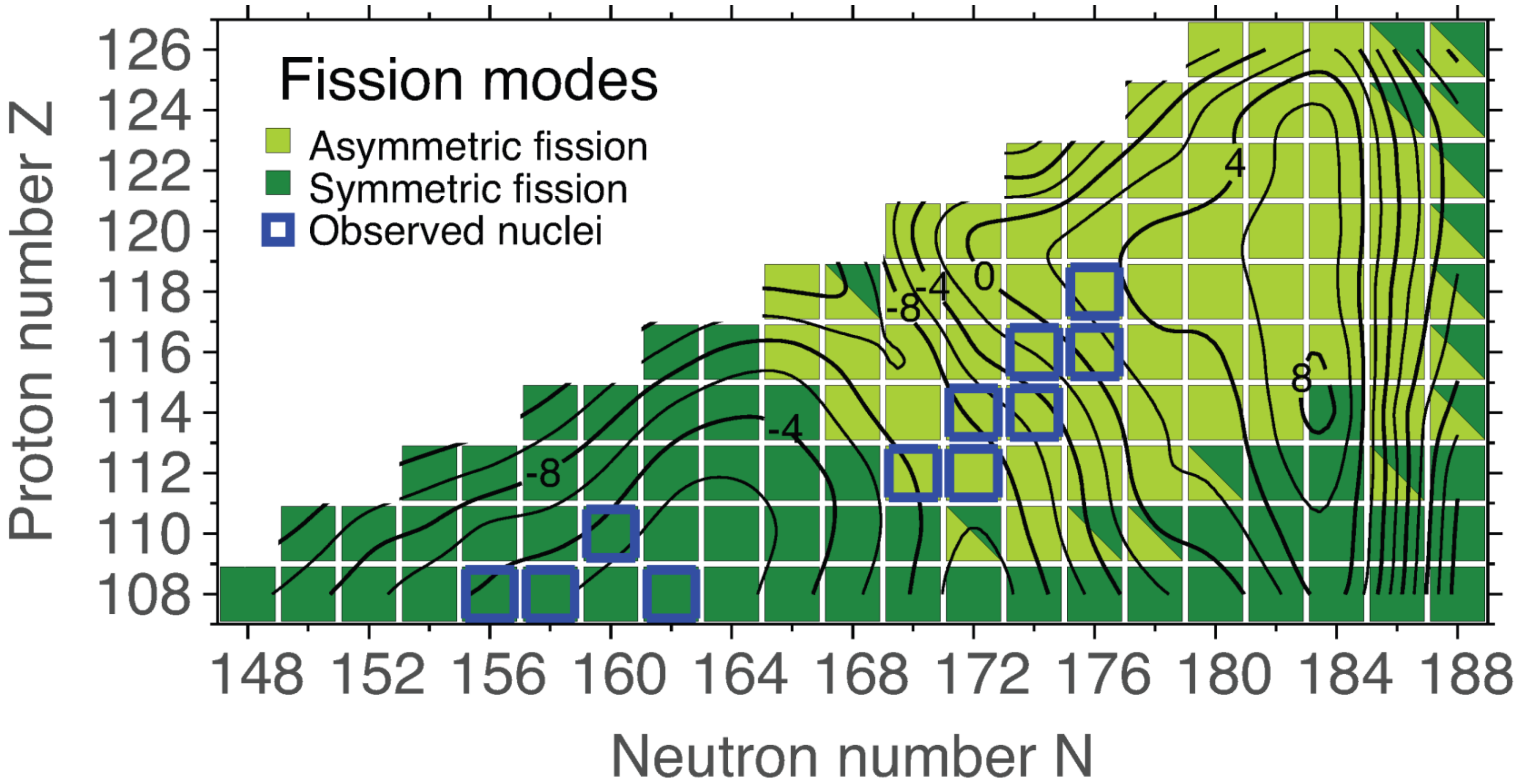

PRC **87**, 024320 (2013)

The contours show the predicted SF half-lives in logarithmic scale in s.

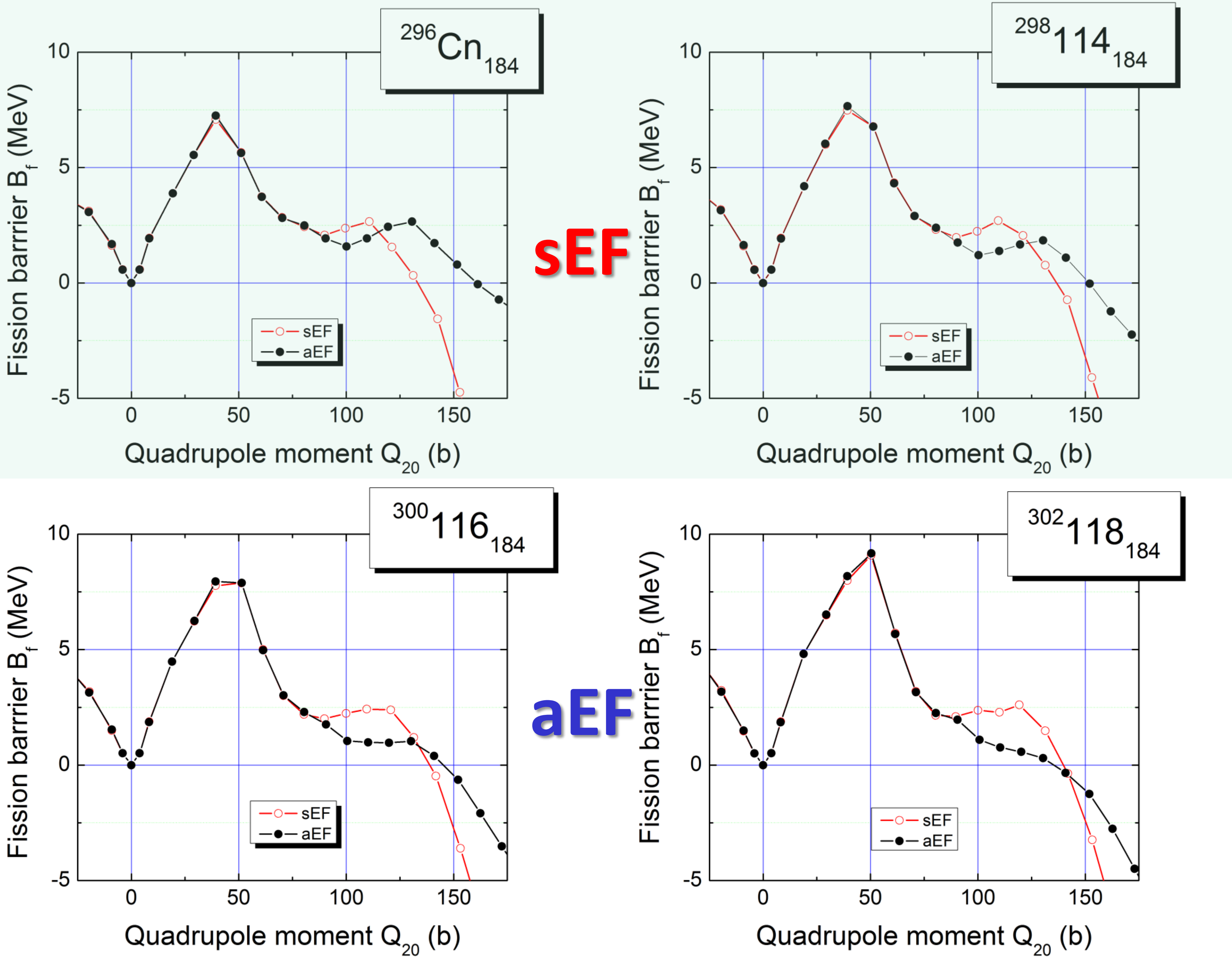

$^{296}Cn_{184}$
$^{298}114_{184}$
$^{300}116_{184}$
$^{302}118_{184}$
sEF
aEF
Fission barrier B_f (MeV)
Quadrupole moment Q_{20} (b)
—○— sEF
—●— aEF

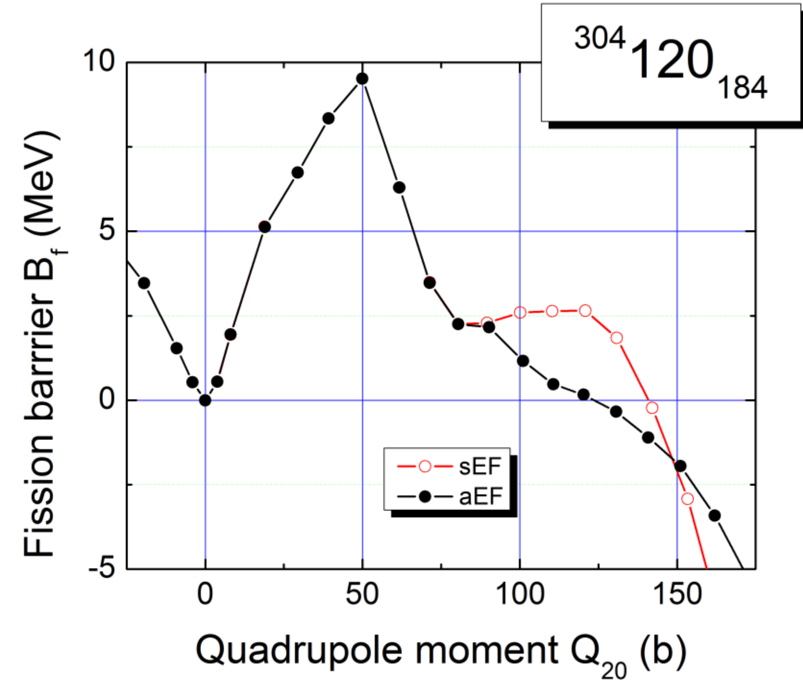

$^{304}120_{184}$
Fission barrier B_f (MeV)
Quadrupole moment Q_{20} (b)
sEF
aEF

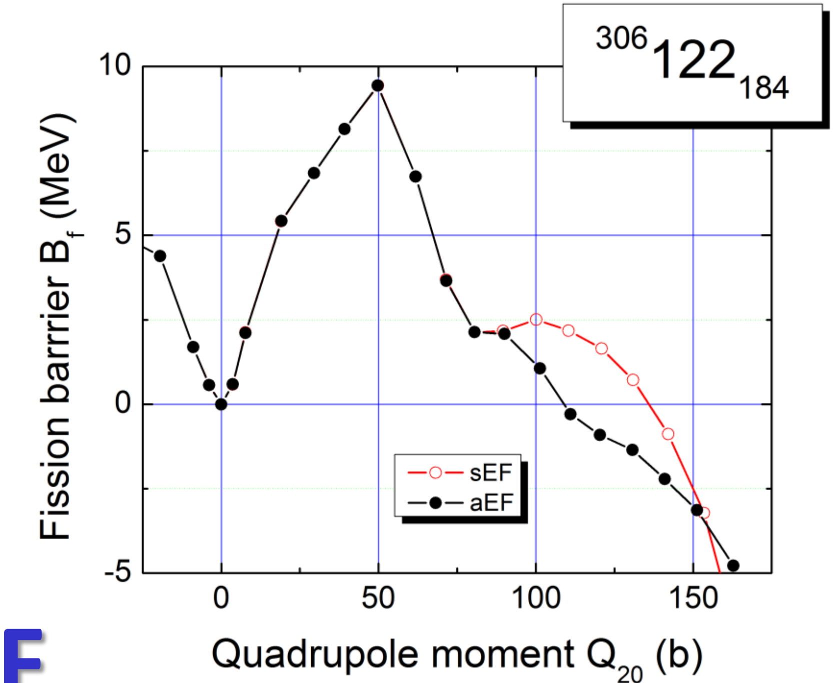

$^{306}122_{184}$
Fission barrier B_f (MeV)
Quadrupole moment Q_{20} (b)
sEF
aEF

aEF

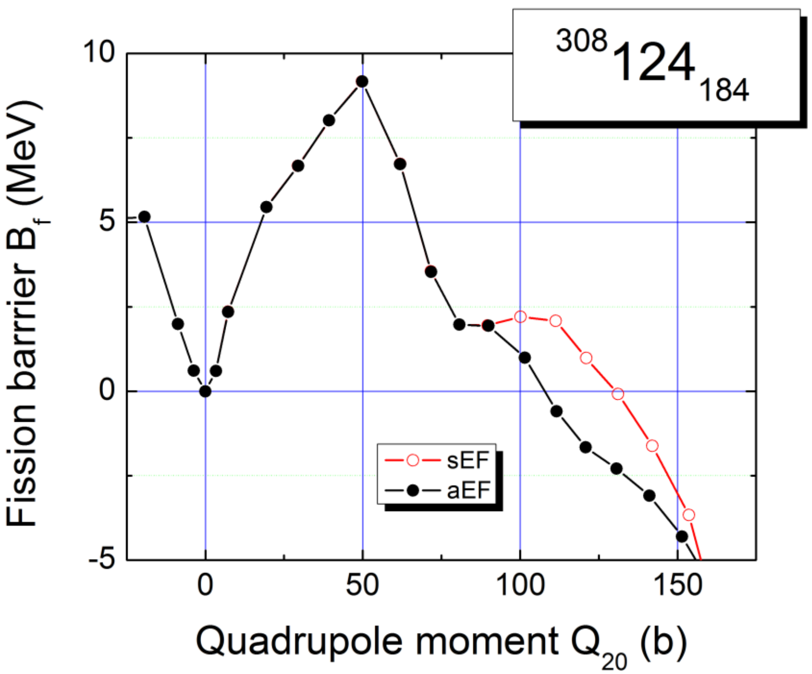

$^{308}124_{184}$
Fission barrier B_f (MeV)
Quadrupole moment Q_{20} (b)
sEF
aEF

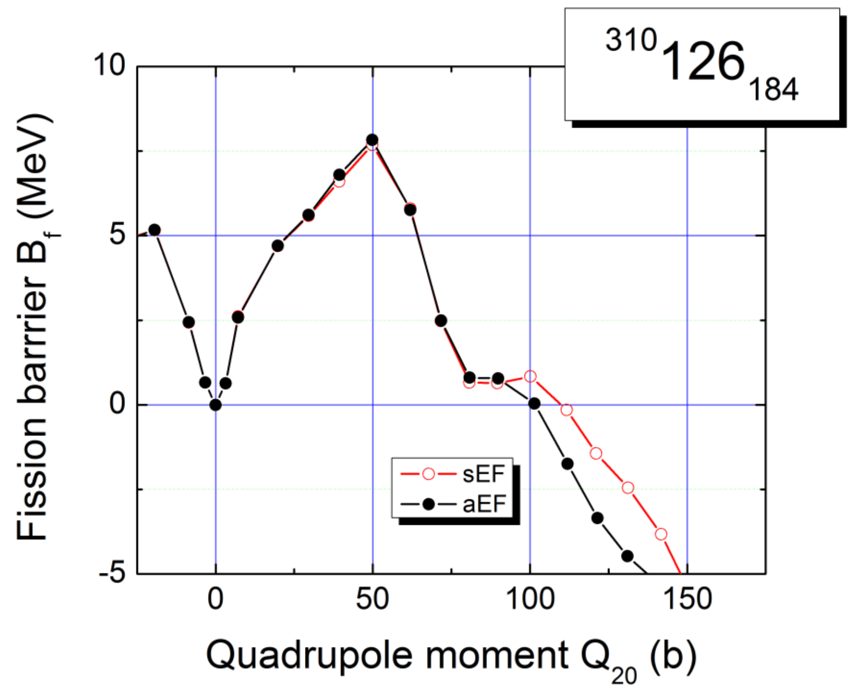

$^{310}126_{184}$
Fission barrier B_f (MeV)
Quadrupole moment Q_{20} (b)
sEF
aEF

HFB-SkM* results for even-even SHN

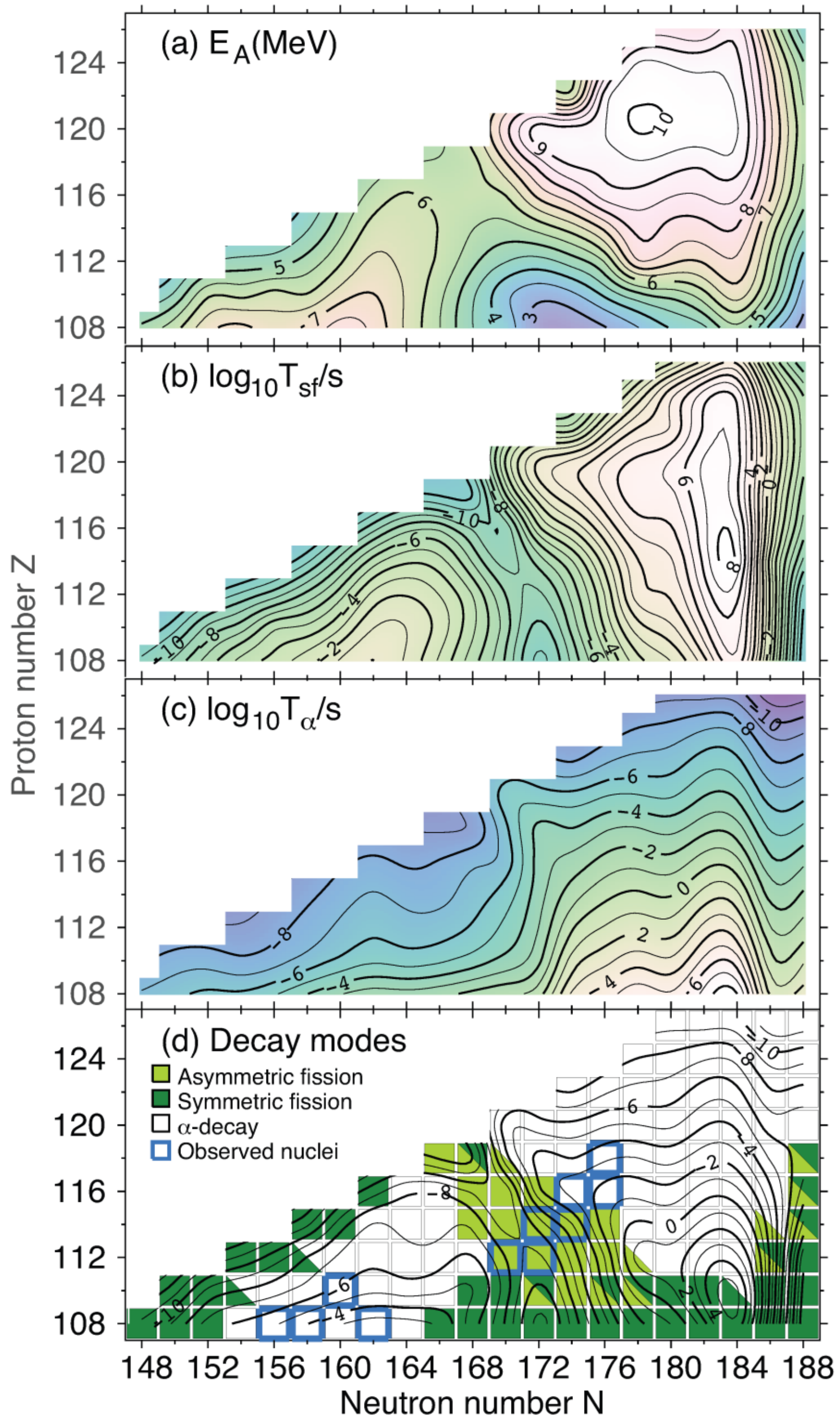

max $E_A \approx 10$ MeV for $^{298,\,300}120$

min $E_A \approx 2.7$ MeV for $^{280,\,282}$Hs

max $T_{sf} \approx 10^{7.7}$s for ^{298}Fl,

$T_{sf} \approx 10^{7.3}$s for ^{300}Lv,

$T_{sf} \approx 10^{7.1}$s for $^{302}120$

min $T_{sf} \sim 10^{-10}$s for ^{280}Hs, ^{284}Fl, $^{284}118$

max $T_{sf+\alpha} \approx 10^{5.1}$s ~ 1.5 days for ^{294}Ds

PRC **87**, 024320 (2013)

SF half-lives of even-even Fm isotopes (II)

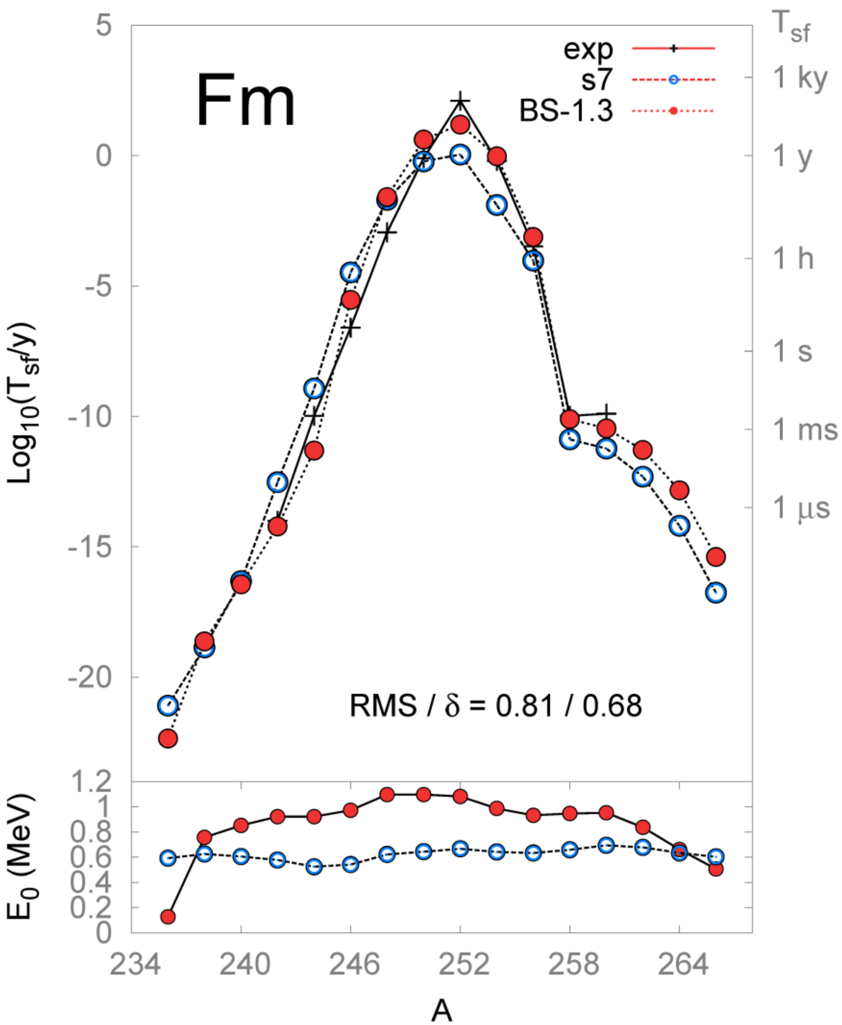

Empty circles – (like before) the constrained HFB-SkM* calculations along Q_{20} coordinate with left-right asymmetry and non-axiality included; the mass parameters were obtained in the perturbative cranking approx. Energy of fissoning nucleus (bottom panel) was assumed to be equal E_0 = 0.7 ZPE(Q_{gs}), where ZPE(Q_{gs}) is zero point energy (GCM+GOA model) at the ground state deformation.

Filled circles – the same as above, but the mass parameters were scaled by a factor 1.3 and E_0 energy was determined from the WKB quantization condition

$$\int_a^b \sqrt{2M(q)\left(E_n - V(q)\right)}\, dq = \pi\left(n + \tfrac{1}{2}\right)\hbar, \quad n = 0,1,2,\ldots$$

HFB-SkM* results for even-even SHN (II)

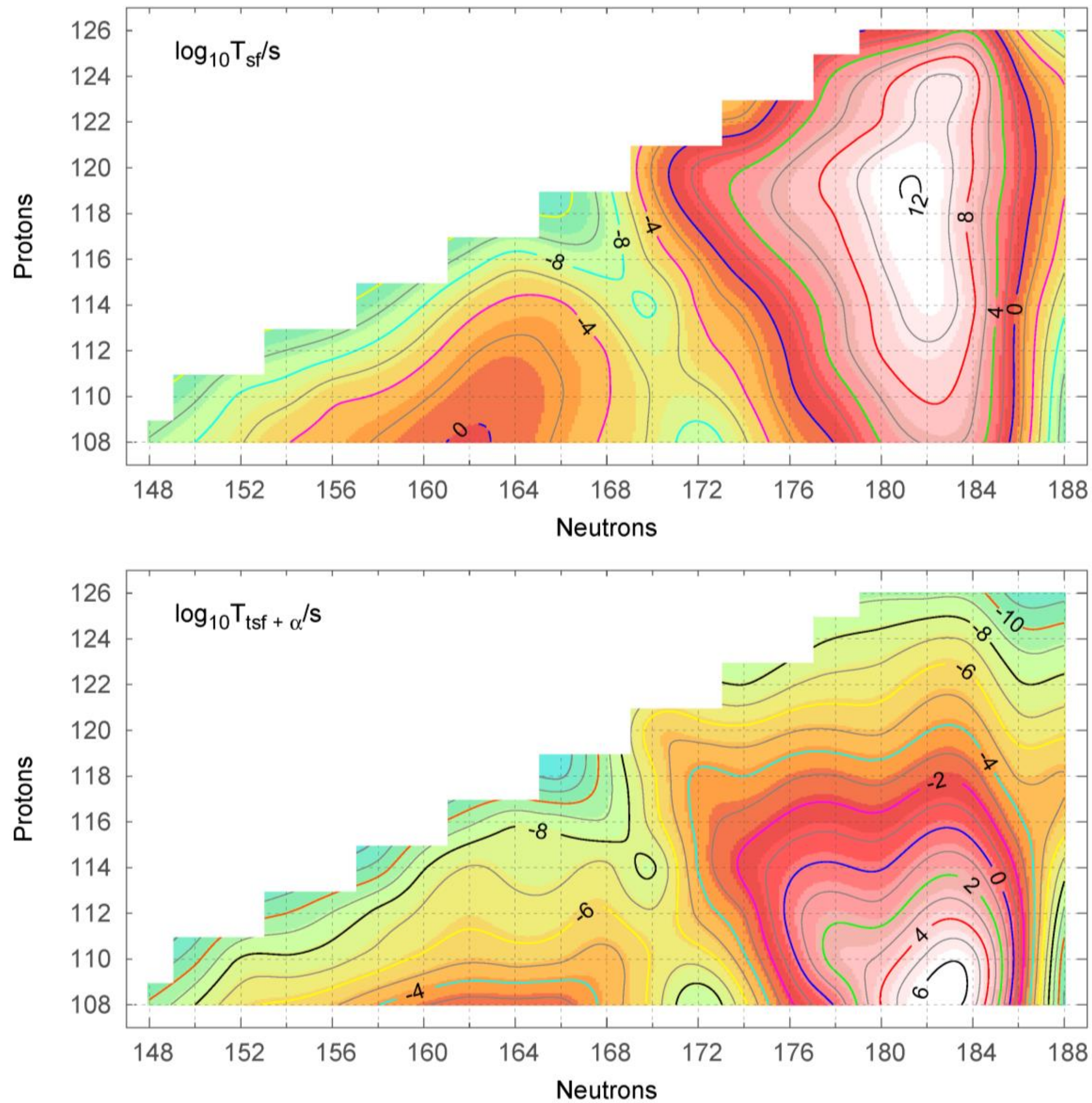

HFB-SkM* results for even-even SHN (II)

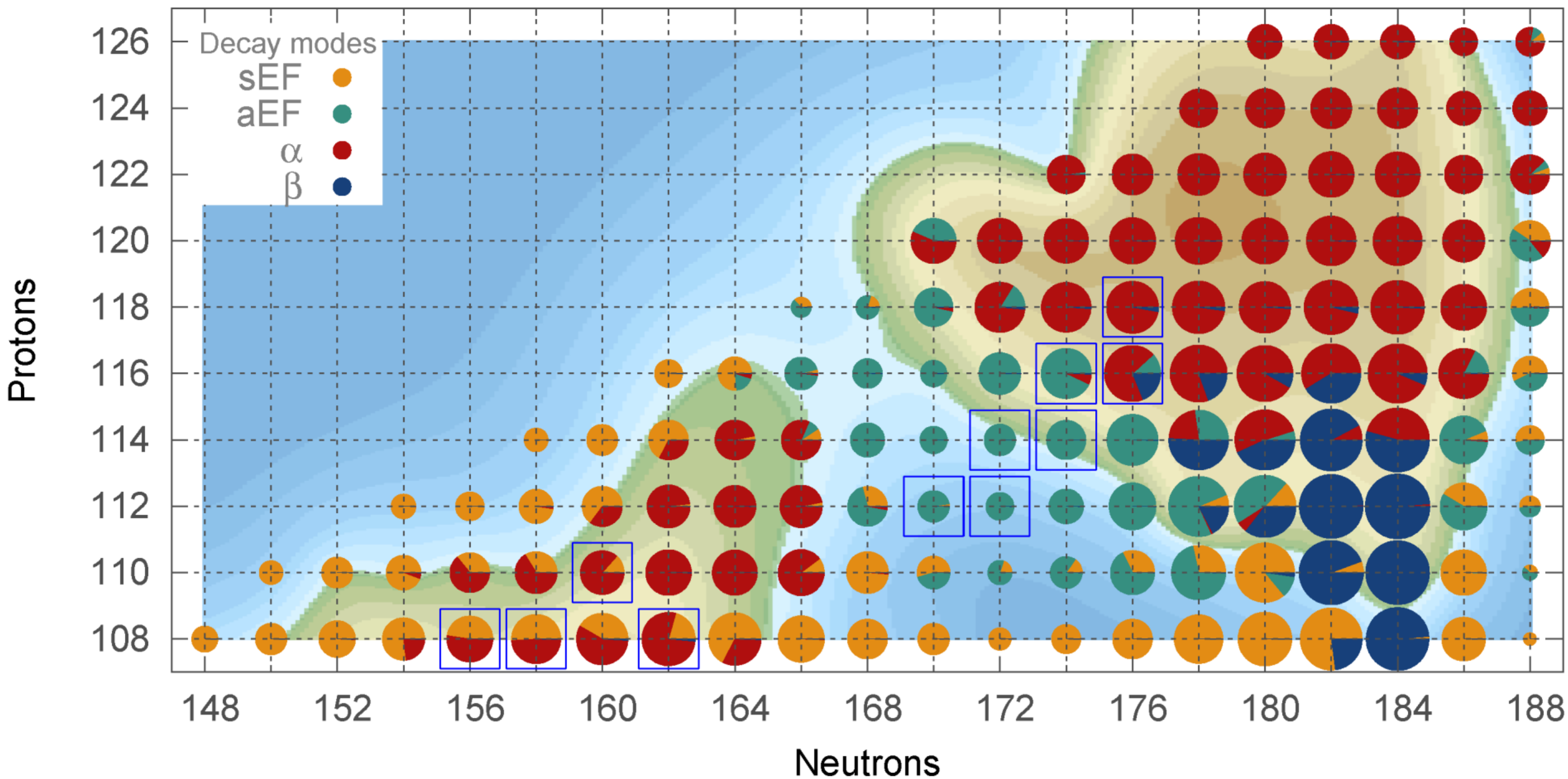

The circle radii are proportional to the decimal logarithms of total half-lives in s.

max $T_{sf+\alpha+\beta} \approx 10^4$ s for $^{294-296}$Cn

SHN with the extreme oblate deformation

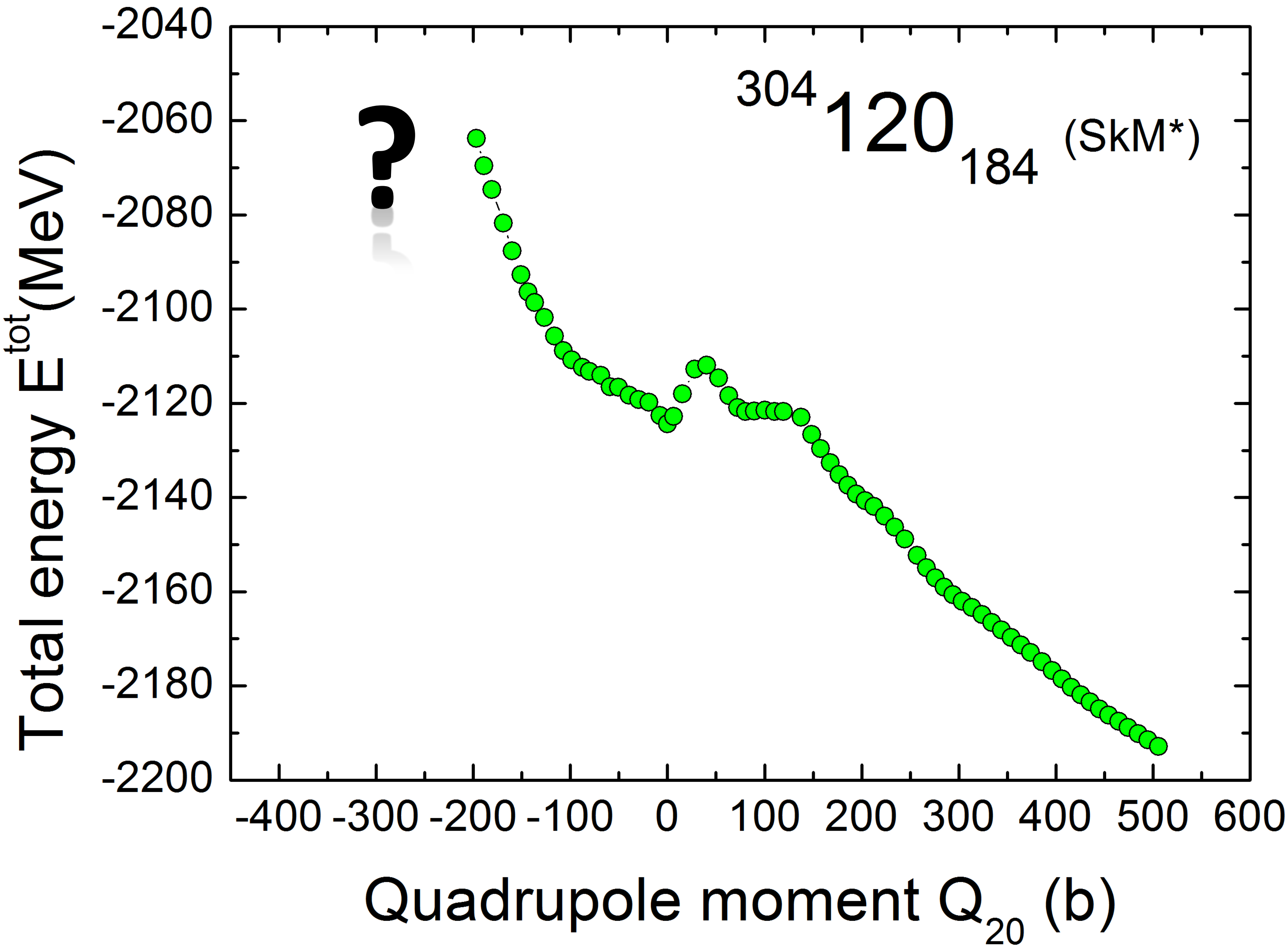

SHN with the extreme oblate deformation

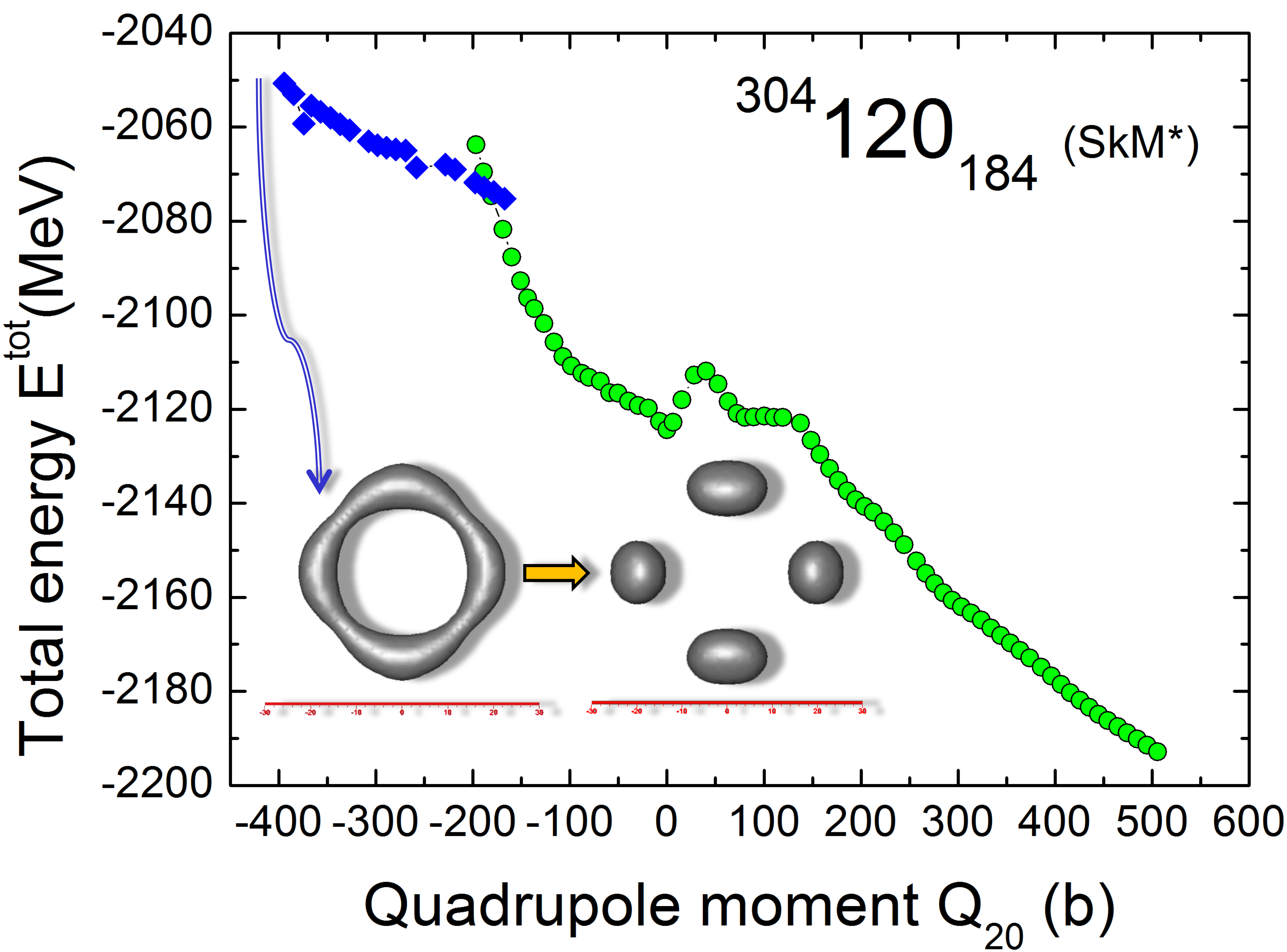

$^{306}122_{184}$ – toroidal shapes

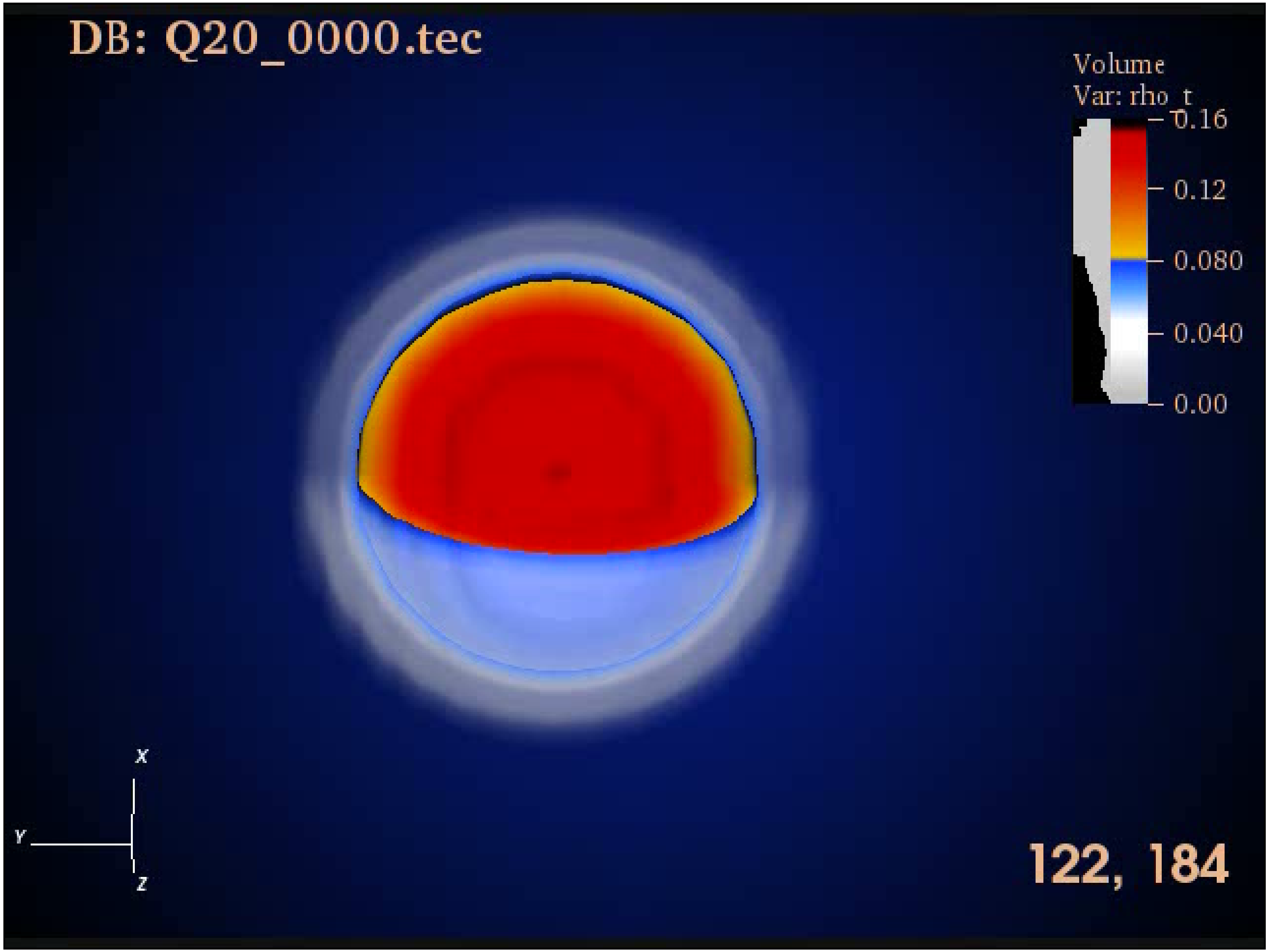

The three-fragment valley in LDM

PHYSICS REPORTS (Section C of Physics Letters) 4, No. 6 (1972) 325–342. NORTH-HOLLAND PUBLISHING COMPANY

FISSION AND FUSION DYNAMICS *

W.J. SWIATECKI

Institute of Physics, University of Aarhus, Denmark and
Lawrence Berkeley Laboratory, University of California, Berkeley, California

and

S. BJØRNHOLM

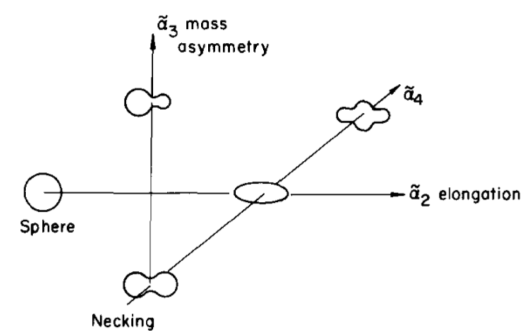

Fig. 1. The three principal degrees of freedom required for the description of fusion and fission.

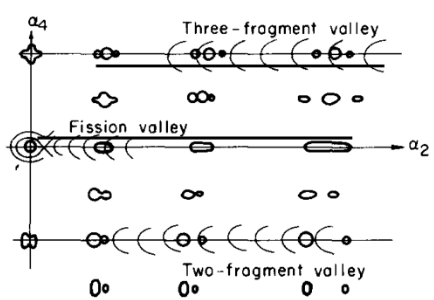

Fig. 2. The fission valley (the three-fragment valley) and the two-fragment valley. The associated shapes are sketched in a rough way.

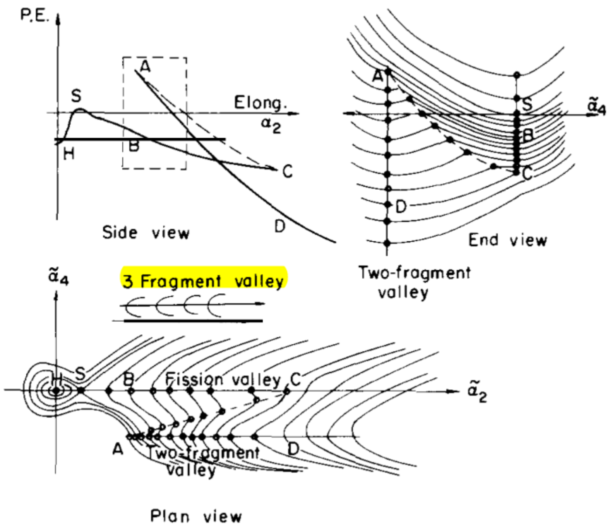

Fig. 3. Schematic energy contour diagrams of the two-fragment valley and the fission valley, including (side view and plan view) the spherical minimum, caused by shell effects.

SHN by 3-body cold fusion ???

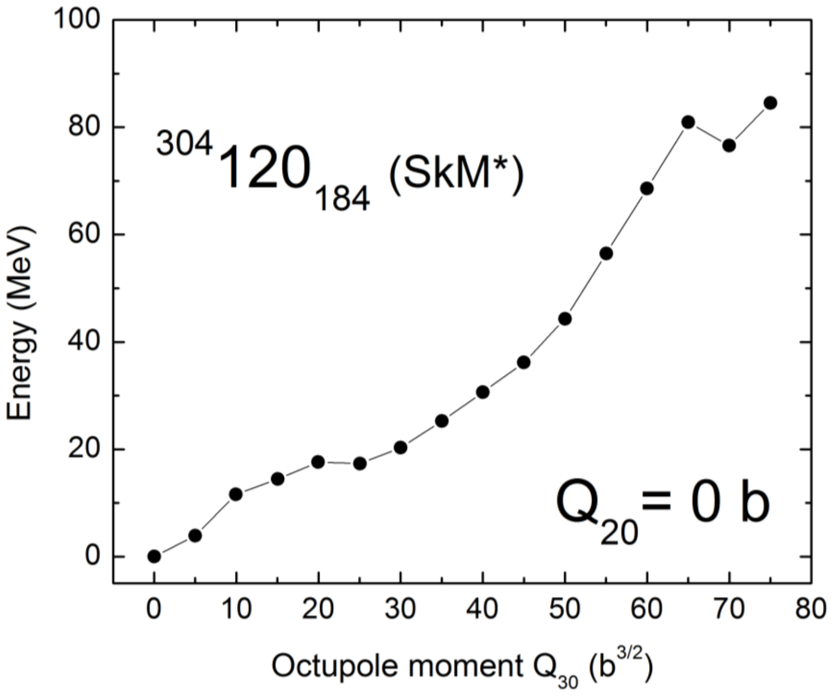

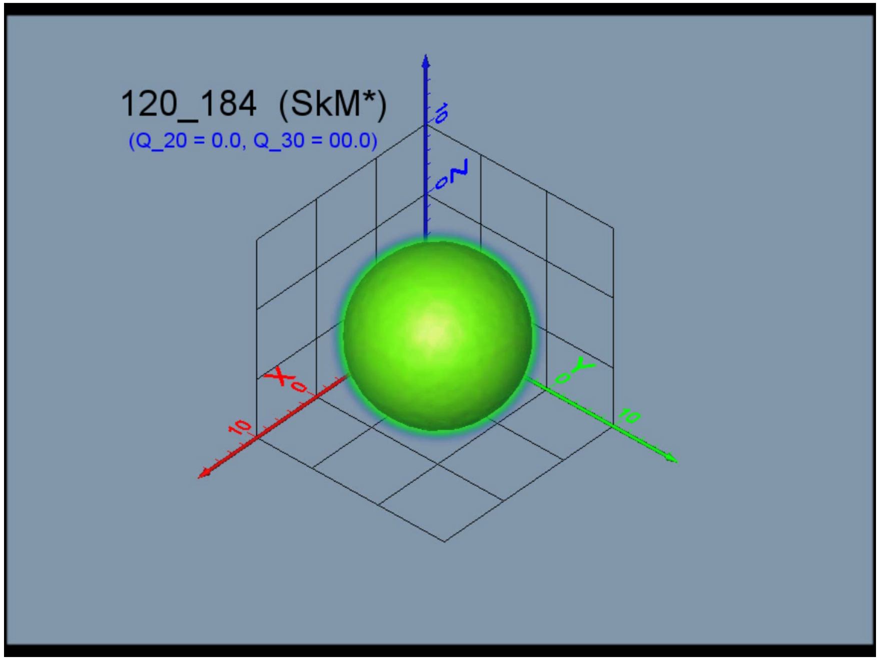

$$^{132}Sn_{82} + {}^{132}Sn_{82} + {}^{40}Ca_{20} \rightarrow {}^{304}120_{184}$$

$$^{48}Ca_{28} + {}^{48}Ca_{28} + {}^{208}Pb_{126} \rightarrow {}^{304}122_{182}$$

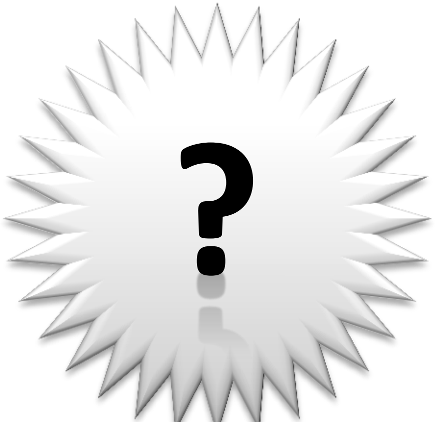

This research has been done in collaboration with

Andrzej Baran (UMCS)

Witek Nazarewicz (UTK-ORNL-UW)

Leszek Próchniak (UW)

Hai Ah Nam (ORNL) – VisIt movies

Thank you!

^{198}Hg: the heteromodal fission

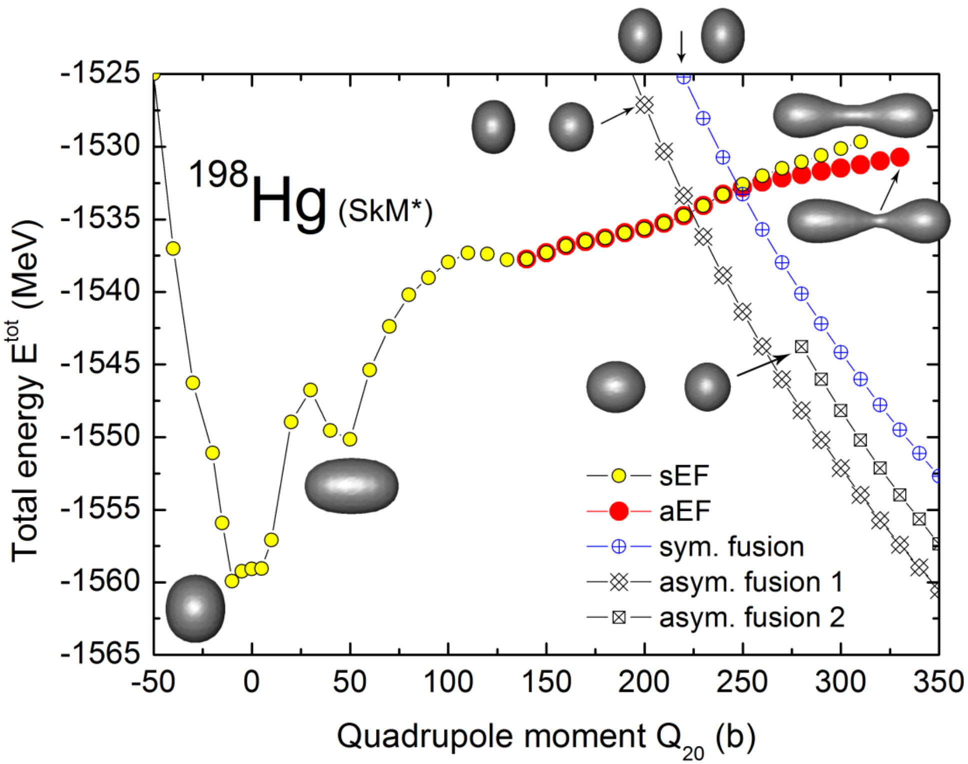

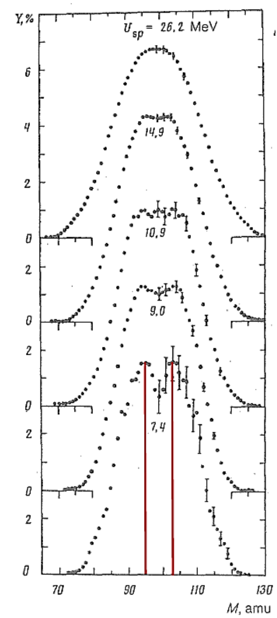

Itkis *et al.*, 1990

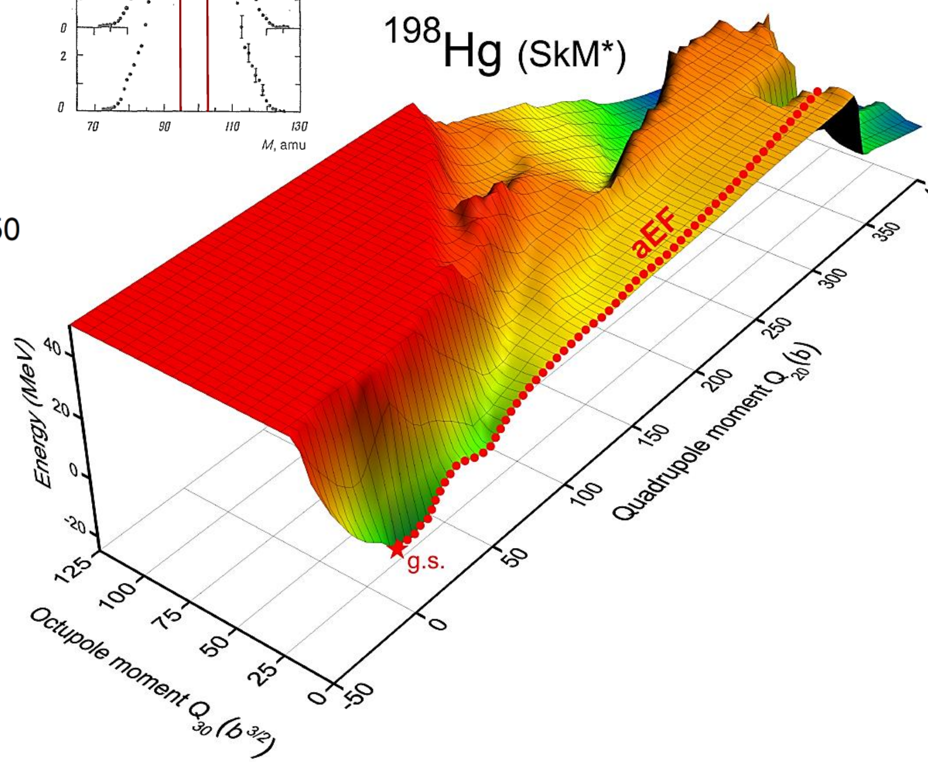

^{180}Hg: asymmetric fission!

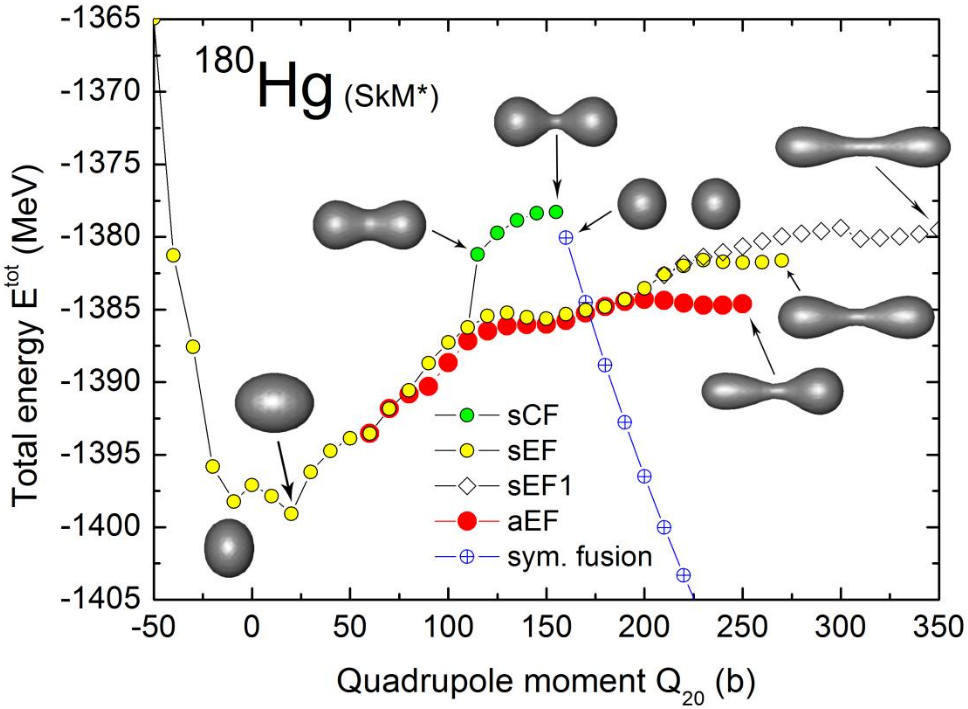

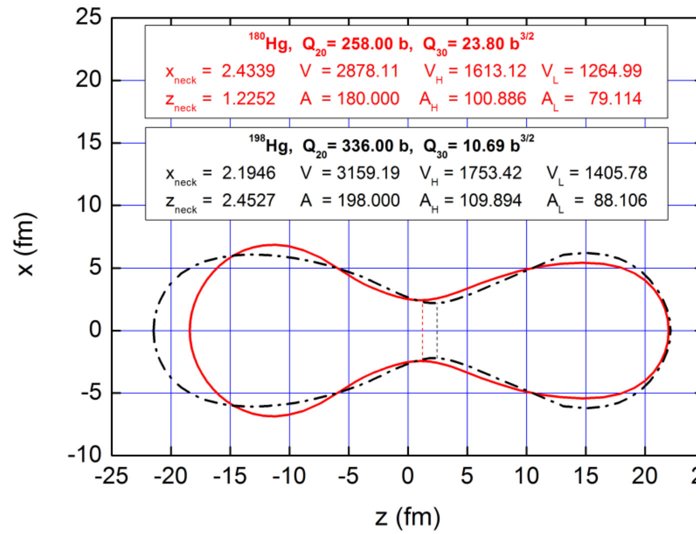

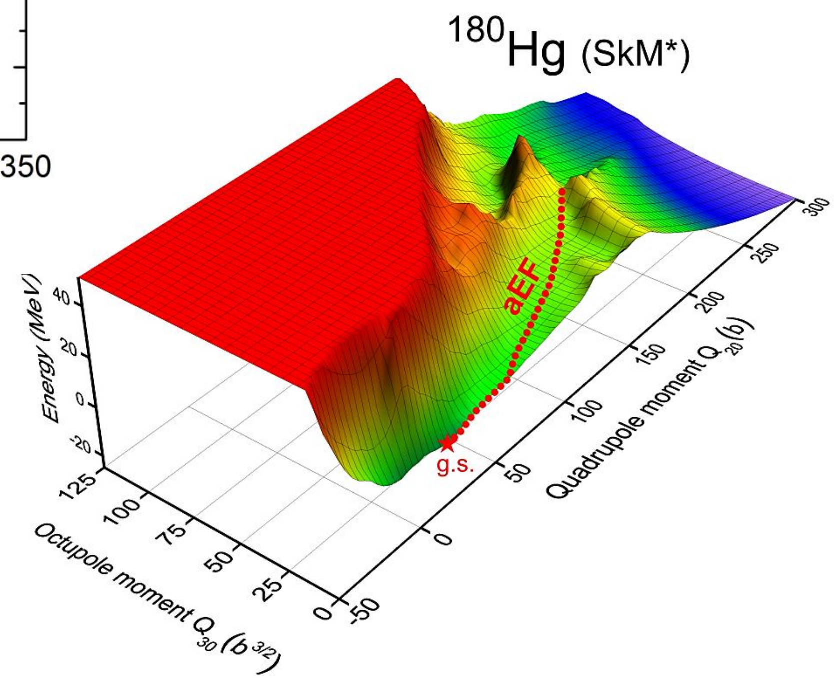

$$ {}^{180}_{80}Hg_{100} \overset{?}{\rightarrow} {}^{90}_{40}Zr_{50} + {}^{90}_{40}Zr_{50} $$

PRC **86**, 024601 (2012)

^{232}Th and ^{232}U : the third minima?

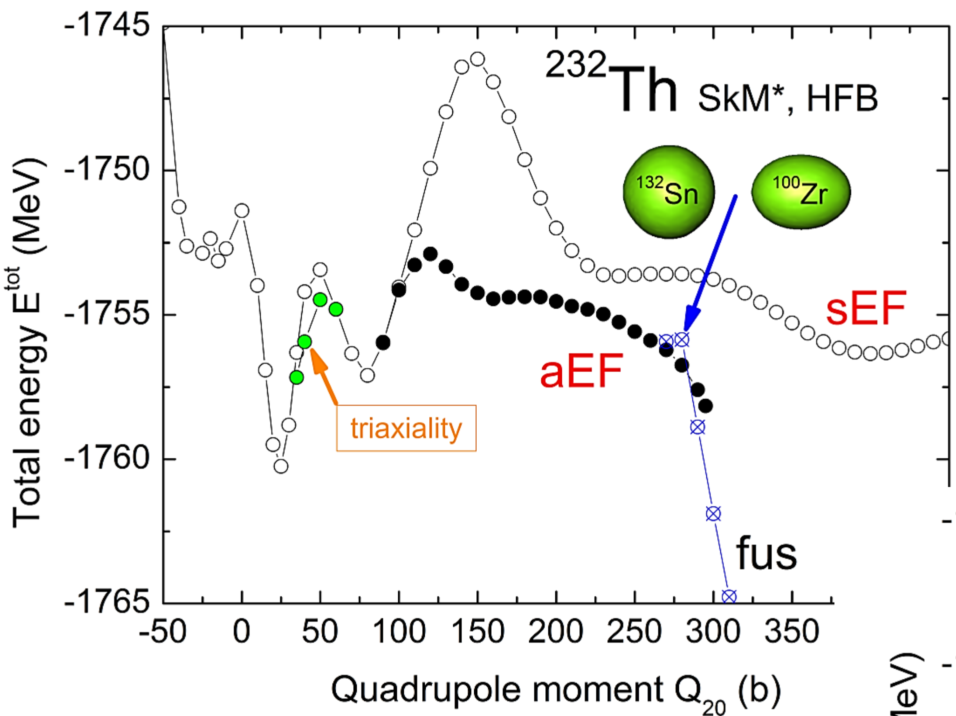

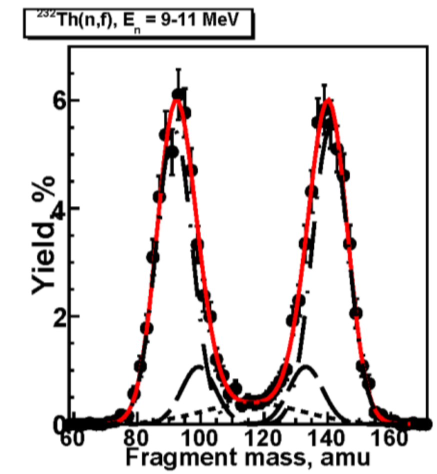

arXiv:1304.2316v1 [nucl-ex]

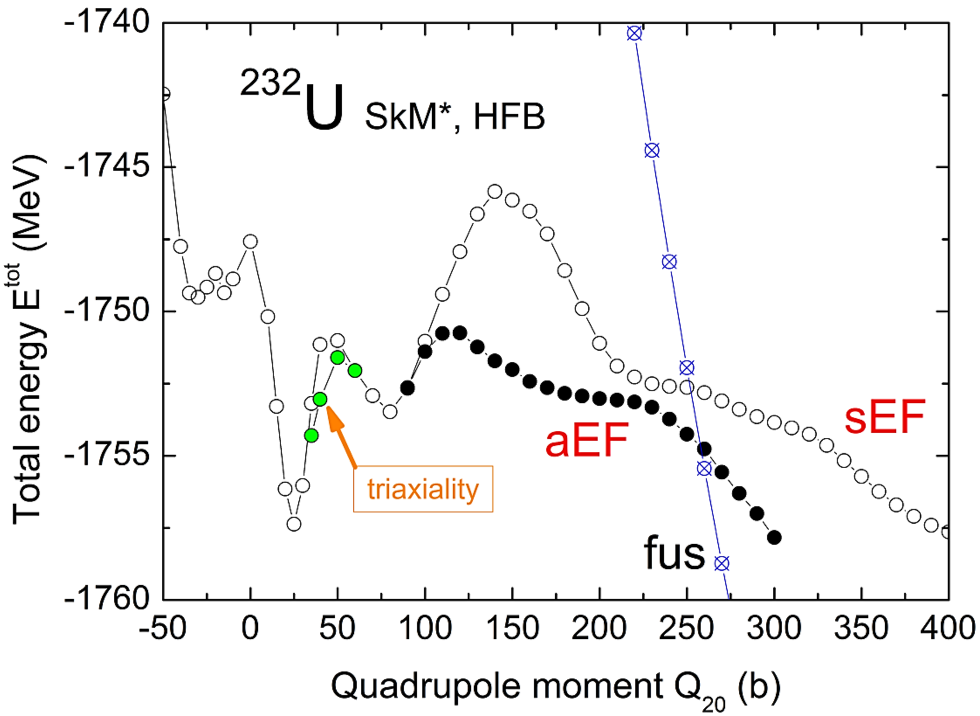

^{232}Th and ^{232}U : the third minima?

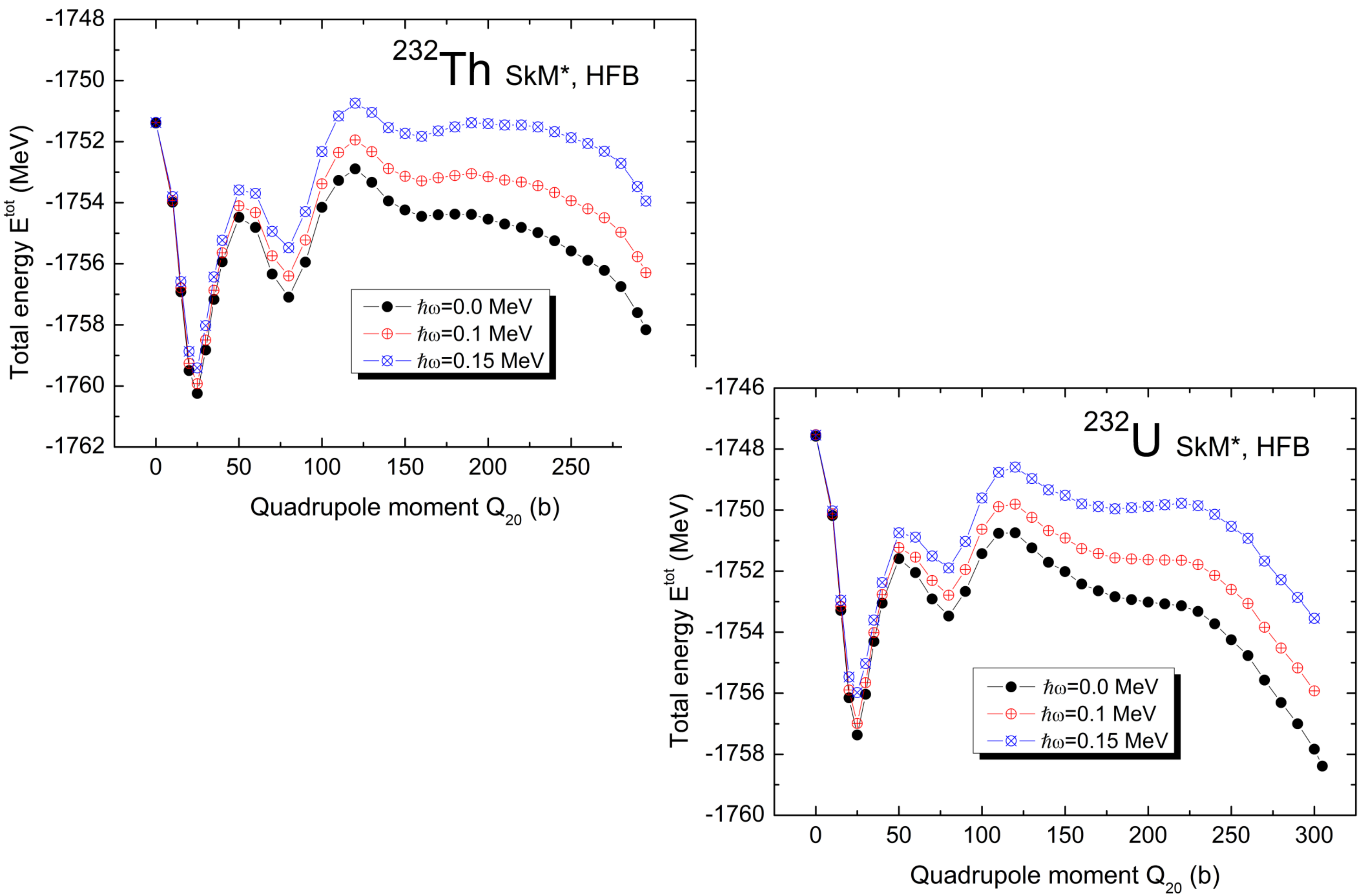


KONIEC